Title
Actin network assembly and force generation: The mechanism of filament nucleation by the Arp2/3 complex and the emergent properties of viscoelastic filament networks

Permalink
https://escholarship.org/uc/item/8qg1r1px

Author
Dayel, Mark J

Publication Date
2005

Peer reviewed|Thesis/dissertation

Actin Network Assembly and Force Generation: The Mechanism of Filament Nucleation by the Arp2/3 Complex and the Emergent Properties of Viscoelastic Filament Networks

by

Mark J Dayel

DISSERTATION

Submitted in partial satisfaction of the requirements for the degree of

DOCTOR OF PHILOSOPHY

in

BIOPHYSICS

in the

GRADUATE DIVISION

of the

UNIVERSITY OF CALIFORNIA, SAN FRANCISCO

Date

University Librarian

Degree Conferred:

Actin Network Assembly and Force Generation: The Mechanism of

Filament Nucleation by the Arp2/3 Complex and the Emergent

Properties of Viscoelastic Filament Networks

Copyright ©2005

by

Mark J Dayel

To my mother and father,

who encouraged me to think for myself

and taught me how.

Acknowledgments

First and foremost my thanks go to my PI, Dyche Mullins, for his enthusiastic support and confidence in me. Dyche has a wonderful outlook on science that I aspire to emulate and I could not have hoped for a better person to work with.

My thanks also to Bence Olveczky, who first encouraged me to come to the United States and was confident of my success; Erik Hom who has been very supportive both personally and intellectually in my time at UCSF and who encouraged me to apply for the PhD program in the first place; John Lever for his confidence and support over the years. And members of the Mullins Lab, for interesting discussions and for their companionship and support.

Special personal thanks to Paul, Jeanne, Linda and Denny. And to Julie Ransom who looks after all us Biophysics students almost as though we are her own children.

Abstract

Actin Network Assembly and Force Generation: The Mechanism of

Filament Nucleation by the Arp2/3 Complex and the Emergent Properties

of Viscoelastic Filament Networks

by

Mark J Dayel

DOCTOR of PHILOSOPHY in BIOPHYSICS

University of California, San Francisco

R Dyche Mullins, Chair

The Arp2/3 complex nucleates actin filaments and crosslinks them into networks that exert the force that drives cell, vesicle and bacterial motility. The activation of Arp2/3 complex is by the WASP family protein VCA region which binds both the Arp2/3 complex and an actin monomer. We show here that the Arp2 and Arp3 subunits of the Arp2/3 complex bind ATP and Arp2 hydrolyzes ATP rapidly upon nucleation of a new actin filament, stimulated by interaction with a single actin monomer co-ordinated by VCA. Our observation that capping of filament pointed ends by the Arp2/3 complex also stimulates rapid ATP hydrolysis on Arp2 identifies this actin monomer as the first monomer at the pointed end of the daughter filament. WASP-family VCA domains therefore activate the Arp2/3 complex by driving its interaction with a single conventional actin monomer to form an Arp2-

Arp3-actin nucleus and the actin monomer becomes the first monomer of the polymerizing the daughter filament.

Actin networks built by Arp2/3 complex behave as viscoelastic gels. It has been proposed that energy can be built up, stored and released by these gels to produce propulsive motion. I create a theoretical framework for computer modeling of such networks and implement the model in C++. The model recreates *in silico* the *in vitro* behavior of bead and *Listeria* motility and validates the viscoelastic energy buildup and release as a simple mechanism for actin-based motility leading to a detailed 'steady-state symmety-breaking' model. This model makes several experimentally testable predictions, including that pulsatile motion is caused by an imbalance in the rate of energy build up and energy release, and that symmetrically coated *Listeria* will move sideways not lengthways.

R Dyche Mullins
Dissertation Committee Chair

Contents

List of Figures

List of Tables

Preface

Biology is rapidly advancing its principal frontiers—investigating the behavior of organisms, of cells and of molecules. The distinction between these three frontiers of knowledge is one of convenience—these are the units that we divide life into for easy study—but we accept that these three are really the same: the relatively simple properties of submicroscopic molecules somehow interact to give rise to the observed behavior of cells and the interactions among cells give rise to the behavior of organisms. The two great challenges of the next phase of biology research will be to bridge the gap between the molecular and cellular world, and the gap between the cellular and organismal world. This thesis begins to address the first of these challenges.

The cytoskeleton (literally, the 'cell-skeleton') gives cells shape and allows them to move. It represents a structure—a self-organizing system—built entirely from molecules. Somehow the properties of these molecules, their binding to and chemical reactions with other molecules, creates a physical structure.

One part of the cytoskeleton is assembled from a polymer-forming molecule called actin—It is the actin cytoskeleton produces force that allows cells to

move and change shape. The Arp2/3 complex is the controller of the assembly of these actin polymers—it orchestrates the creation of new actin filaments and pins them together into arrays that build up the structures. The part I of this thesis investigates how the Arp2/3 complex works.

Part II of the thesis begins to investigate how a viscoelastic polymer network such as the actin cytoskeleton produces force. I use a computational model to show that the observed behavior of actin networks that lead to force generation and movement can be explained as a direct result of the network properties themselves.

In Part I, chapter 2 discusses the Arp2/3 complex and summarizes the findings of my papers (included as chapters 3 and 4.) Chapter 5 shows in graphical form the implications of these results for how the Arp2/3 complex works. Chapter 6 continues with some unpublished data and chapter 7 casts the Arp2/3 complex as a player in a larger cycle of formation and disassembly of actin structures, taking the discussion in the direction of the function of ATP hydrolysis by the Arp2/3 comples. Chapter 8 suggests future directions that to answer the remaining questions raised by this research.

In Part II, chapter 9 introduces the question of how actin networks produce force, sketching out the current models and their target behavior. Chapter 10 explains the plans for my computational model, and chapter 11 outlines their technical implementation. Finally, chapter 12 describes the results of the first generation model, their implications and the future directions of the project.

Chapter 1

Background

1.1 Actin-based motility

Actin cytoskeleton is responsible for almost all[1] eukaryotic cell movement. During wound healing for example, the actin cytoskeleton drives the movement of cells to close the wound. Figure 1.1a shows a goldfish scale, plucked from the fish and placed in medium overnight. The irregular grey material surrounding the scale is a single layer of fish cells that were attached to the bottom of the scale spreading out over the glass in an attempt to close the wound. Treating this layer of cells with the trypsin breaks down the proteins involved in cell-cell adhesion and causes the layer to dissociate into individual cells, and the mechanism of migration can be seen to be a flat, actin-rich structure at the front of the cell (Figure 1.1b). Movies of this migration show material in the lamellipod being swept

---

[1] the exception is sperm which in most cases move by flagellar swimming, but in the case of *Ascaris* sperm use MSP (another polymerizing protein) instead of actin

back with the movement of the cell as though it is being continually deposited at the front of the lamellipod, and studies have shown one of the major components of this material to be actin (Waterman-Storer et al., 1998).

1.2   The Lamellipod

Figure 1.2 shows an electron micrograph of the goldfish keratocyte lamellipodium. In this image, the membrane is stripped away to reveal the actin-rich network beneath. These filaments are crosslinked into a network that provides the driving force for the lamellipod (see Pollard and Borisy, 2003, for review).

The actin protein exists in two forms within the cell, free-floating monomeric actin (sometimes associated with proteins such as profilin that prevent spontaneous polymerization), and actin filaments (made of actin momomers that bind to one another in a helical arrangement.) Actin filaments are polarized: they have a fast growing 'barbed' end and a 'pointed' end which does not elongate[2]. An exposed 'barbed' end will spontaneously elongate by the addition of monomers from solution, making the control of barbed ends critical for the regulation of actin assembly. Actin filament barbed ends are created by the Arp2/3 complex, which nucleates actin filaments from the sides of existing filaments to create branched 'dendritic' arrays (Mullins et al., 1998).

---

[2]Profilin prevents monomers adding onto the pointed end *in vivo*. Without profilin the pointed end does elongate, albeit much more slowly than the barbed end
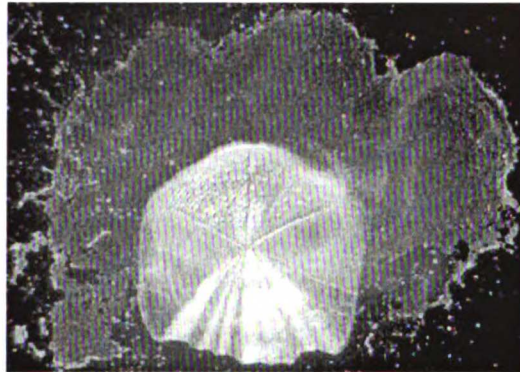
(a) A monolayer of cells moves outwards from an excised goldfish scale

0 min   1 min   2 min   3 min
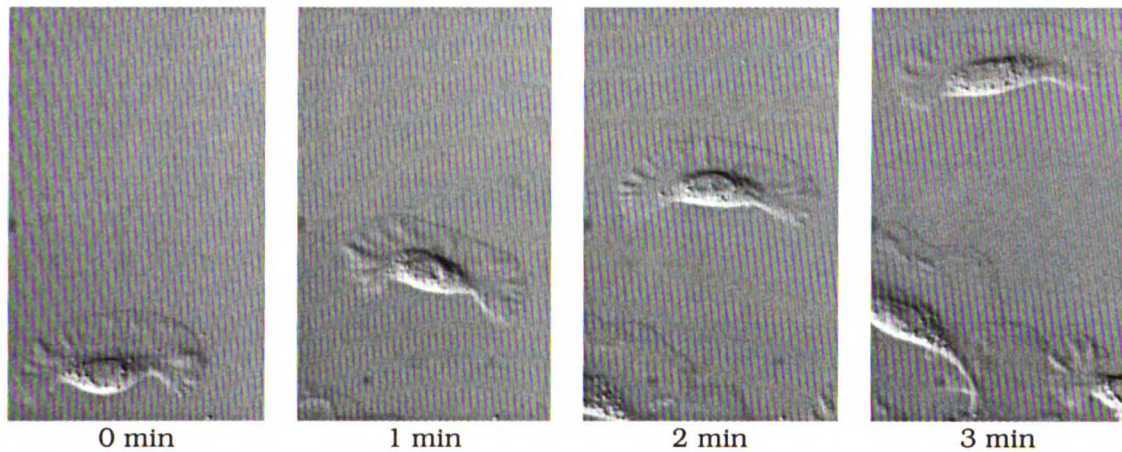
(b) Dissociated from the monolayer using trypsin, an individual cell moves across the glass coverslip at ~10 μm per minute. The broad, flat lamellipod at the front of the cell is an actin-rich structure that drives cell movement.

Figure 1.1: An example of cell motility: Fish epidermal keratocytes crawl over a glass coverslip
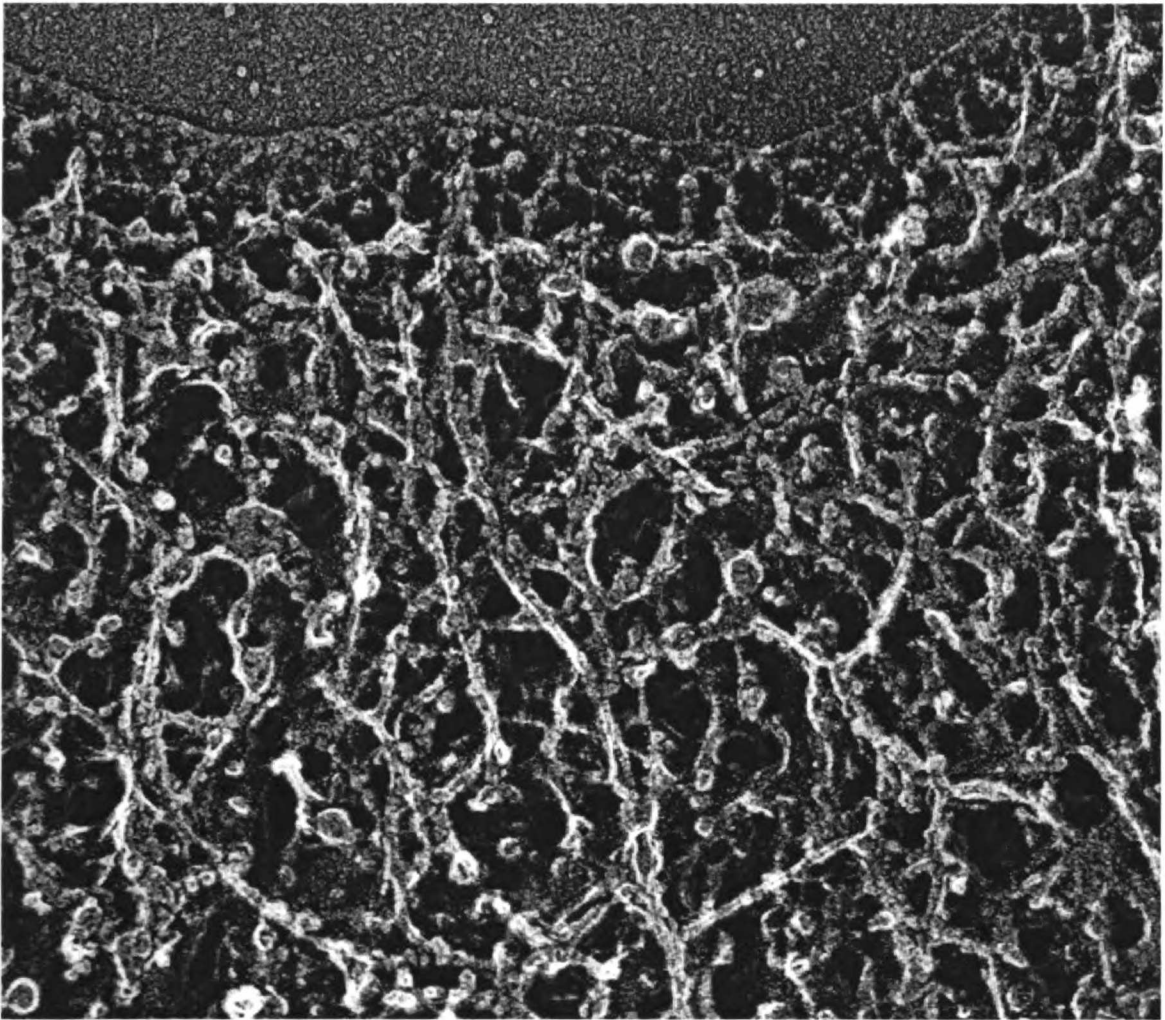
Figure 1.2: The fish keratocyte lamellipod, seen using electron microscopy shows a dense actin network beneath the cell membrane. (Keratocytes were grown on glass coverslips then visualized by freeze-fracture deep-etch platinum replica EM)

1.3 The Lamellipodial Motor

To produce motile force, we believe that two primary mechanisms are active, localized nucleation of new filaments at the front of the lamellipod by Arp2/3 complex, and global decommissioning of old barbed ends by capping protein.

Figure 1.3 shows our cartoon model for how the lamellipodial motor works. In step 1, an Arp2/3 activator protein is itself turned on (e.g. by a small GT-Pase) and recruits and activates Arp2/3 complex, nucleating a new actin filament which is attached to an existing filament. In step 2, the newly nucleated filaments grow by addition of monomers onto their barbed ends. They are growing in the direction of the membrane, and since they are semi-flexible polymers, they push against and bend away from the membrane. The elastic restoring force tends to push on the membrane forwards, exerting the motile force. Step 3 shows how filaments that are growing away from the membrane are capped by capping protein, resulting in localized filament elongation at the front of the lamellipod. Since this whole system operates continuously, the components must be disassembled (step 4) and recycled to the front of the lamellipod again (step 5).

1.3.1 Filament Nucleation

Proteins that activate the Arp2/3 complex to nucleate new filaments have a VCA domain, and activation of native Arp2/3 activators (Wasp family proteins) is thought to involve the VCA domain switching from a protected state to an exposed state that can bind and activate Arp2/3 complex as shown in Figure 1.4a (Abdul-
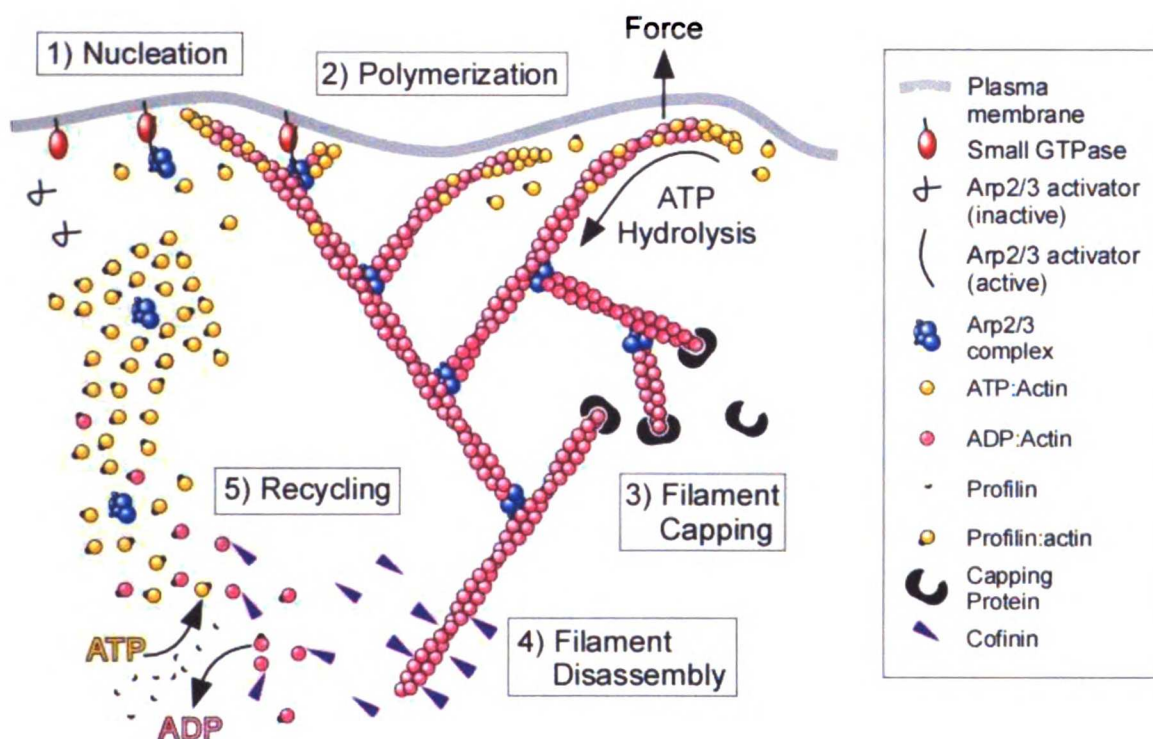
Figure 1.3: Simplified model for the protein components that assemble and de-construct the lamellipodial actin network. Arp2/3 nucleates filaments into actin branches that exert force at the membane, capping protein localizes filament elongation, and the network is disassembled at the rear of the lamellipod
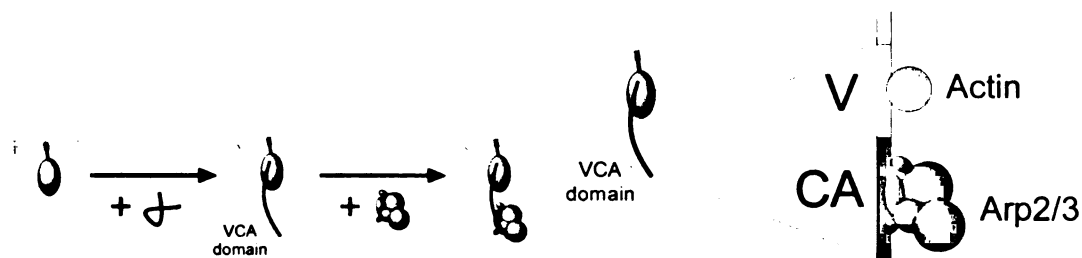
(a) G-protein turns on Arp2/3 activator, exposing VCA domain

(b) V domain of VCA binds monomeric actin, and CA domain binds Arp2/3 complex

Figure 1.4: VCA domain is the active domain of Arp2/3 activators

Manan et al., 1999; Gautreau et al., 2004). The VCA domains consists of an acidic domain (A) that binds Arp2/3 complex, a verprolin-homology (V) domain that binds monomeric actin and a connecting (C) domain that binds weakly to both Figure 1.4b (Marchand et al., 2001). Part I of this thesis deals in detail with the mechanism of nucleation of new filaments by the Arp2/3 complex and how the complex is activated by Wasp family proteins.

1.3.2 Network Elasticity

The simultaneous nucleation and crosslinking of actin filaments by the Arp2/3 complex leads to the creation of a filamentous network that can extend many microns. The network is composed of semi-flexible actin polymers, and on a micron scale the actin network behaves as a viscoelastic gel (Gardel et al., 2004). The intracellular pathogen *Listeria* uses actin-based motility to propel itself from one infected cell to the next directly and so avoids the host immune system. The viscoelastic nature of actin filament networks has been measured in

(Gerbal et al., 2000b) and proposed as an explanation for (Gerbal et al., 2000a)

the force generation that drives propulsion of *Listeria*. Part II of this thesis in-

troduces a computational model that explores in detail the mechanism of force

generation by crosslinked filament networks.

Part I

The Molecular Mechanism of Arp2/3 Activation
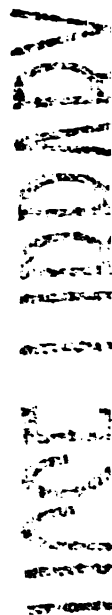
Chapter 2

Introduction
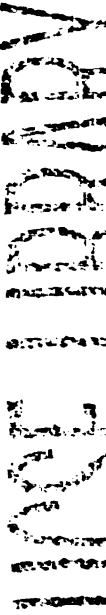
2.1 Background

The results of this work address some of the fundamental questions of how the Arp2/3 complex is activated on a molecular level, and by extension, how actin itself functions.

When work began on this project we had a reasonable understanding of what the Arp2/3 complex does, but little understanding of how it does it—how it works on a molecular level. Its fundamental function—that of nucleating new actin filaments from the sides of existing filaments and keeping them attached (crosslinked) had already been established, in large part thanks to Dyche's previous work in the lab of Tom Pollard (Mullins et al., 1998). We also knew from kinetic experiments (Machesky et al., 1999) that existing 'mother' filaments and the VCA domain of an Arp2/3 activator are needed to activate the complex (Figure 2.1). We knew that the Arp2/3 complex has 7 subunits and that two of these subunits have significant sequence similarity to conventional actin (Machesky et al., 1994), and the hypothesis had been proposed by the Pollard lab (Kelleher et al., 1995) that these two actin related subunits, Arp2 and Arp3 were the key to the nucleation of the new filaments. The exposed 'barbed-end' of an actin filament will spontaneously elongate by the addition of monomers from the cytoplasm and a filament barbed end is composed of two adjacent actin subunits in a specific conformation. Since Arp2/3 complex contains the two actin related proteins Arp2 and Arp3, the possibility that the complex might nucleate an actin filament by bringing its two actin related proteins together to mimic the barbed

end of an actin filament seemed very intuitive, and has been supported by the results of this work and others since.

To understand the functioning of the Arp2/3 complex, our approach has been to concentrate on the Arp2 and Arp3 subunits. These were expected to bind ATP because of their sequence similarity to actin, which was known to bind ATP and to use ATP hydrolysis to regulate its interation with monomers within a filament. We set out to discover whether the Arp2/3 complex binds ATP, and to determine if and when ATP is hydrolysed, and find out the function of ATP hydrolysis.

2.2 Arp2/3 as a molecular device: balancing conflicting kinetic requirements

Since ATP hydrolysis is used to release energy for cellular processes, we approached the question of the function of ATP hydrolysis by Arp2/3 complex by looking for aspects of Arp2/3 function that might require energy.
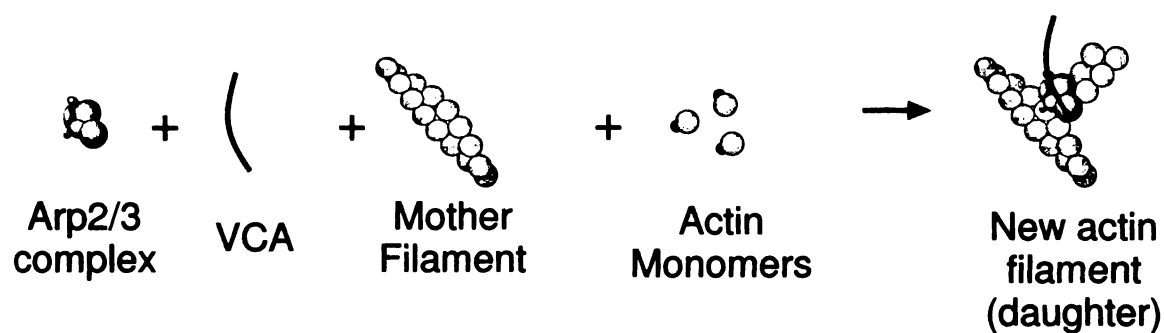
Figure 2.1: The components of an Arp2/3 nucleated actin branch

Most processes in biology are achieved by equilibrium reactions—driven by increasing entropy. Processes that hydrolyse ATP break the constrains of equilibrium kinetics and achieve a local entropy decrease (at the expense of the ATP), allowing non-equilibrium behaviors such as directional movement or irreversible steps in a reaction. The Arp2/3 complex has two behaviors which seemed in advance to be good candidates for requiring ATP hydrolysis:

Arp2/3 is:

- **A low-noise switch.** Arp2/3 becomes active in response to a signal by another activator protein (e.g. NWASP-VCA) and the presence of a mother filament but is inactive otherwise

- **A reversible structural anchor.** Arp2/3 forms an actin nucleus that attaches strongly to both the daughter and mother filament to provide structural rigidity, but can be disassembled later.

2.2.1 Arp2/3 as a low-noise switch

Upon activation, the Arp2/3 complex must switch from a state in which the proteins (the Arp2/3 complex and actin subunits) are free in solution, to a state in which they are bound tightly together. For many biological processes which require regulated interaction, alterations in off-rate are sufficient to shift the equilibrium one way or the other and change the bound and free population as desired. For the Arp2/3 complex, however, the result of activation is the creation of a nucleus and the polymerization of a new actin filament—an energy

expensive and not easily reversible process. Because of the release of the latent energy of polymerization of the monomers, activation of the complex is a kinetic trap—a state that once achived is very hard to reverse. To prevent accidental triggering, such a system would be expected to have a high energetic barrier for entry, i.e. the association of the actin monomers that form the daughter filament and the simplest mechanism to activate such a system would by something that transiently lowers this barrier, and the energy released by ATP hydrolysis could conceivably accomplish this.

2.2.2 Arp2/3 as a reversible structural anchor

The Arp2/3 complex nucleates and crosslinks actin filaments together in an array that can exert sustained protrusive force (Figure 1.3). This requires that the crosslinks be stable. A network of crosslinked actin filaments whose crosslinking proteins are in relatively rapid equilibrium will yeild to applied force, but a network of stably crosslinked filaments will resist the force (Xu et al., 1998). To form a force-producing network, the Arp2/3 complex must therefore have slow kinetics (primarily a slow off-rate) from both the mother and daughter filament, presenting a potential problem for disassembly of the network, once formed. Just as ATP hydrolysis on actin itself (more accurately the phosphate release following ATP hydrolysis) causes a destabilisation of the monomer-monomer contacts and a disassembly of the filament, ATP hydrolysis on Arp2/3 complex could potentialy be used to destabilize the branch and allow disassembly.
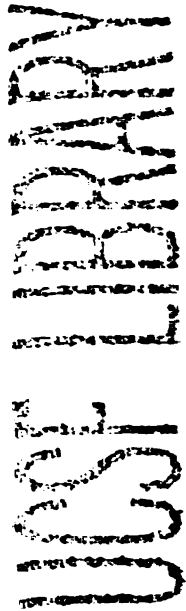
2.3 Published Findings

Our initial hypothesis was that hydrolysis of ATP by the Arp2/3 complex might be used to overcome an energy barrier and allow nucleus formation (Section 2.2.1). Our initial results (Chapter 3 on page 19) showed that the Arp2/3 complex binds two molecules of ATP on the Arp2 and Arp3 subunits as expected (Section 3.4.1). We showed that ATP is required by the complex for filament nucleation, whilst ADP or AMP-PNP (an ATP analogue) does not work (Section 3.4.3), supporting our initial hypothesis (Section 3.4.6).

The next challenge was to determine when ATP is hydrolysed by the complex on which subunits (Chapter 4 on page 43). To do this we covalently crosslinked a radioactive version of ATP, γ^{32}P-AzidoATP, to the complex and looked for the cleavage of the radioactive γ^{32}P. Using this assay we showed that Arp2 hydrolyses ATP rapidly upon filament nucleation (section 4.4.2), then used this assay to look for the precise requirements to stimulate hydrolysis.

We determined that Arp2 could be stimulated to hydrolyse ATP by two different routes:

- The presence of a mother actin filament, the VCA domain and actin monomers stimulate ATP hydrolysis. Importantly, the momomers are required, but do not need to be polymerisable (Latrunculin B binds to momomers and prevents them polymerizing, but they still work in this reaction to stimulate ATP hydrolysis on Arp2)

- Actin filament 'pointed-ends' are enough to stimulate ATP hydrolysis on Arp2. This pointed-end capping is thought to mimic the interaction between the Arp2/3 complex and the daughter filament.

2.4 Interpretation

Together these results suggested that the key to promoting ATP hydrolysis on Arp2 was interaction with an actin momomer, and that this momomer could be driven to interact with the complex by VCA, or by the pointed end of the actin filament.

Chapters 3 and 4 are reproductions of published papers detailing these results. Chapter 5 on page 75 details the structural implications of these results for the mechanism of activation of the Arp2/3 complex and chapter 6 continues the discussion with further, unpublished results leading to questions of the role of ATP hydrolysis on Arp2/3 complex discussed in chapters 7 and 8.

Chapter 3

Arp2/3 complex requires hydrolyzable ATP for nucleation of new actin filaments

Mark J. Dayel, Elizabeth A. Holleran, and R. Dyche Mullins.
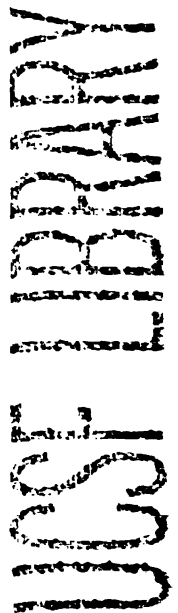
3.1 ABSTRACT

The Arp2/3 complex, a seven-subunit protein complex containing two actin-related proteins Arp2 and Arp3, initiates formation of actin filament networks in response to intracellular signals but the molecular mechanism of filament nucleation is not well understood. Arp2 and Arp3 are predicted to bind ATP via a highly conserved nucleotide-binding domain found in all members of the actin superfamily and to form a heterodimer than mimics a conventional actin dimer. We show here that adenosine nucleotides bind with micromolar affinity to both Arp2 and Arp3 and that hydrolyzable ATP is required for actin nucleation activity. Binding of N-WASP WA increases the affinity of both Arp2 and Arp3 for ATP but does not alter the stoichiometry of nucleotides bound in the presence of saturating concentrations of ATP. Arp2/3 complex bound to ADP or the non-hydrolyzable ATP analogue AMP-PNP cannot nucleate actin filaments but addition of the phosphate analogue BeF_3 partially restores activity to ADP-Arp2/3. Bound nucleotide also regulates the affinity of Arp2/3 complex for its upstream activators N-WASP and ActA. We propose that the active nucleating form of the Arp2/3 complex is the $ADP-P_i$ intermediate in the ATPase cycle and that the ATPase activity of Arp2/3 controls both nucleation of new filaments and release of Arp2/3 from membrane-associated activators.

3.2 INTRODUCTION

The actin cytoskeleton determines the shape, motility, and internal organization of eukaryotic cells. Many actin-based structures, especially those involved in membrane protrusion, are assembled by coordinated polymerization and crosslinking of new actin filaments from actin monomers into either orthogonal or parallel filament networks (Pollard et al., 2000). In these structures work is accomplished by the free energy of polymerization. Subsequent ATP hydrolysis by filamentous actin then allows the networks to be disassembled. The rapid and regulated assembly and disassembly of actin filament networks lies at the heart of many cellular processes that involve membrane protrusion such as cell locomotion, endocytosis and phagocytosis (Taunton, 2001).

The Arp2/3 complex plays a central role in the regulated assembly of actin-based structures. Arp2/3 nucleates formation of new actin filaments in response to upstream signaling events and simultaneously crosslinks them into orthogonal networks. Activation of Rho-family G-proteins, including Rac and Cdc42, leads to dramatic reorganization of the actin cytoskeleton (Ridley and Hall, 1992; Ridley et al., 1992). Rac and Cdc42 promote activation of members of the WASP family of proteins (Miki et al., 1998a,b; Rohatgi et al., 1999) that include WASP, N-WASP and several isoforms of Scar (Mullins, 2000). WASP family proteins, in turn, recruit and activate Arp2/3 (Machesky and Insall, 1998; Rohatgi et al., 1999; Yarar et al., 1999). Arp2/3 nucleates formation of new actin filaments from the sides of older filaments, creating a dendritic network of cross-linked actin filaments

in vitro (Blanchoin et al., 2000a; Mullins et al., 1998) and *in vivo* (Svitkina and Borisy, 1999).

We previously proposed that activation of Arp2/3 complex involves the two actin-related proteins, Arp2 and Arp3, forming a heterodimer that mimics a conventional actin dimer and nucleates a new actin filament (Kelleher et al., 1995; Mullins and Pollard, 1999b). Actin-related proteins and other members of the actin superfamily such as molecular chaperones like Hsc70, apyrases like ecto-apyrase HB6, and sugar kinases like hexokinase and glycerokinase share a core structural fold, the actin fold, that forms an adenosine nucleotide binding site (Bork et al., 1992). In these proteins the actin fold couples ATP hydrolysis and phosphate release to conformational changes that control, for example, actin filament stability (Belmont et al., 1999; Korn et al., 1987; Maciver et al., 1991) and the affinity of Hsc70 for unfolded proteins (Liberek et al., 1991). Actin monomer-monomer interactions within a filament are stronger in the ATP and the ADP-Pi states (Orlova and Egelman, 1992; Otterbein et al., 2001), than in the ADP state. In contrast, Hsp70 binds its substrates weakly in the ATP state but tightly the ADP state (Takeda and McKay, 1996). Bound nucleotide regulates the affinities of several members of the actin superfamily for their substrates so we speculated that bound nucleotide might also regulate the interaction of Arp2 and Arp3 and control the formation of an Arp2-Arp3 nucleus. To address these questions we characterized nucleotide binding and hydrolysis by Arp2/3 and investigated the role of the bound nucleotide in the biochemical activity of Arp2/3.

3.3 MATERIALS AND METHODS

3.3.1 Purification of proteins

We purified Arp2/3 from *Acanthamoeba Castellini* by a combination of conventional and affinity chromatography. We resuspended 75 g *Acanthamoeba* in two volumes of lysis buffer (11% sucrose, 10mM Tris pH 8.0, 5mM DTT, 1mM ATP, 1mM EGTA, 2mM PMSF, 0.1mM Benzamidine, 1mg Leupeptin, 4mg Soybean Trypsin Inhibitor, 1mg Pepstatin A, 1mg Aprotinin) and lysed cells in a dounce homogenizer. We spun the lysate at 13,000 RPM in a Sorvall GSA rotor for 20 minutes to remove cell debris, and then in a Ti50.2 rotor at 38,000 rpm for 90 minutes. We collected the layer of supernatant between the pellet and lipid layer and bound it in batch for 20 minutes to 100mL DEAE resin equilibrated in column buffer (100 μM ATP, 1mM Ca^{2+}, 2mM Tris pH 8.0, 1mM DTT). DEAE flow-through was loaded on a 15mL C200 column (Cellufine 200(m); Millipore, Bedford, MA). We collected the flow-through; added 25mM KCl and passed it over a 2 mL CH-Sepharose (Activated CH-Sepharose 4B, Amersham Pharmacia Biotech, Uppsala, Sweden) N-WASP WA (398-501) affinity column. We washed the resin with 10 volumes each of 25mM and 100mM KCl in column buffer. Arp2/3 was eluted with 400mM $MgCl_2$ and passed over a 400 μL phenyl-sepharose column (#6 Fast-Flow low sub, Amersham) then either gel filtered on a 30 mL Superdex S-200 column equilibrated with KMEI buffer or exchanged into KMEI using a PD-10 desalting column (Amersham). The complex was concentrated by dialysis against sucrose and dialyzed overnight into KMEI buffer + 100 μM ATP for use in assays. Typical

yields were ~6mg pure Arp2/3 from 75 grams of packed cells. The protein was never freeze-thawed or stored for more than a week. Typically it was used within 24 hours of purification. KMEI buffer: 50 mM KCl, 1 mM MgCl$_2$, 1 mM EGTA, 0.5mM TCEP, 10 mM Imidazole, pH 7.0.

Actin was purified from *Acanthamoeba* by the method of MacLean-Fletcher and Pollard (MacLean-Fletcher and Pollard, 1980). Actin filaments used as seeds for polymerization or in ATP hydrolysis experiments were polymerized for 30 minutes at room temperature by adding of 0.1 volume of 10x KMEI to monomeric actin, followed by the addition of 1.2 molar excess phalloidin. Phalloidin-actin was allowed to continue polymerizing overnight on ice and nucleotide was removed the following day by 2 treatments with 5% Dowex resin (Bio-Rad AG 1-X8 resin) at 4°C. Residual denatured actin monomers were removed by centrifugation at 20,000×g for 10 minutes.

Rat N-WASP-WA (398-502) with an N-terminal 6His tag was purified by Ni-affinity chromatography using standard methods.

3.3.2 Assay Conditions

All assays were performed in KMEI buffer (50 mM KCl, 1 mM MgCl$_2$, 1 mM EGTA, 0.5mM TCEP, 10 mM Imidazole, pH 7.0) at 25°C, except for buffer exchange to measure bound nucleotide (Table 3.2) which was performed at 4°C. Free nucleotide was removed from Arp2/3 before assays by 2–4 treatments for 3 minutes each with 5% volumes of Dowex resin.

3.3.3 UV crosslinking studies

Arp2/3 was used at 1–2 μM, F-actin at 10 μM and N-WASP WA at 25 μM. For normal ATP crosslinking a stock solution of 300 μM ATP in KMEI was doped with 150 μCu [α–^{32}P]ATP. For azido-ATP crosslinking we used a stock of [α–^{32}P] azido-ATP at 500 μM. Free nucleotide was removed from Arp2/3 by 4 treatments with 5% Dowex resin. We incubated Arp2/3 in KMEI for 20 minutes with labeled ATP and then photo-crosslinked bound nucleotide to the protein by exposing the mixture to ultraviolet light. For ATP, the ultraviolet exposure was 30s and for azido-ATP 1.5 to 19 seconds (Fisher Scientific 312 nm UV handlamp) (Biswas and Kornberg, 1984). Subunits were separated by SDS-PAGE, ^{32}P labeling quantified using a phosphoimager (Storm 840, Molecular Dynamics) and data fit to a binding quadratic using Dynafit (Biokin Ltd., Pullman, WA) to obtain dissociation constants.

3.3.4 HPLC

Arp2/3 in KMEI plus 100 μM ATP was exchanged into KMEI plus 50nM, 1.4 μM or 10 μM ATP using a PD-10 buffer-exchange column (Amersham Pharmacia Biotech) Exchange took less than 2 minutes and flow-through was collected in 150 μL fractions. Arp2/3 concentration was determined by A290 (7.14 μM / OD). The peak fraction (~5 μM) was heat denatured and buffer plus released nucleotide was separated from denatured protein by filtration through a 10 kD MWCO filter (UltraFree-MC, Millipore, Bedford, MA). Nucleotide was quantified by HPLC in

75mM KH$_2$PO$_4$ pH 4.0, 1.5mM Tetrabutylammonium phosphate, 12% Methanol on a C18 column (Waters DeltaPak 15 μM 100A 300 × 3.9 mm; Waters Corporation, Milford, MA) at 1 ml / minute (Childs et al., 1996). The concentration of nucleotide in the column buffer was subtracted from that in the sample and this was divided by the Arp2/3 concentration to calculate the number of bound nucleotides per complex. For the N-WASP WA condition, the PD-10 column was pre-equilibrated in 25 μM N-WASP WA, and 25 μM N-WASP WA was added to the Arp2/3 before loading onto the column.

3.3.5 Etheno-ATP affinity measurement

Free nucleotide was removed from Arp2/3 by 4 treatments with 5% Dowex resin. Etheno-ATP fluorescence was measured (λ_{ex} = 340 nM, λ_{em} = 420 nM) for 100 μL KMEI + 0.8 μM Arp2/3 + 30 μM etheno-ATP + 200 mM acrylamide (as a dynamic quencher (Rosenfeld and Taylor, 1984)). This solution was serially diluted with 50% volumes of 0.8 μM Arp2/3 + 200 mM acrylamide in KMEI to titrate down etheno-ATP concentrations. Etheno-ATP + Arp2/3 fluorescence was linear with etheno-ATP concentration, for concentrations greater than 10 μM, and we fit this linear portion of the data to $f = a + b[\text{eATP}]$ to find b, the contribution of unbound etheno-ATP to the measured fluorescence. We subtracted background protein fluorescence and free etheno ATP fluorescence from the measured fluorescence to obtain the enhancement due to etheno ATP binding and data fit to the binding quadratic to obtain dissociation constants.

3.3.6 Measurement of ATP Hydrolysis

We determined steady-state ATP hydrolysis rates at 25° C in KMEI buffer. Arp2/3 was used at 4.4 μM, N-WASP WA at 25 μM, F-actin at 15 μM. Free nu- cleotide was removed from Arp2/3 by 2 treatments with 5% Dowex resin and Arp2/3 was brought up to room temperature. 50 μCi of $[\alpha^{32}P]$ATP and 500 μM ATP concentrations were added to start the reaction. 5 μL aliquots were quenched with equal volumes of 5M formic acid at timepoints shown, spotted on polyethyleneimine- cellulose TLC plates and separated by chromatography with 0.6M KH_2PO_4 pH 3.4. $[\alpha^{32}P]$ATP and product $[\alpha^{32}P]$ADP were quantified using a phosphorimager and normalized by the starting ATP concentration.

3.3.7 Kinetic Assays

We measured the time course of nucleotide release from Arp2/3 by the in- crease in fluorescence intensity of etheno-ATP (λ_{ex} = 360 nM, λ_{em} > 389 nM) on binding to Arp2/3 using a hand-operated rapid mixer (SFA-20; HiTech Scientific, Salisbury, UK) and fluorimeter (K2; ISS, Champange, IL). Samples were excited at 360 nM, and emission measured at >389 nM using a long pass filter (KV389; Schott Glass Technologies, Duryea, PA). We used 1-2 μM Arp2/3 in KMEI buffer, treated 2x with 5% Dowex just before use to remove free nucleotide. For ATP, ADP and AMP off rate measurements, 100 μM nucleotide was added to the buffer, excess removed once more using Dowex and 5 μM nucleotide added immediately before use. The dissociation rate for nucleotide was measured by competing off

the bound nucleotide with 50 µM etheno-ATP. Fluorescence data were analyzed

by non-linear least squares fitting to a single exponential function.
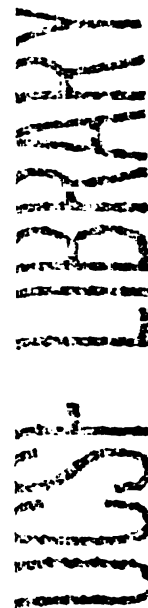
3.3.8 Polarization Anisotropy

N-WASP WA (398–501) was labeled on cysteine 427 in 2 mM HEPES 500mM

KCl plus 4-fold molar excess of rhodamine maleimide (Molecular Probes, Eugene,

OR) overnight at 4° C. The sample was centrifuged at 350,000 g for 20 minutes

and the supernatant gel filtered on a Sephacryl S-300 column to remove free dye

and denatured protein. ActA (30–170) was labeled as in Zalevsky et al. (Zalevsky

et al., 2001a). By this procedure, proteins were ~25% labeled as determined by

A280 and A554. Polarization anisotropy was measured for 250nM labeled protein

in the presence of various concentrations of Arp2/3 in KMEI plus 1mM nucleotide

(ATP, ADP or AMP-PNP), and Arp2/3 concentration was titrated by serial dilution.

Relative affinities of labeled and unlabeled protein were measured by monitoring

anisotropy of labeled protein in competition with unlabeled protein. Labeled N-

WASP WA was determined to bind 4-fold tighter than unlabeled N-WASP WA in

the presence of ATP and ADP. Anisotropy data was fit to a model accounting for

fraction of unlabeled protein and their different affinities using Dynafit (Biokin

Ltd., Pullman, WA).

3.3.9 Actin Polymerization Assays

Acanthamoeba actin doped with 10% pyrene labeled actin was used to mon-

itor actin polymerization by fluorescence (λ_{ex} = 365 nM, λ_{em} = 407 nM) (Cooper and

Pollard, 1982; Mullins and Machesky, 2000). ATP- and ADP-Actin were prepared on ice by incubating in respective nucleotides for >10 minutes before briefly treating twice with 5% Dowex resin to remove unbound nucleotide. Polymerization reactions were performed at room temperature. We started seeded polymerization assays by mixing pre-polymerized filamentous actin seeds in 1.1× KMEI plus 110 µM nucleotide with 10 µL ATP- or ADP-actin. Arp2/3 nucleated polymerization was started by mixing 90 µL of 11nM Arp2/3 plus 1.2 µM N-WASP WA plus 110 µM nucleotide in 1.1× KMEI (+/- filamentous actin seeds) with 10 µL doped ATP- or ADP-actin. Kinetic modeling was done using the Macintosh version of Berkeley Madonna (Robert Macey, Tim Zahnley, and George Oster, University of California, Berkeley)

3.4 RESULTS AND DISCUSSION

3.4.1 The Arp2 and Arp3 subunits of the Arp2/3 complex bind nucleotide with micromolar affinity

To identify the subunits of Arp2/3 complex that bind nucleotide we crosslinked the radiolabeled photo-reactive ATP derivative[α^{32}P] Azido-ATP to Arp2/3 complex using ultraviolet light. For short crosslinking times, Arp2 is preferentially labeled, and for longer crosslinking times labeled Azido-ATP specifically crosslinks to both the Arp2 and Arp3 subunits (Figure 3.1A). This supports the prediction of Kelleher et al. that Arp2 and Arp3 contain nucleotide binding sites similar to the nucleotide binding pocket of conventional actin (Kelleher et al., 1995).

We measured the affinity of Arp2/3 for nucleotide by three methods, UV crosslinking, etheno-ATP fluorescence and nucleotide dissociation kinetics, and obtained essentially identical results. Radiolabeled nucleotides lacking the photoreactive azido group can be crosslinked to both Arp2 and Arp3 but with greatly reduced crosslinking efficiency. We measured the affinities of each of the actin related proteins to ATP by analysis of the photocrosslinking with[α^{32}P] ATP. This is possible because photo-crosslinking with ATP crosslinks only a small fraction of the total protein (see Supplementary Material). We crosslinked [$\alpha-^{32}$P] ATP to Arp2/3 with ultraviolet light and quantified labeling of Arp2 and Arp3 with increasing concentrations of [α^{32}P] ATP to construct a binding isotherm (Figure 3.1B,C). At saturation, Arp2 labels only 20% as strongly as Arp3, presumably reflecting a lower relative crosslinking efficiency because of different amino acid

A [α³²P] Azido-ATP photocrosslinking

AR
CB 0.5" 1.5" 2.5" 3.5" 6" 9" 14" 19"

Arp3
Arp2

B [α³²P] ATP photocrosslinking
Coomassie   Autoradiogram

Arp3
Arp2

Arp2/3   Arp2/3+NW   Arp2/3   Arp2/3+NW

D

εATP fluorescence increase (a.u.)

Arp2/3 + N-WASP WA

Arp2/3

[εATP] (μM)

C

[α³²P] ATP labelling (a.u.)

Arp3

Arp3 + N-WASP WA

Arp2

Arp2 + N-WASP WA

[ATP] (μM)

E

EthenoATP fluorescence (a.u.)

Arp2/3 + N-WASP WA

Arp2/3

Residuals

time (s)
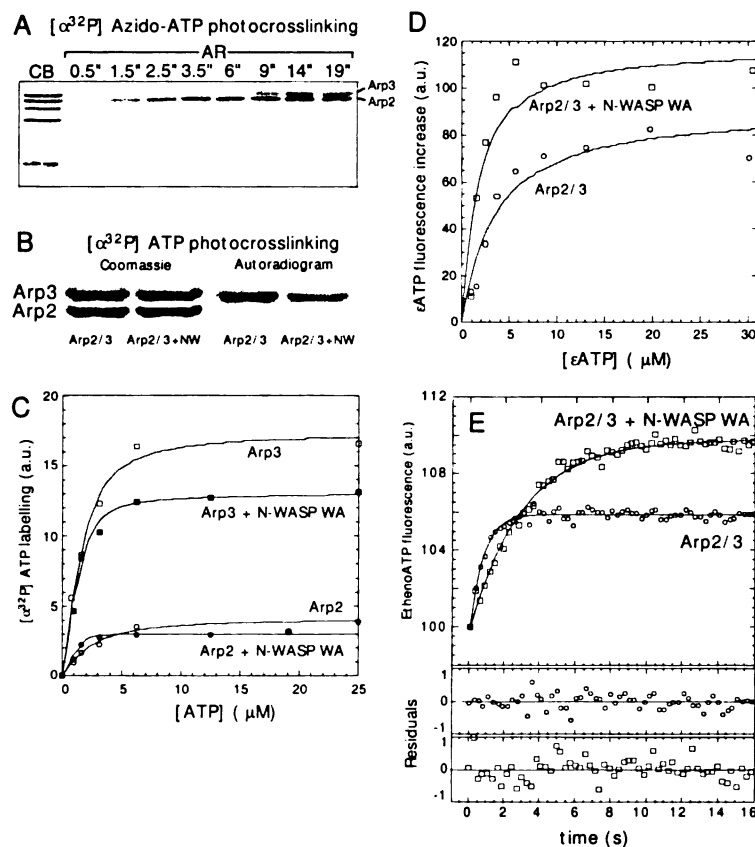
Figure 3.1: **Both the Arp2 and Arp3 subunits of the Arp2/3 complex bind nucleotide with micromolar affinity(A)** Ultraviolet crosslinking of 5 μM [α³²P] Azido-ATP to 1 μ M Arp2/3 shows both Arp2 and Arp3 bind nucleotide and that [α³²P] Azido-ATP crosslinking efficiency is greater on Arp2. **(B)** Crosslinking of ATP doped with [α³²P]ATP to 2 μM Arp2/3 using UV light. In the presence of 100 μM ATP radiolabeling occurs mainly on Arp3 with less efficient labeling on Arp2 both in the absence and presence of 25 μM N-WASP. **(C)** Quantitation of (B) for a range of ATP concentrations fit to the binding quadratic to obtain dissociation constants: Arp3 K_d = 0.6 μM, Arp2 K_d = 1.3 μM Arp3+N-WASP K_d = 0.25 μM, Arp2+N-WASP K_d= 0.5 μM. **(D)** We measured the affinity of Arp2/3 for etheno-ATP by monitoring fluorescence enhancement due to binding. Etheno-ATP fluorescence increase was measured for a range of etheno-ATP concentrations in the presence of a constant concentration of Arp2/3 by subtracting the contribution of free etheno-ATP fluorescence from the total measured intensity. Arp2/3 alone binds etheno-ATP with an affinity of 3.1 μM and N-WASP-Arp2/3 binds etheno-ATP with an affinity of 1.3 μM. **(E)** ATP dissociation kinetics. In 5 μM ATP, nucleotide was driven from 1 μM Arp2/3 by mixing with 50 μM etheno-ATP and binding kinetics measured by fluorescence enhancement of etheno-ATP on binding. k_{off} Mg^{2+}ATP = $2.6s^{-1}$. Dissociation slows in the presence of N-WASP k_{off} Mg^{2+}ATP = $0.7s^{-1}$ and fluorescence of etheno-ATP approximately doubles.

| Nucleotide | Arp2/3 | | Arp2/3 + N-WASP | | |
	k_{off} (s^{-1})	K_d (μM)	k_{off} (s^{-1})	K_d (μM)	Method
ATP	2.6	0.5*	0.7	0.15*	Stopped Flow
ATP(Arp2)		0.6		0.25	32P UV Crosslinking
ATP(Arp3)		1.3		0.5	32P UV Crosslinking
ADP	0.7	0.14	0.3	0.06*	Stopped Flow
EthenoATP		3.1		1.3	Fluorescence

* Equilibrium constants calculated assuming k_{on} = 5 $\mu M^{-1}s^{-1}$. (De La Cruz and Pollard, 1995)

Table 3.1: **Kinetic and equilibrium constants of Arp2/3 complex for adenosine nucleotides at 25°C**

residues contacting the nucleotide (Bai et al., 1998). From this binding isotherm we determined that Arp3 binds ATP with a K_d of 0.6 μM and Arp2 with a K_d of 1.3 μM (Figure 3.1C; Table 3.1). In the presence of the Arp2/3 activator N-WASP WA, the nucleotide affinity increases approximately 3-fold on both subunits to 0.25 μM on Arp3 and to 0.5 μM on Arp2. In addition, the efficiency of Arp3 labeling decreases in the presence of N-WASP WA suggesting that it induces a change in the structure of the nucleotide binding pocket.

We also measured the affinity of the entire Arp2/3 complex for the fluorescent nucleotide analog, etheno-ATP by monitoring the increase in etheno-ATP fluorescence upon binding to Arp2/3 complex (Figure 3.1D). Consistent with the UV crosslinking results etheno-ATP binds Arp2/3 with an affinity of 3.1 μM and the affinity increases to 1.3 μM in the presence of N-WASP WA. There is also an increase in the magnitude of the etheno-ATP fluorescence change in the presence of N-WASP WA, further evidence that N-WASP alters the structure of the nucleotide binding pocket of Arp2 and/or Arp3. To test this hypothesis we added 1.0 μM

etheno-ATP to 6 μM nucleotide free Arp2/3 complex. Under these conditions 90% of the etheno-ATP will be bound to Arp2/3. Subsequent addition of N-WASP increased etheno-ATP fluorescence a further 2-fold (unpublished observations), indicating that the fluorescence enhancement is due entirely to a change in the local environment of the nucleotide. The binding of N-WASP WA has been shown to cause a conformational change on Arp2/3 complex (Zalevsky et al., 2001b). We would expect that a conformational change might alter the residues that contact the adenosine ring of ATP or the etheno group of etheno-ATP. Such changes would explain the observed changes the efficiency of crosslinking of [α^{32}P] ATP and the degree of fluorescence enhancement for etheno-ATP.

We measured the dissociation rates for non-fluorescent nucleotides by competing off bound unlabeled nucleotide with etheno-ATP (Figure 3.1E), and assuming association rate constants equal to actin (De La Cruz and Pollard, 1995) calculated the dissociation rate constants summarized in Table 3.1. Arp2/3 binds Mg^{2+}ATP with an affinity of 0.5 μM, 400 times less tightly than actin binds Mg^{2+}ATP (1.2 nM (De La Cruz and Pollard, 1995)), and binds Mg^{2+}ADP 3-fold tighter than it binds Mg^{2+}ATP. In the presence of N-WASP, the affinity for ATP increases and we note an enhancement of the fluorescence change of approximately 2-fold.

The efficiency of UV crosslinking of ATP and the fluorescence of etheno-ATP change upon binding of N-WASP to Arp2/3. To be certain that the number of nucleotides bound is the same in the presence and absence of N-WASP WA, we

| | Stoichiometry of bound nucleotide | | | | |
| | Measured | | | Normalized to actin | |
Exchange buffer	Actin ($n = 4$)	Arp2/3	Arp2/3 +N-WASP	Arp2/3	Arp2/3 +N-WASP
No added ATP		0.24	0.21	0.45	0.4
1.4 μM ATP		0.76	0.83	1.4	1.6
10.0 μM ATP	0.53	1.2	1.1	2.3	2.1

Table 3.2: **Number of nucleotides bound per Arp2/3 complex.** We investigated the total number of nucleotides bound to the Arp2/3 complex by using a buffer-exchange column to rapidly exchange the Arp2/3 complex into a low concentration of ATP and measure the total nucleotide present. We heat-denatured the Arp2/3 complex to release bound nucleotide into solution, removed protein by filtration through a 10-kD MWCO filter, and analyzed nucleotide content of the filtrate by HPLC, subtracting the contribution caused by buffer alone. To correct for systematic error, results were normalized to actin.

used HPLC to quantitate the total amount of nucleotide bound by the complex

(Table 3.2). In buffer containing enough free ATP to saturate both the binding

sites (10 μM), Arp2/3 complex binds more than one nucleotide per complex and

this number does not change in the presence or absence of N-WASP WA.

3.4.2 Bound nucleotide controls the affinity of the Arp2/3 complex for its upstream activators

Arp2/3 complex binds its activators NWASP WA and ActA 3–4 fold more

tightly in saturating concentrations of ATP than in ADP (Figure 3.2). Rapid re-

lease of Arp2/3 complex from its activators is a general requirement for efficient

motility. In the case of *Listeria* motility the Arp2/3 activator, ActA, is perma-

nently attached to the bacterium while the Arp2/3 complex remains part of the

actin network which treadmills away from the bacterium surface during motility.

High resolution positional measurements (Kuo and McGrath, 2000) suggest that the speed of *Listeria* movement is limited by release of attachments between the bacterium and actin filaments in the tail. We know of two such attachments (1) via VASP and (2) via the Arp2/3 complex. VASP binds to the sides of filaments with 10nM affinity (Laurent et al., 1999) and to ActA with ~10 μM affinity (Ball et al., 2000). The Arp2/3 complex binds to the pointed ends of new filaments with 10–50 nM affinity (Mullins et al., 1998) and to ActA with an affinity of 0.6 μM (Zalevsky et al., 2001a). If these are the only connections between the bacterium and the actin comet tail, ActA binding to ATP-Arp2/3 would be the rate-limiting interaction. If the ATP on Arp2/3 complex is hydrolyzed to ADP upon nucleation, ActA would bind the Arp2/3 complex 4-fold less tightly (Figure 3.2, inset) and its effect on motility would be decreased. This could be a mechanism to allow an Arp2/3 activator to bind and recruit the Arp2/3 complex with high affinity and then release it before the binding retards motility. We propose that the same may be true for the endogenous WASP-family proteins. WASP and N-WASP associate with the membrane-anchored G-protein Cdc42 and the affinity of N-WASP for Arp2/3 complex also depends on the bound nucleotide (Figure 3.2). Although these proteins are not permanently membrane-anchored like the transmembrane ActA protein, we hypothesize that these upstream activators remain at the membrane after activating Arp2/3 complex, released by a decrease in affinity after nucleotide hydrolysis.
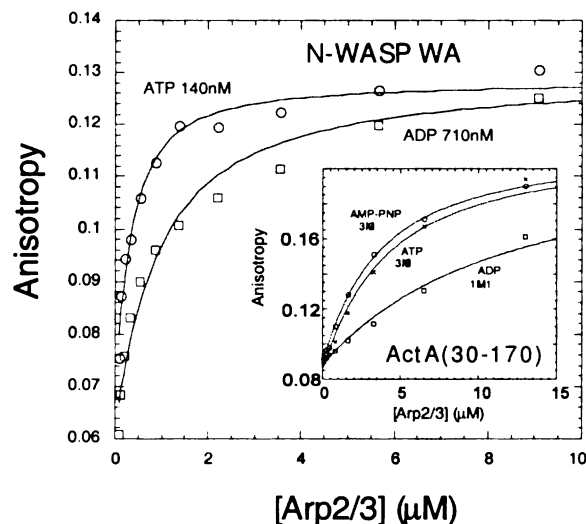
Figure 3.2: **The affinity of N-WASP and ActA for Arp2/3 depends on the bound nucleotide.** We used polarization anisotropy to measure the affinity of nucleation promoting factors to Arp2/3 in the presence of 1mM ATP, ADP, and AMPPNP. 250nM rhodamine ActA (30-170) binds Mg^{2+}ATP-Arp2/3 with k_d of 3.5μM, Mg^{2+}ADP-Arp2/3 with k_d of 11.1μM and MgAMP-PNP-Arp2/3 with k_d of 3.0μM Inset: 250nM Rhodamine N-WASP WA binds Mg^{2+}ATP-Arp2/3 with k_d of 140nM and Mg^{2+}ADP-Arp2/3 with k_d of 710nM.

3.4.3 The Arp2/3 complex requires hydrolyzable ATP to nucleate new actin filaments

We carried out pyrene-actin polymerization assays to test the ability of N-WASP stimulated Arp2/3 complex to nucleate new filaments when bound to different nucleotides or nucleotide analogues. Because actin itself binds nucleotide, we needed to be certain that we were observing an effect of nucleotide on Arp2/3 nucleation and not an effect that nucleotide in solution might have on actin polymerization. We therefore measured the elongation of 2 μM Mg^{2+}ATP-actin with no free ATP from phalloidin-stabilized actin seeds in the presence of 100 μM ATP, ADP and AMP-PNP (Figure 3.3A). Kinetics of polymerization are independent of added

nucleotide within the first 100 seconds of starting the reaction, but diverge soon after this, because of the exchange of nucleotide on the monomeric actin with nucleotide in solution (Selden et al., 1999). Therefore, in subsequent experiments with Arp2/3 we limited our observations to the first 100 seconds of the reaction. We used N-WASP WA at 3 times its saturating concentration for ATP-Arp2/3 to be certain that we were not simply seeing an effect of nucleotide on N-WASP affinity. As expected in this 100 second time window ATP-Arp2/3 activated by N-WASP WA rapidly nucleates new actin filaments (Figure 3.3B). ADP-Arp2/3 cannot nucleate new filaments, but we were able to partially restore nucleation activity by adding BeF$_3$ to simulate an ADP-Pi state (Figure 3.3B) (Combeau and Carlier, 1988; Orlova and Egelman, 1992). We also found that Arp2/3 complex bound to the non-hydrolyzable ATP analog, AMP-PNP, is unable to nucleate new filaments (Figure 3.3B). This is consistent with our previous results showing that G-protein stimulated, Arp2/3-dependent actin polymerization in amoeba extracts requires hydrolyzable ATP (Mullins and Pollard, 1999a). AMP-PNP appears to be a good mimic of ATP for Arp2/3 complex, as both AMP-PNP-Arp2/3 and ATP-Arp2/3 have similar affinities for ActA (30–170), 3–4 fold higher than that of ADP-Arp2/3. These data suggest that both the ADP- and ATP-bound forms of the complex are inactive. We conclude that the ADP-Pi state of Arp2/3 complex, reached either through hydrolysis of ATP, or mimicked by adding BeF$_3$ to ADP, is the active nucleating form of Arp2/3 complex.

(A) Polymerization from F-actin seeds

ATP buffer

AMPPNP buffer

ADP buffer
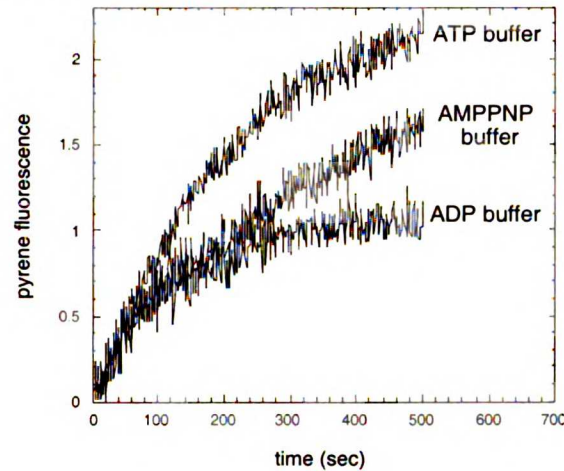
(B) Arp2/3 nucleated polymerization

ATP

ADP +BeF$_3$

AMPPNP

ADP
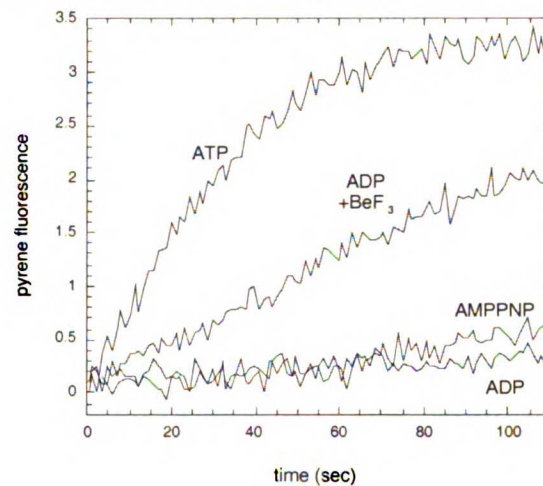
Figure 3.3: **Actin nucleation by Arp2/3 requires ATP hydrolysis**. **(A)** We tested elongation of 2 μM Mg^{2+}ATP-actin from F-actin seeds in the presence of 100 μM ATP, ADP and AMP-PNP. Kinetics of polymerization are independent of solution nucleotide within the first 100 seconds of starting the reaction, but diverge soon after this, because of the exchange of nucleotide with solution. We therefore limited our observations to the first 100 seconds when using ATP-actin. **(B)** Arp2/3 induces polymerization of Mg^{2+}ATP-actin in the presence of ATP, or ADP-BeF$_3$ but not AMP-PNP or ADP. We used the fact that nucleotide in solution exchanges onto Arp2/3 within seconds (Figure 1E), but takes much longer to exchange onto actin monomers to load one type of nucleotide onto Arp2/3, but keep ATP bound to actin. We mixed 2 μM Mg^{2+}ATP-actin with a solution of 10nM Arp2/3 and 1.2 μM N-WASP WA (3-fold above saturating concentration) with 100 μM ATP, ADP, ADP + 2mM BeF$_3$ or AMP-PNP.

3.4.4 The hydrolysis of ATP by Arp2/3 complex can account for the first-order activation step in Arp2/3-dependent actin assembly

We propose that the Arp2/3 complex must hydrolyze ATP to nucleate a new filament. Marchand et al. (2001) and Zalevsky et al. (2001a) noticed that affinity of wild type and mutant WASP family proteins for Arp2/3 complex does not correlate with ability to activate Arp2/3 and suggested that some further activation step(s) must occur between activator binding and filament nucleation (Marchand et al., 2001). ATP hydrolysis may be the rate-limiting activation step in nucleation. ATP hydrolysis is a first-order reaction and we can incorporate this hydrolysis step into a kinetic scheme for filament formation:

$$F + A_{ATP} + N + G \overset{k_a}{\rightleftharpoons} F.A_{ATP}.N.G \overset{k_{hyd}}{\rightarrow} F.A_{ADP-Pi}.N.G$$

where F is F-actin, A is Arp2/3 complex, N is N-WASP, G is G-actin and the F.A$_{ADP-Pi}$.N.G form is the active nucleus. We fixed the association constants for the components in the reaction (here grouped together as k_a) to previously determined values (Mullins et al., 1998). We fit this scheme to polymerization data collected during N-WASP stimulated pyrene-actin polymerization experiments and calculated the hydrolysis rate, k_{hyd} for Arp2/3 complex during the polymerization reaction to be 0.02 s^{-1}. To achieve this ATP hydrolysis rate, Arp2/3 complex must be stimulated by some combination of filamentous actin, monomeric actin and N-WASP.

3.4.5 N-WASP and F-actin do not stimulate ATP hydrolysis by Arp2/3 complex

To investigate the basal ATP hydrolysis rate of the Arp2/3 complex we incubated Arp2/3 complex with 500 μM ATP doped with [α^{32}P]-ATP and quantified the amount of [α^{32}P]-ADP produced over time by thin layer chromatography. We were unable to detect ATP hydrolysis within the limits of our measurement, suggesting that the basal Arp2/3 complex ATP hydrolyses rate is less than 0.1×10^{-3} s^{-1}(data not shown). We could not use the TLC method to directly measure the ATPase rate of Arp2/3 complex in the presence of F-actin, N-WASP and actin monomers, because the actin monomers themselves hydrolyze ATP as they polymerize. We measured Arp2/3 complex ATPase activity in the presence of N-WASP and F-actin in the absence of the actin monomers but found no significant ATPase activity above control levels (data not shown). Since adding F-actin and N-WASP to Arp2/3 complex does not change the hydrolysis rate, we suggest that actin monomers must be required to stimulate Arp2/3 complex ATPase activity. All Arp2/3 complex activators that promote rapid nucleation contain actin monomer-binding WH2 domains in close proximity to an Arp2/3 binding domain. We suggest the role of the WH2 domain may be to place a monomer in contact with a filament-bound Arp2/3 complex and stimulate ATP hydrolysis. Hydrolysis of ATP to an ADP-Pi state could then cause a conformational change that allows Arp3 to associate with Arp2 to form a nucleus.

3.4.6 Model for ATP hydrolysis and nucleus formation

Based on our data, we propose a model relating Arp2/3 ATPase activity to its actin filament nucleation activity (Figure 3.4) **Step 1**: Arp2/3 complex binds to the activator, with high affinity because Arp2/3 complex is ATP-bound. Binding N-WASP brings the actin monomer attached to the WH2 domain of N-WASP in contact with the Arp2/3 complex, and this stimulates ATP hydrolysis. **Step 2**: Hydrolyzing ATP to ADP-Pi causes a conformational change on the complex forming a stable nucleus between Arp3, Arp2 and the conventional actin monomer. **Step3**: A new actin filament polymerizes from this nucleus. **Step 4**: Phosphate release from Arp2/3 decreases the affinity for N-WASP and allows the Arp2/3 complex to release its membrane-associated activator.
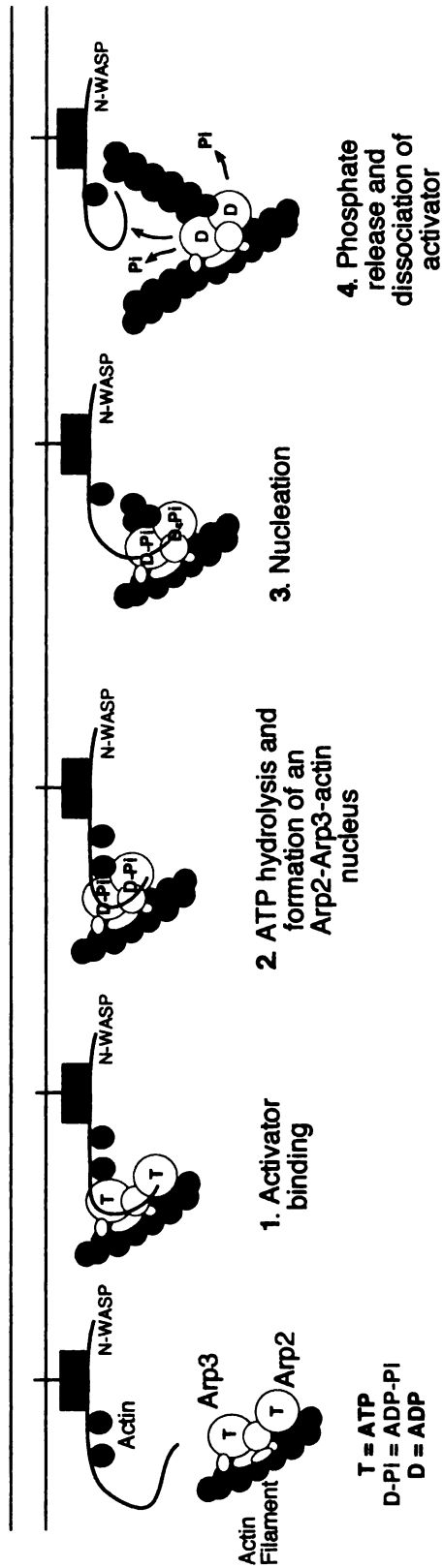
Figure 3.4: **Model for the role of Arp2/3 nucleotide binding and hydrolysis in the formation of new actin filaments. Step 1:** Arp2/3 complex binds to the activator, in this case N-WASP, with high affinity because Arp2/3 complex is ATP-bound. Binding N-WASP brings the actin monomer attached to the WH2 domain of N-WASP in contact with the Arp2/3 complex, and this stimulates ATP hydrolysis. **Step 2:** Hydrolyzing ATP to ADP-Pi causes a conformational change on the complex forming a stable nucleus between Arp3, Arp2 and the conventional actin monomer. **Step3:** A new actin filament polymerizes from this nucleus. **Step 4:** Phosphate release from Arp2/3 decreases the affinity for N-WASP and allows the Arp2/3 complex to release its membrane-associated activator.

Chapter 4

Mechanism of Arp2/3 complex activation: WASP family proteins mediate the addition of the first actin monomer of the daughter filament, triggering rapid ATP hydrolysis on Arp2

Mark J. Dayel and R. Dyche Mullins.

4.1 ABSTRACT

In response to activation by WASP family proteins, the Arp2/3 complex nucleates new actin filaments from the sides of pre-existing filaments. The Arp2/3-activating (VCA) region of WASP family proteins binds both the Arp2/3 complex and an actin monomer. The Arp2 and Arp3 subunits of the Arp2/3 complex bind ATP and we show that Arp2 hydrolyzes ATP rapidly—with no detectable lag—upon nucleation of a new actin filament. Filamentous actin and VCA, together, do not stimulate ATP hydrolysis on the Arp2/3 complex, nor do monomeric and filamentous actin in the absence of VCA. Actin monomers bound to the marine macrolide Latrunculin B do not polymerize but, in the presence of phalloidin-stabilized actin filaments and VCA, they stimulate rapid ATP hydrolysis on Arp2. These data suggest that ATP hydrolysis on Arp2/3 complex is stimulated by interaction with a single actin monomer, and that the interaction is co-ordinated by VCA. We show that capping of filament pointed ends by the Arp2/3 complex (which occurs even in the absence of VCA) also stimulates rapid ATP hydrolysis on Arp2, identifying the actin monomer which stimulates ATP hydrolysis as the first monomer at the pointed end of the daughter filament. We conclude that WASP-family VCA domains activate the Arp2/3 complex by driving its interaction with a single conventional actin monomer to form an Arp2-Arp3-actin nucleus. This actin monomer becomes the first monomer of the polymerizing the daughter filament.

4.2 INTRODUCTION

The actin cytoskeleton determines the shape, mechanical properties, and motility of most eukaryotic cells. To change shape and to move, cells precisely control the location and timing of actin filament assembly by regulating the number of fast-growing (barbed) filament ends (Pollard et al., 2000). The Arp2/3 complex, a seven-subunit protein complex that contains two actin-related proteins, generates these new barbed ends in response to cellular signals (Machesky et al., 1999; Rohatgi et al., 1999; Welch et al., 1998). In a process called 'dendritic nucleation', the Arp2/3 complex nucleates new actin filaments from the sides of pre-existing filaments to produce a rigid and highly crosslinked filament array (Blanchoin et al., 2000a; Machesky et al., 1999; Mullins et al., 1998). Such crosslinked arrays form the core of many motile cellular structures, including the leading edges of amoeboid cells and the actin comet tails that propel endosomes and bacterial pathogens through eukaryotic cytoplasm. To understand the construction, function, and regulation of these structures, it is important to understand the molecular mechanism of Arp2/3 activation.

Arp2/3 must be activated by both a WASP family protein and a pre-existing actin filament before it will nucleate a new actin filament (Blanchoin et al., 2001; Machesky et al., 1999; Zalevsky et al., 2001b). The structure and the orientation of the Arp2 and Arp3 subunits within the crystal structure of the complex suggest that these subunits may nucleate a new filament by forming an actin-like heterodimer that mimics the barbed end of an actin filament (Robinson et al.,

2001). In the crystal structure of the unactivated complex, however, Arp2 and Arp3 are separated by 40Å so that formation of an actin-like dimer would require a conformational change (Robinson et al., 2001). Binding of the Arp2/3 complex to both a preformed filament and a WASP-family protein is thought to drive at least part of this conformational change (Blanchoin et al., 2001; Marchand et al., 2001; Panchal et al., 2003). The Arp2/3-activating region of WASP-family proteins is composed of three sequences arranged in tandem: (1) an actin-binding verprolin-homology (or V) domain (also known as a WASP-homology 2 or WH2 domain), (2) a conserved 'connecting' (or C) region that interacts with both Arp2/3 complex and monomeric actin (Marchand et al., 2001) and (3) an acidic (or A) region that binds the Arp2/3 complex. This 'VCA' domain is both necessary and sufficient for efficient Arp2/3 activation. We and others have previously suggested that an actin monomer provided by the VCA domain to the Arp2/3 complex may drive the formation of an Arp2-Arp3-actin hetero-trimer and form a nucleus for actin polymerization (Dayel et al., 2001; Marchand et al., 2001).

Both the Arp2 and Arp3 subunits of the complex bind ATP (Dayel et al., 2001). Hydrolysis of this ATP could be used to perform work, to provide a signal, or, like the GTP bound to the beta subunit of tubulin heterodimers, may simply stabilize a protein fold. On conventional actin, ATP hydrolysis is a timing mechanism that promotes construction of dynamic and polarized filament networks. Actin rapidly hydrolyses ATP upon polymerization (Blanchoin and Pollard, 2002) and releases bound phosphate several hundred seconds later (Melki et al.,

1996). ATP hydrolysis and phosphate dissociation do not cause immediate filament disassembly, but enable interaction with depolymerizing factors like cofilin (Blanchoin and Pollard, 1999). ATP hydrolysis by actin thereby determines the overall rate of filament turnover.

We show here that the Arp2/3 complex rapidly hydrolyzes ATP on the Arp2 subunit upon filament nucleation, and that phosphate release follows hydrolysis with a half-time of 40 seconds. There are several events in the Arp2/3 nucleation reaction that might trigger ATP hydrolysis on Arp2: (1) binding of N-WASP VCA to Arp2/3, (2) binding of VCA-Arp2/3 to the side of a preformed filament, (3) binding of a VCA-tethered actin monomer to the Arp2/3 complex, or (4) binding of a second or third actin monomer to form a stable daughter filament. We find that ATPase activity requires the combination of a preformed actin filament, a VCA domain and an actin monomer, but does not require actin polymerization. This indicates that hydrolysis is triggered relatively early in the nucleation reaction— before completion of a stable daughter filament. Capping the pointed ends of actin filaments also stimulates Arp2 to rapidly hydrolyze ATP, in the absence of monomeric actin and VCA and without branch formation. Thus ATP hydrolysis on Arp2 is stimulated directly by interaction with conventional actin: either presented to the complex as a monomer attached to the VC domain of the WASP family protein, or as the pointed end of a pre-formed filament. This is the first direct evidence that the monomer supplied by the VCA domain is the first monomer

of the new daughter filament. From these observations we propose a model for

the mechanism of Arp2/3 complex activation by WASP family proteins.

4.3 MATERIALS AND METHODS

4.3.1 Purification of proteins

We purified Arp2/3 from *Acanthamoeba castellini* by a combination of conventional and affinity chromatography (Dayel et al., 2001). We flash-froze Arp2/3 complex in aliquots of ~40 μM in 10% glycerol, 0.5 μM TCEP, 2mM Tris pH 8.0 and stored them at -80°C for later use. We purified actin from *Acanthamoeba* by the method of MacLean-Fletcher and Pollard.(MacLean-Fletcher and Pollard 1980). Actin was stored in fresh G-buffer (0.5 μM TCEP, 0.1 μM CaCl₂, 0.2 μM ATP, 2mM Tris pH 8.0) and gel-filtered before use. Rat N-WASP-VCA (398–502) and Human Scar1-VCA (489–559) with N-terminal 6His tags and TEV cleavage sites were bacterially expressed and purified by nickel affinity chromatography.

We prepared phalloidin-stabilized actin filaments by adding 1/10 volume of 10x KMEI to monomeric actin at room temperature for 20 minutes to initiate polymerization then adding twice the concentration of phalloidin and incubating for a further hour at room temperature. (1× KMEI buffer: 50 mM KCl, 1 mM MgCl₂, 1 mM EGTA, 10 mM Imidazole, pH 7.0.) We took care not to unintentionally shear the phalloidin-stabilized actin filaments by using wide-bore pipette tips.

4.3.2 Arp2/3 ATPase assay

We diluted freshly thawed aliquots of Arp2/3 to 2.0 μM in 1 mM MgCl₂, 50 mM KCl, 10 mM Imidazole pH 7.0 and added 6 μM γ^{32}P labeled 8-AzidoATP (Affinity Labeling Technologies, Lexington, KY). After a two-minute incubation to

allow nucleotide exchange we crosslinked for 10 seconds using a UV hand lamp (Fisher Scientific 312 nM), added 1 mM ATP and 1 mM DTT to quench the reaction and buffer exchanged into 1X KMEI + 100 µM ATP, 1mM DTT using a NAP5 column (Amersham Pharmacia Biotech). We used the Arp2/3 for assays within 10 minutes of crosslinking. The same actin (including 7% pyrene-actin) was used for both ATP hydrolysis assays and correlative pyrene-fluorescence polymerization assays. We took ATPase time points by mixing 400uL of the reaction mixture with pre-mixed 400uL methanol and 100uL chloroform. We ran the precipitated protein on SDS-PAGE gel to separate the subunits and quantified ^{32}P labeling using a phosphoimager (Storm 840, Molecular Dynamics). For phosphate cleavage assays, we quenched timepoints into 1/10 volume 26 M Formic acid, spotted on cellulose TLC plates and separated components in 0.4 M KH_2PO_4 pH 3.4. We separately ran ^{32}P-ATP and ^{32}P-ATP treated with apyrase as standards to confirm the separation of ^{32}P-ATP and cleaved ^{32}P respectively (unpublished observations). As an alternative method of quantifying cleaved ^{32}P, phosphomolybdate was extracted as in Shacter (1984) and quantified using a scintillation counter. To distinguish the ADP-Pi state of Arp2 from the ADP state, the kinetics of phosphate release were measured by performing the reaction in the presence of 2 mM maltose and 2 U/ml maltose phosphorylase (Sigma-Aldrich) which uses only the released Pi to form glucose phosphate. Glucose phosphate was separated from free ATP, protein-ATP and Pi using TLC.

4.3.3 Actin Polymerization Assays

We doped Acanthamoeba actin with 7% pyrene labeled actin to monitor actin polymerization by fluorescence (λ_{ex} = 365 nM, λ_{em} = 407 nM, 25°C) (Mullins and Machesky, 2000). We calculated the number of ends produced over time from [ENDS] = $\frac{\frac{d}{dt}[\text{F-actin}]}{[\text{free G-actin}]}$ × 10 μMs^{-1} (c.f. Zalevsky et al. (2001b)). Polymerization reactions were performed in G-buffer + 1/10 volume 10× KMEI. The Ca^{2+} cation on monomeric actin was pre-exchanged with Mg^{2+} 30 s before use.

4.3.4 Microscopy

We prepared filamentous actin as above and stabilized filaments with stoichiometric Alexa-488 phalloidin (Molecular probes). We mixed 2 μM Alexa-488-phalloidin-F-actin with 20nM Arp2/3, passed twice through a 30 gauge needle to shear the filaments, and incubated at room temperature. Timepoints were taken by diluting 500-fold and rapidly applying to poly-1-lysine coated coverslips for visualization. Filament images were quantified for length distribution and branch frequency by a custom MATLAB (Mathworks Inc) routine.

4.4 RESULTS

4.4.1 γ^{32}P-AzidoATP can be covalently crosslinked to Arp2 and Arp3 with approximately equal efficiency

Previously we used SDS-PAGE to show that UV irradiation covalently crosslinks α^{32}P-8-AzidoATP to the Arp2 and Arp3 subunits of the Arp2/3 complex (Dayel et al., 2001). Here we crosslink γ^{32}P-AzidoATP instead of α^{32}P to Arp2 and Arp3 in order to measure ATPase activity. Using SDS-PAGE, we can separate the subunits and monitor cleavage of the labeled γ-phosphate from ATP bound to both Arp2 and Arp3 simultaneously. This technique allows us to measure ATP hydrolysis specifically on the Arp2/3 complex in spite of a 100-fold molar excess of actin, which also binds and hydrolyzes ATP. We crosslinked γ^{32}P-AzidoATP to the Arp2/3 complex by brief (9 second) exposure to UV light. In the presence of γ^{32}P-AzidoATP at concentrations above the K_d for ATP (Dayel et al., 2001), γ^{32}P-AzidoATP crosslinks to both Arp2 and Arp3 with approximately equal efficiency (Figure 4.1a). Addition of large amounts of monomeric actin to the labeled Arp2/3 distorts the shape of the Arp2 band, but the ^{32}P signal from Arp2 remains separately quantifiable, and the magnitude is unaffected (Figure 4.1a). The efficiency of crosslinking for both Arp2 and Arp3 is approximately 10% (unpublished observations), therefore only 1% of the Arp2/3 complex has γ^{32}P-AzidoATP crosslinked to both Arp2 and Arp3. For simplicity we refer to this partially crosslinked Arp2/3 complex as γ^{32}P-AzidoATP-Arp2/3. Reactions using γ^{32}P-AzidoATP-Arp2/3 are performed in the

presence of 100 μM ATP, to occupy the non-crosslinked sites and ensure 100% of the Arp2/3 complex is active.

4.4.2 Arp2 hydrolyzes ATP rapidly upon actin filament nucleation

We mixed 20nM γ^{32}P-AzidoATP-Arp2/3 with 2 μM monomeric actin in polymerization buffer and initiated polymerization by adding 750nM VCA, which activates rapid actin filament nucleation by Arp2/3 complex. (Unless otherwise stated, VCA refers to 6His-N-WASP-VCA (398-502). Cleavage of the 6His tag did not affect the kinetics of Arp2/3-mediated actin polymerization (unpublished observations)). We assayed timepoints both by SDS-PAGE and TLC during the same reaction to monitor remaining and cleaved ^{32}P respectively (Figure 4.1b–d). ATP is hydrolzed by Arp2/3 complex at the earliest timepoints after the addition of VCA (monitored by ^{32}P cleavage) and cleavage has ceased by 90 seconds (Figure 4.1d). SDS-PAGE analysis separates the subunits and shows that the γ^{32}P is cleaved rapidly from Arp2 upon addition of VCA, but not significantly from Arp3 (Figure 4.1c). The kinetics of ATP hydrolysis assayed by SDS-PAGE match the kinetics of phosphate cleavage by TLC (Figure 4.1e). Since the nucleation reaction is autocatalytic, the rate increases over time and therefore it is not possible to derive an exact ATPase rate constant from our data, but we can define a conservative lower bound: $k_{hyd} > 0.05$ s^{-1}, noting that the true rate constant may be much higher. Isolated Arp2/3 complex in polymerization buffer shows very slow spontaneous cleavage of γ^{32}P from both Arp2 and Arp3 ($< 1 \times 10^{-4}$s^{-1}, unpublished observations). ^{32}P-ATP hydrolysis is only seen when the Azido-ATP is covalently
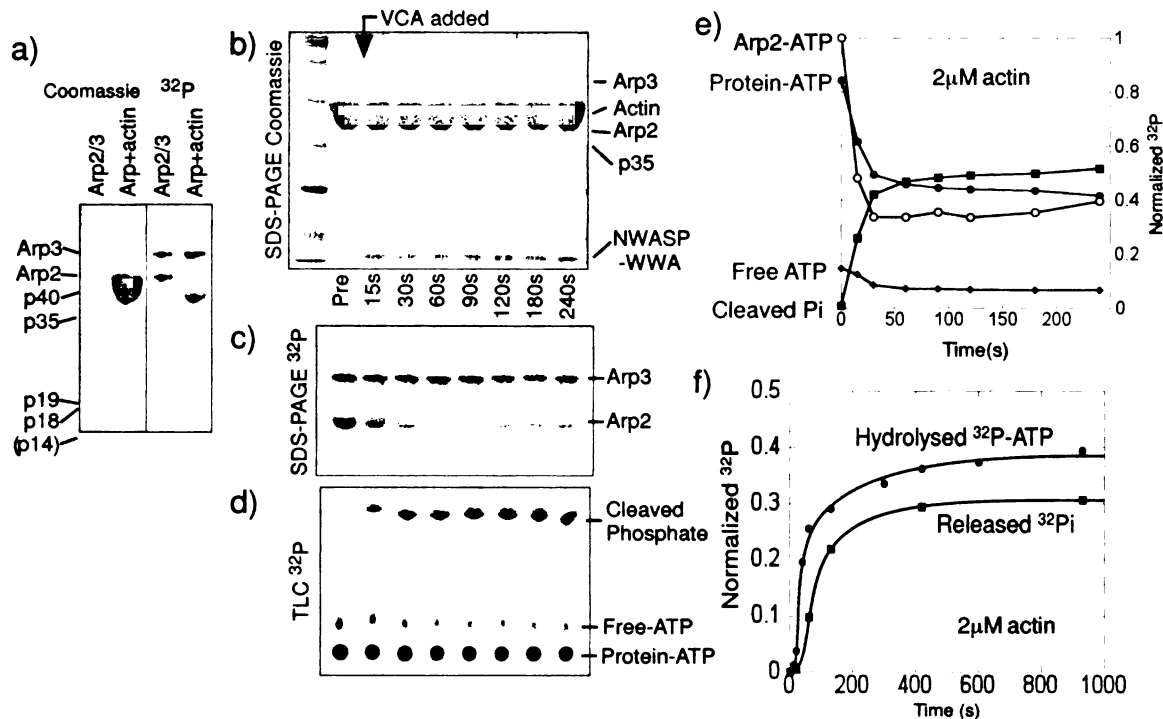
Figure 4.1: **Arp2 hydrolyses ATP rapidly upon initiation of Arp2/3-mediated filament nucleation.** **(a)** 2 μM Arp2/3 was covalently crosslinked to γ^{32}P-AzidoATP by exposure to UV light. Both Arp2 and Arp3 crosslink with approximately equal efficiency (lane 1) Addition of 100-fold excess monomeric actin (lane 2) distorts the shape of the Arp2 band but the Arp2 signal remains separate and quantifiable. **(b-e)** 20 nM γ^{32}P-AzidoATP-Arp2/3 was mixed with 2 μM monomeric actin in polymerization buffer. Samples were taken before and at indicated times after the addition of 750 nM VCA which initiates actin rapid filament nucleation by Arp2/3 complex. **(b)** Subunits were separated by SDS-PAGE and stained with coomassie. **(c)** ^{32}P signal shows remaining uncleaved γ^{32}P on Arp2 and Arp3 subunits. Arp2 rapidly loses γ^{32}P after addition of VCA. **(d)** Cleaved γ^{32}P was separated from free ^{32}P-ATP and protein-^{32}P-ATP by TLC. **(e)** Quantitation of (b-d): Protein-ATP(●), Cleaved Phosphate (■), Free ATP(◊) and Arp2-ATP from SDS-PAGE(○, normalized separately). **(f)** Arp2 releases phosphate soon after ATP hydrolysis. Reaction conditions were the same as (b-e) but with the addition of 2mM maltose and 2U/ml maltose phosphorylase. Timepoints were quenched into formic acid and assayed by TLC. Hydrolysed ^{32}P-ATP was quantified from the decrease in protein conjugated ^{32}P, and Released ^{32}P was quantified from the ^{32}P-Glucose phosphate produced.

crosslinked to Arp2/3 complex (Figure 4.3d, open vs. closed circles), indicating that the signal is due to only to hydrolysis of ATP covalently bound to Arp2/3 complex, and not on ATP hydrolysis by polymerizing actin. This is further confirmed by observations of ATP hydrolysis on Arp2/3 complex under conditions where no actin polymerization takes place (Figure 4.3e,f, Figure 4.4).

4.4.3 Phosphate release by Arp2 lags hydrolysis by ~ 40 seconds

To investigate the kinetics of phosphate release from Arp2/3 during the polymerization reaction, we added maltose and maltose phosphorylase to the nucleation reaction. In the presence of ^{32}P-labeled Arp2/3 complex maltose phosphorylase conjugates the ^{32}P-orthophosphate released from Arp2 to a hydrolyzed maltose molecule to make ^{32}P-glucose phosphate. The phosphate from ADP-Pi Arp2 is inaccessible to the enzyme and remains unconjugated orthophosphate. We quantified hydrolysed ^{32}P-ATP and released phosphate by TLC (figure 1f). Phosphate release from Arp2 lags behind ATP hydrolysis by approximately 40 seconds.

4.4.4 The rate of filament nucleation matches the rate of ATP hydrolysis by Arp2

To determine whether ATP hydrolysis on Arp2 is coupled to filament nucleation, we varied the rate of nucleation and looked to see if the rate of ATP hydrolysis by Arp2 varied accordingly. We varied the nucleation rate by using N-WASP and Scar1 VCA domains which stimulate different rates of Arp2/3 complex-dependent actin nucleation(Zalevsky et al. 2001). To slow the nucleation reaction

and allow more accurate kinetic measurements we used only $1\,\mu M$ monomeric actin. We used pyrene-actin polymerization data (Figure 4.2a) to calculate the concentration of barbed ends produced over time (Figure 4.2b, open symbols)(see Methods and Zalevsky et al. 2001). Note that this calculation of nucleation rate is model-independent, and simply uses the established kinetic parameters for actin polymerization, and the change in the amount of monomeric and filamentous actin over time measured from the pyrene-actin curves. The same reagents were used to monitor ATP hydrolysis by Arp2 under the same conditions. We used loss of $\gamma^{32}P$ labeling as a probe for ATP hydrolysis as before, and scaled the initial labeling intensity to the Arp2/3 concentration used in the reaction (20 nM) to calibrate the stoichiometry of ATP hydrolyzed by Arp2 (Figure 4.2b). Using Scar1 VCA instead of N-WASP VCA halves both the rate of nucleation of actin filaments and the rate of ATP hydrolysis on Arp2.

We note that the total amount of Arp2 that hydrolyzes ATP in the polymerization reaction is 30% less for Scar1 VCA than for NWASP VCA, which we interpret as 30% fewer filaments produced. Although it is possible to calculate the *rate* of end production from the pyrene-actin polymerization curve in a model-independent way, it is not possible to calculate the *total* number of barbed ends produced, since once the monomeric actin is polymerized, the pyrene-actin curve will not change even if new barbed ends continue to be produced. From the ATP hydrolysis data, therefore, the Arp2/3 complex produces filament ends more slowly when activated by Scar1 and under our conditions the reaction ends when
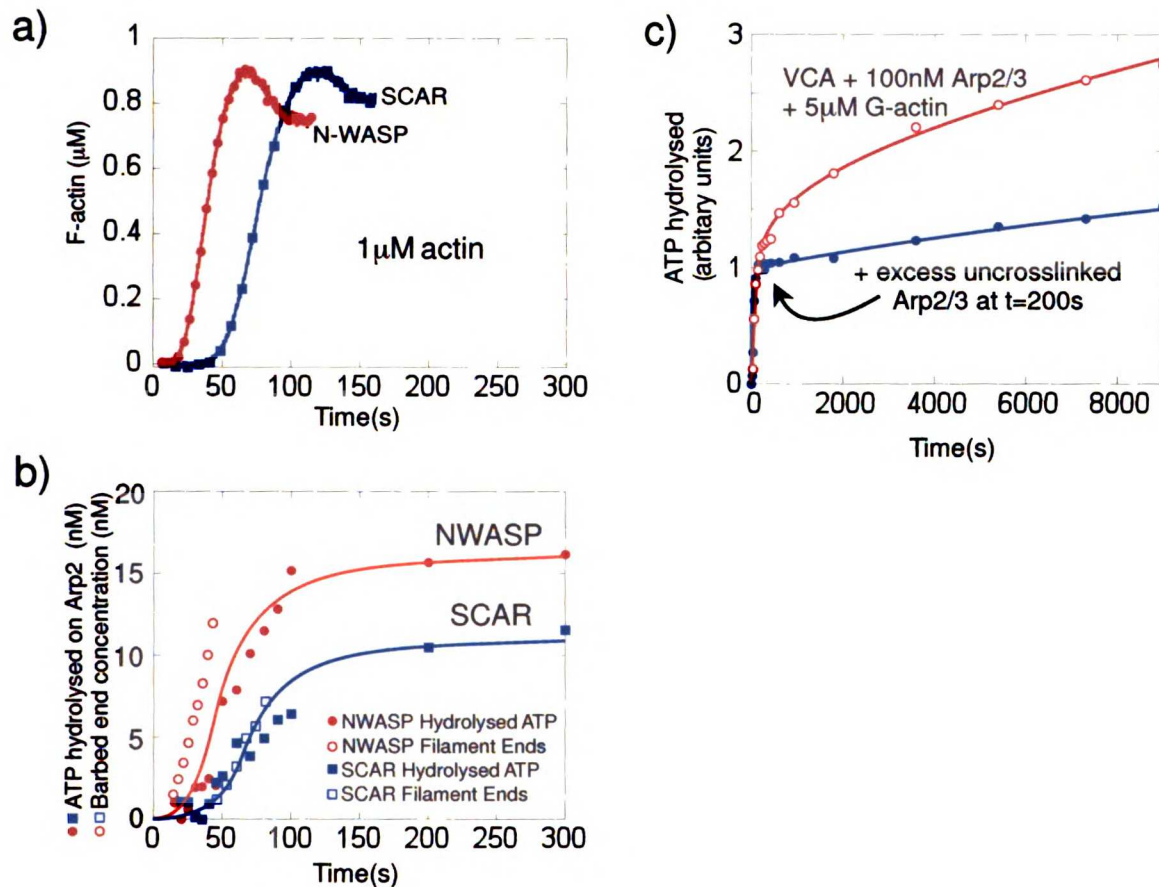
Figure 4.2: **ATP hydrolysis by Arp2 coincides with nucleation of new actin filaments, and not filament debranching.** The kinetics of nucleation were slowed by using only 1 μM monomeric actin (compared to 2 μM for Figure 4.1). 20 nM γ^{32}P-AzidoATP-Arp2/3 was mixed with either 750 nM N-WASP WWA (●) or Scar1 WA (■) and 1 μM 7% pyrene-labeled monomeric actin **(a)** Actin polymerization measured by pyrene fluorescence **(b)** The concentration of new filament ends (open symbols) was calculated from the polymerization data in a model-independent way (see Methods) and Arp2 ATP hydrolysis (closed symbols) was measured under same reaction conditions for both N-WASP WWA (●,○) and Scar1 WA (■,□). **(c)** ATP hydrolysis on Arp2 does not accompany filament debranching. Using a large excess (100nM) of γ^{32}P-AzidoATP-Arp2/3 creates a slow hydrolysis phase that follows the rapid nucleation phase. The slow phase of ATP hydrolysis can be inhibited by excess (1.5 μM) uncrosslinked Arp2/3 added at t = 200 s, showing that the slow phase ATP hydrolysis is from Arp2/3 being recruited from solution and not from that already incorporated in branches.

monomeric actin is depleted by incorporation into the new filaments, and therefore fewer total filaments are produced by the less active VCA domain.

4.4.5 ATP hydrolysis does not accompany filament debranching

A previous study claimed that ATP hydrolysis on Arp2 occurs very slowly ($t_{1/2} \approx 800s$), co-incident with filament debranching (Le Clainche et al., 2003). We performed the ATP hydrolysis assay using similar conditions to Le Clainche et al. 2003, who used a much higher concentration of Arp2/3 complex (100nM) than is used up during the polymerization reaction (5nM, estimated by Le Clainche et al. 2003). Under these conditions, we find that Arp2/3 complex hydrolysis ATP in two discrete phases: a fast (nucleation) phase, followed by a slow, approximately linear phase (Figure 4.2c, open symbols). This slow phase does not plateau, and is similar to the data points presented in Le Clainche et al. (2003). To demonstrate that this slow ATP hydrolysis is not due to Arp2/3 complex hydrolyzing ATP upon debranching, we added an excess of unlabelled Arp2/3 into solution at t = 200s, after the polymerization phase is complete. This unlabelled Arp2/3 competes with γ^{32}P-AzidoATP-Arp2/3 in solution, but not γ^{32}P-AzidoATP-Arp2/3 already incorporated in branches. Addition of excess of unlabelled Arp2/3 abolishes the slow phase of ATP hydrolysis (Figure 4.2c, closed symbols), indicating that the slow phase is due to Arp2/3 being recruited from solution and not that already in branches. This slow hydrolysis probably represents a low rate of filament nucleation by the excess unused Arp2/3 complex, the rate of nucleation

being limited by the low monomeric actin concentration that remains after most of the actin has polymerized.

4.4.6 Both VCA and monomeric actin are required to stimulate ATP hydrolysis by Arp2 during the polymerization reaction

Although the kinetics of ATP hydrolysis on Arp2 match the kinetics of actin polymerization, these data do not rule out the possibility that VCA alone, or the filamentous actin created during the polymerization reaction stimulate the ATPase activity independent of nucleation. To more specifically determine what stimulates ATP hydrolysis on Arp2, we varied the order of addition of the components that initiate the polymerization reaction. Incubation of Arp2/3 complex with VCA does not induce ATP hydrolysis by the complex until monomeric actin is added to the reaction (Figure 4.3a), showing that VCA alone does not stimulate the ATPase activity. Similarly, monomeric actin alone does not stimulate the Arp2/3 complex to hydrolyze ATP until the addition of a VCA (Figure 4.3b). To test whether actin filaments themselves stimulate Arp2/3 ATP hydrolysis we used phalloidin-stabilized actin filaments to ensure that no monomeric actin would be present and took care not to shear the filaments in order to reduce the number of free pointed ends. ATP hydrolysis is not stimulated on the Arp2/3 complex by filamentous actin, even in presence of VCA (Figure 4.4c). As controls, we found that neither phalloidin nor 20 mM phosphate inhibit the kinetics of ATP hydrolysis by Arp2 during the polymerization reaction (unpublished observations)

(a) Arp2/3 + VCA → Added G-actin

Normalised ^{32}P

1
0.8
0.6
0.4
0.2
0

Arp3
Arp2

0 300 600 900 1200 1500
Time(s)

(b) Arp2/3 + G-actin → Added VCA

Normalised ^{32}P

1
0.8
0.6
0.4
0.2
0

Arp3
Arp2

0 300 600 900 1200 1500
Time(s)

(c) Arp2/3 + F-actin → Added VCA

Normalised ^{32}P

1
0.8
0.6
0.4
0.2
0

0 300 600 900 1200 1500
Time(s)

(d)
ATP hydrolysed (arbitary units)

6
5
4
3
2
1
0

VCA+G-Actin

VCA+LatB:G-Actin
VCA + G-actin + Non-crosslinked Arp2/3

0 200 400 600 800 1000
Time(s)

(e)
ATP hydrolysed (arbitary units)

6
5
4
3
2
1
0

F-actin + VCA + LatB:G-actin
F-actin + VCA + G-actin
F-actin + LatB:G-actin

0 100 200 300 400 500 600 700 800
Time(s)

(f)
Polymerized actin (arbitarty units)

1
0.8
0.6
0.4
0.2
0

Arp2/3 + F-actin + VCA + G-actin

F-actin + G-actin

Arp2/3 + F-actin + VCA + LatB:G-actin

0 100 200 300 400 500
Time(s)

Figure 4.3: **A single actin monomer, in the presence of actin filaments and VCA, stimulates ATP hydrolysis on Arp2, without requiring actin polymerization. (a-c)** Remaining unhydrolyzed γ^{32}P-AzidoATP on Arp2(•) and Arp3(○) was quantified to assay ATP hydrolysis (same conditions as Figure 4.1b–d). 20nM γ^{32}P-AzidoATP labeled Arp2/3 was mixed at indicated times with either **(a)** 750nM VCA then 2μM G-actin **(b)** 2μM G-actin then 750nM VCA or **(c)** 2μM F-actin then 750nM VCA. **(d)** Latrunculin B (□) inhibits the ability of VCA plus monomeric actin (○) to stimulate ATP hydrolysis on Arp2/3 complex in the absence of actin filaments. Also, ^{32}P ATP hydrolysis signal requires covalent crosslinking to Arp2/3. Arp2/3 was mixed with 6μM γ^{32}P-AzidoATP and exposed to UV either before (○) or after (•) the addition of excess (2mM) unlabelled ATP. Excess ATP added before the UV exposure prevents crosslinking and abolishes the ATP hydrolysis signal, indicating that all the ^{32}P ATP hydrolysis signals measured are due to ATP hydrolysis on Arp2/3 and not from ATP hydrolysis on actin. **(e,f)** In the presence of phalloidin-stabilized actin filaments, actin monomers are prevented from polymerizing by Latrunculin B, but still stimulate ATP hydrolysis on Arp2/3 complex. 20nM γ^{32}P-AzidoATP labeled Arp2/3 was pre-mixed with 1μM phalloidin-stabilized actin filaments. The reaction was initiated by mixing with 750nM N-WASP VCA, 1uM G-actin and 4μM Latrunculin B as indicated, and actin polymerization was monitored by pyrene-actin fluorescence **(e)** and, separately, cleaved γ^{32}P was assayed by phosphomolybdate extraction **(f)**.

When Arp2/3 concentration is low (20 nM), and nucleation is rapid (using NWASP VCA), initiation of the polymerization reaction causes striking and near-complete ATP hydrolysis on Arp2 (~80%, i.e. ~16nM). ATP hydrolysis on Arp3 has similar kinetics but much lower stoichiometry (10-20%, Figure 4.3b,c). The decrease is not caused by the dilution effect of adding the second component (~4%) which is already compensated for in the data presented.

4.4.7 In the presence of both VCA and actin filaments, a non-polymerizable actin monomer is sufficient to trigger rapid ATP hydrolysis on Arp2

The timing of ATP hydrolysis and the combination of factors required to stimulate it suggest that Arp2 hydrolyses ATP during the filament nucleation reaction. Kinetic and light microscopy data indicate that most or all Arp2/3 dependent filament nucleation occurs from Arp2/3 complex bound to the sides of filaments produced earlier in the polymerization reaction (Blanchoin et al., 2000a, 2001; Zalevsky et al., 2001b). To test whether filament side binding is necessary for ATP hydrolysis on Arp2 we blocked filament formation with the actin-monomer binding toxin, Latrunculin B. Latrunculin B binds to monomeric actin and prevents it polymerizing, but does not affect its binding to VCA (A.E. Kelly, R.D.M., unpublished observations). The combination of VCA and Latrunculin B:actin monomers does not stimulate ATP hydrolysis on Arp2/3 complex (Figure 4.3d, compare open symbols), nor do pre-formed, phalloidin-stabilized actin filaments

Conditions					Results	
VCA	G-actin	LatB	F-actin	Shearing	ATP Hydrolysis	Polymerisation
+	+	-	Produced	-	+	+
-	-	-	-	-	-	-
+	-	-	-	-	-	-
-	+	-	-	-	-	-
-	-	-	Added	-	-	-
+	-	-	Added	-	-	-
+	+	+	-	-	-	-
+	+	+	Added	-	+	-
-	+	+	Added	-	-	-
-	-	-	Added	+	+	-

Table 4.1: Requirements to Stimulate ATP Hydrolysis on the Arp2 Subunit of Arp2/3 Complex

and Latrunculin B-actin monomers without VCA (Figure 4.3e, filled squared). In the presence of pre-formed actin filaments and VCA, however, Latrunculin B:actin monomers stimulate rapid ATP hydrolysis on Arp2/3 (Figure 4.3e, filled circles), without actin polymerization (Figure 4.3f). Table 4.1 summarizes the requirements for stimulation of ATP hydrolysis on Arp2. These data indicate that during the nucleation reaction, actin filament side-binding is a pre-requisite for VCA and monomeric actin to stimulate ATP hydrolysis on Arp2. The observation that polymerization of the daughter filament is unnecessary implies that, mediated by VCA, the interaction of a single actin monomer with the Arp2/3 complex is the trigger for ATP hydrolysis on Arp2.

4.4.8 Pointed end capping by the Arp2/3 complex stimulates rapid ATP hydrolysis by Arp2 in the absence of either branch formation or a WASP family VCA domain

Arp2/3 complex is known to cap the pointed ends of pre-formed actin filaments *in vitro*, inhibiting both polymerization and depolymerization from the pointed ends of gelsolin-capped filaments (Mullins et al., 1998). (Arp2/3 complex does not cap the barbed ends of actin filaments and does not affect the rate of addition of monomers from the barbed ends of spectrin-capped filaments (unpublished observations)). We speculated that the way the Arp2/3 complex caps a free filament pointed end in solution might mimic the way the Arp2/3 complex anchors the pointed end of the new daughter filament in a branch. If the actin monomer that triggers ATP hydrolysis during nucleation is the first monomer of the daughter filament, pointed-end capping, like nucleation, should drive interaction with this monomer and trigger ATP hydrolysis on Arp2. To test this, we sheared pre-formed, phalloidin-stabilized actin filaments in the presence of Arp2/3 complex. Mechanical shearing fragments long actin filaments into many short filaments, creating many new filament ends that rapidly re-anneal to produce long filaments again. This re-annealing process is blocked by proteins that cap filament ends (Andrianantoandro et al., 2001; Murphy et al., 1988). Without shearing, the addition of 20nM Arp2/3 does not alter the length distribution of phalloidin-stabilized actin filaments (Figure 4.4a, compare (i) and (iii)). After shearing in the presence of 20nM Arp2/3 complex, pointed end-capping by

Arp2/3 complex blocks re-annealing and results in significantly shorter filaments (Figure 4.4a compare (ii) and (iv)). No branches form within this time—it takes take several hours for even a few branches to assemble under these conditions (unpublished observations). To assay for ATP hydrolysis by the complex, we incubated γ^{32}P-AzidoATP-Arp2/3 complex with actin filaments under the same conditions as the microscopy experiment. We split the mixture into two parts; sheared one half; and took timepoints to assay for ATP hydrolysis from both samples (Figure 4.4b and quantified in 3c). No ATP hydrolysis occurs in the unsheared condition, confirming that binding to the sides of actin filaments is not sufficient to stimulate ATP hydrolysis. ATP hydrolysis occurs rapidly in the sheared condition and occurs only on Arp2 (Figure 4.4c). Since this occurs well before any branches form, pointed end capping by the Arp2/3 complex is sufficient to stimulate ATP hydrolysis on Arp2 not only in the absence VCA, but also in the absence of filament side binding.
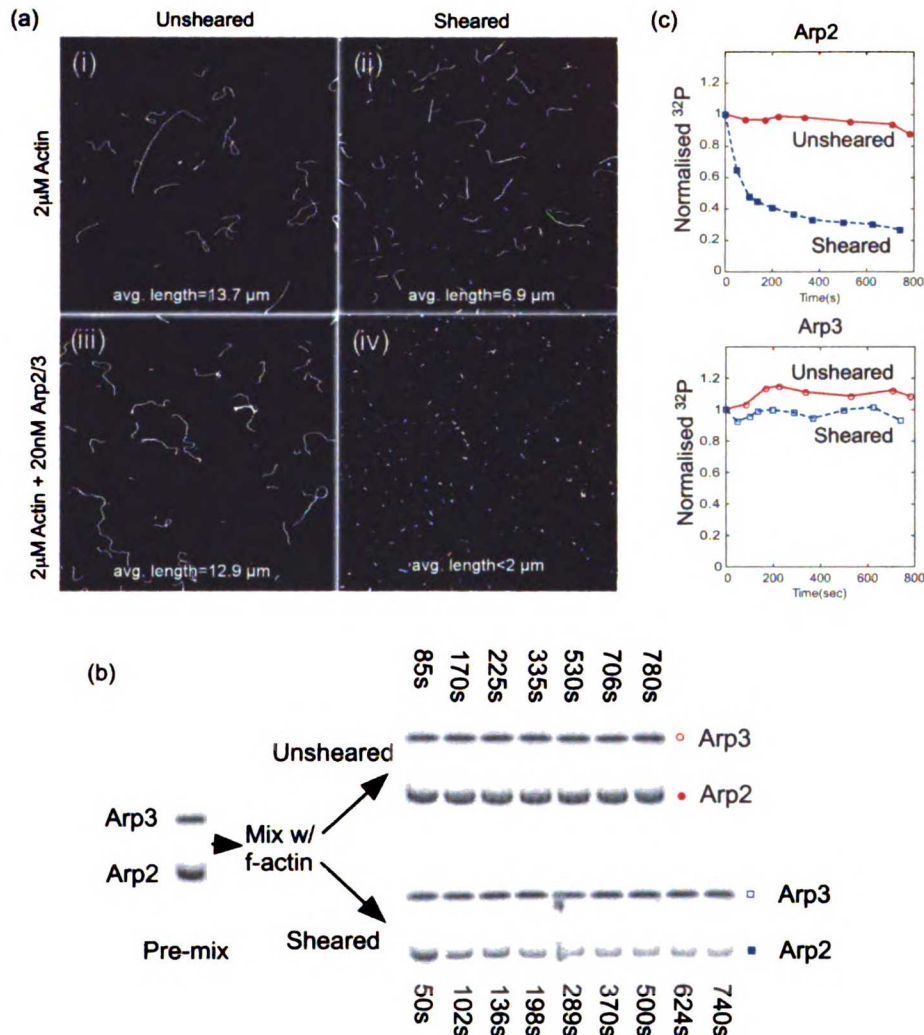
Figure 4.4: **Pointed end filament capping is sufficient to stimulate ATP hydrolysis on Arp2 in the absence of VCA**. **(a)** Arp2/3 complex prevents actin filament re-annealing by capping the pointed ends. The length distribution of 2μM Alexa-488 phalliodin-stabilized actin filaments is unaffected in the absence **(i)** or presence **(iii)** of 20nM Arp2/3 complex. **(ii)** 5 minutes after shearing the filaments, filament have begun to re-anneal in the absence of Arp2/3 complex, but 20nM Arp2/3 complex **(iv)** maintains short filaments, preventing re-annealing by capping filament pointed ends. **(b)** ATP hydrolysis on Arp2 is stimulated by pointed-end capping. 20nM crosslinked γ^{32}P-AzidoATP-Arp2/3 was mixed with 2μM phalloidin-stabilized actin filaments. The mixture was split in two and one sample was sheared. Timepoints were taken as shown. **(c)** Uncleaved ^{32}P on Arp2 (unsheared (•) and sheared (○)) and Arp3 (unsheared (•) and sheared (○))) were quantified from (b). Arp2 rapidly hydrolyzes bound ATP upon filament pointed end capping.

4.5 DISCUSSION

Conventional actin and all actin-related proteins share a conserved nucleotide binding pocket. Actin monomers bind ATP but do not hydrolyze it until they are induced to polymerize. Actin polymerization triggers rapid ATP hydrolysis followed by a slow release of cleaved phosphate from the filament (Blanchoin and Pollard, 2002). Arp2 also hydrolyzes its bound ATP and we find that the conditions that promote ATP hydrolysis and the kinetics of the reaction are remarkably similar to those of conventional actin. In the presence of VCA and actin filaments, monomeric actin stimulates ATP hydrolysis on Arp2. We also find that binding of Arp2/3 complex to the pointed end of a pre-formed actin filament is sufficient to trigger Arp2 ATP hydrolysis, even in the absence of VCA. The stimulation of Arp2 ATPase activity by both filament pointed ends and by actin monomers under nucleating conditions suggests that the geometry of the Arp2/3-actin interaction is the same in both cases.

Interaction between Arp2/3 complex and conventional actin can occur in three distinct ways: (1) Arp2/3 complex binds the sides of pre-formed actin filaments; (2) Arp2/3 complex binds to the pointed ends of filaments, either by remaining associated with the daughter filament following nucleation or by capping preformed pointed ends; and (3) Arp2/3 complex may interact with an actin monomer bound to the VCA domain of a WASP-family protein. There is abundant experimental evidence for filament side- and pointed end-binding by the complex (Amann and Pollard, 2001a,b; Blanchoin et al., 2000a, 2001; Mullins et al.,

1998). Evidence that a VCA-bound actin monomer interacts with Arp2/3 complex is more circumstantial and is supported by four observations: (1) VCA-domains can simultaneously bind both the Arp2/3 complex and monomeric actin (Marchand et al., 2001; Panchal et al., 2003); (2) removal of the actin monomer-binding WH2 (V) domain from a WASP-family protein severely decreases the efficiency of Arp2/3 activation (Marchand et al., 2001); (3) Kinetic modeling suggests that the Arp2/3 complex requires monomeric actin to form a filament nucleus (Zalevsky et al., 2001b) but, on its own, it has no detectable affinity for monomeric actin; and (4) Arp2/3-dependent nucleation is not limited to the end of the mother filament (Amann and Pollard, 2001b), indicating that the VCA-bound actin monomer does not incorporate into the mother filament. Two of the three interactions between the Arp2/3 complex and conventional actin—nucleation and pointed end capping—are thought to be mediated by the actin related subunits, analogous to actin-actin interactions in a filament. Both interactions stimulate rapid ATP hydrolysis by Arp2.

Based on sequence conservation and biochemical similarities, ATP hydrolysis on Arp2 is probably driven by a mechanism similar to that which stimulates ATP hydrolysis on actin. The molecular details of how polymerization activates ATP hydrolysis on conventional actin, however, are not well understood. A leading hypothesis is that a 'hydrophobic plug'—a loop between subdomains 3 and 4 of actin (Kuang and Rubenstein, 1997, residues 262–274 in yeast)—undocks from the monomer surface and binds to a hydrophobic cleft formed by adja-

cent monomers in the opposite strand of the two-start filament helix (Kuang and Rubenstein, 1997; Lorenz et al., 1993). Our data are consistent with stimulation of ATP hydrolysis by docking of a hydrophobic plug sequence on Arp2 into a hydrophobic cleft created by Arp3 and the first actin monomer of the daughter filament (Figure 4.5). In the crystal structure of the inactive Arp2/3 complex, Arp2 and Arp3 are oriented like a pair of actin monomers in opposite strands of the two-start filament helix (Robinson et al., 2001), but they are separated by a 40 Å cleft. Activation of the complex probably involves closure of the cleft, allowing actin to polymerize from an Arp2-Arp3 heterodimer (Kelleher et al., 1995; Robinson et al., 2001), which then remains attached to the pointed end of the new daughter filament, anchoring it to the branch (Figure 4.5b(iv)). Based on the geometry of the subunits in the crystal structure and the hydrophobic plug model we expect that the Arp3-actin contact creates a pocket to bind the hydrophobic plug of Arp2 (residues 265–277 in yeast Arp2). The geometry of the interaction would stimulate the ATPase activity of Arp2, but not Arp3 (Figure 4.5a).

Monomeric actin does not interact directly with the Arp2/3 complex in the absence of VCA but, under conditions that promote nucleation, a single actin monomer triggers VCA-dependent ATP hydrolysis on Arp2. By analogy with capping-induced ATP hydrolysis, the monomer that triggers ATPase activity is therefore the first monomer of the new daughter filament (Figure 4.5b (i–iii)). The hydrophobic pocket formed between Arp2, Arp3 and the actin monomer would therefore
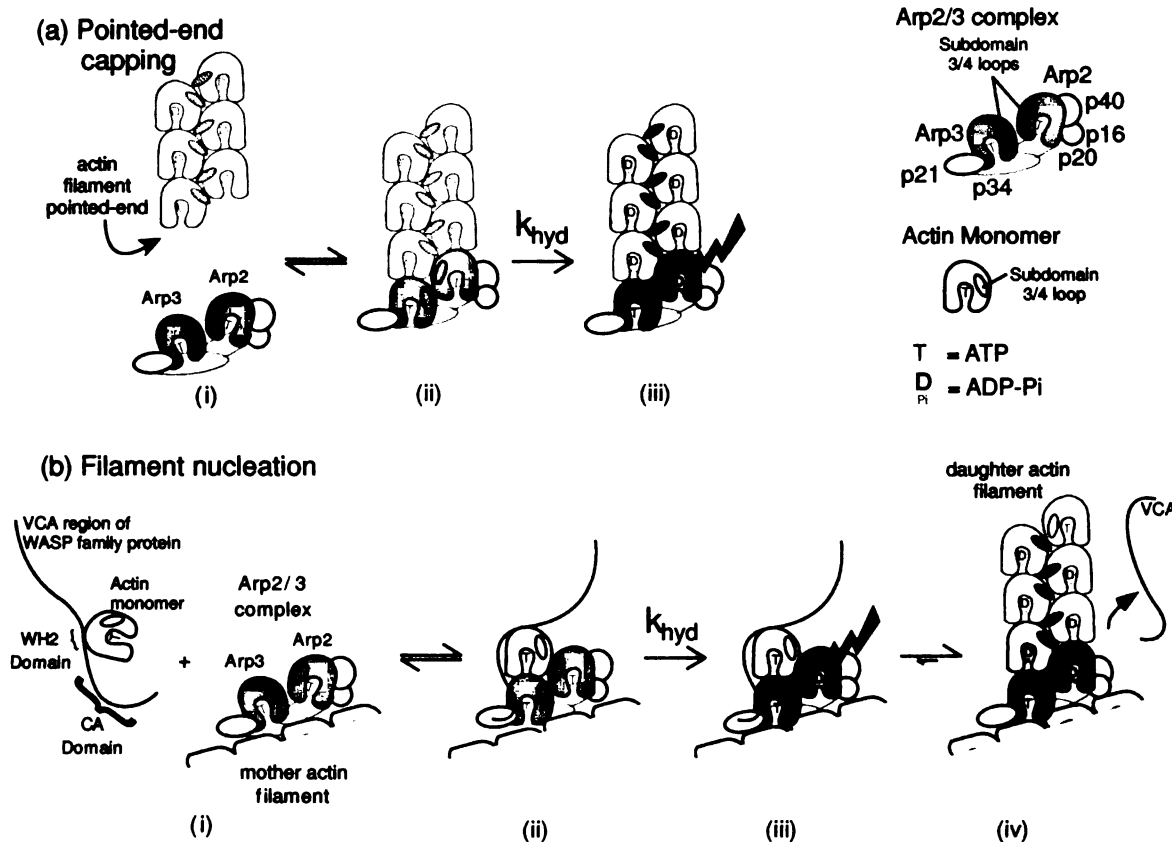
Figure 4.5: **Model for activation of ATP hydrolysis on Arp2/3 complex, and mechanism by which WASP family proteins activate Arp2/3 complex to nucleate new actin filaments.** (a) Filament pointed-end capping stimulates ATP hydrolysis on Arp2. (i) Arp2 and Arp3 are separated when Arp2/3 complex is free in solution (ii) Upon pointed-end capping, the binding energy of the actin-Arp2/3 interface drives Arp2 and Arp3 together and (iii) a conformational change on Arp2 (shown by the red the subdomain 3/4 loop flipping out) triggers ATP hydrolysis by Arp2. (filament pointed-end capping is probably not a significant function of the Arp2/3 complex *in vivo*) (b) A VCA-bound actin monomer drives the activation of the Arp2/3 complex and stimulates ATP hydrolysis on Arp2. (i) Arp2/3 complex must first be bound to the side of an actin filament, and an actin monomer is bound to the VC domain of the WASP family protein. (ii) The VC domain of the WASP family protein docks the first monomer of the daughter filament onto the Arp2/3 complex, stabilizing the Arp2-Arp3-actin interaction and promoting the active conformation of the complex. (C.F. (a)(ii)) (iii) the active conformation of the Arp2-Arp3-actin monomer triggers a conformational change on Arp2 and ATP hydrolysis by the subunit. (iv) Actin polymerizes from the activated Arp2/3 complex. ATP hydrolysis by Arp2 may promote dissociation of the CA domain of the WASP family protein from Arp2/3 complex, aided by actin polymerization which competes its WH2 domain from the first actin monomer.

promote a similar conformational change in Arp2 and stimulate ATP hydrolysis (Figure 4.5b (iv)).

Interaction of Arp2/3 complex with the sides of filaments is not sufficient to trigger Arp2 ATPase activity, even in the presence of VCA. Binding of Arp2/3 to the sides of filaments is, however, required for ATP hydrolysis on Arp2 stimulated by VCA and monomeric actin. These data suggest that binding the side of an actin filament induces a conformational change in the Arp2/3 complex that enables it to interact with monomeric actin bound to VCA. The filament side-binding activity of Arp2/3 does not require the presence of the Arp2 or Arp3 subunits, and can be reconstituted by a combination of the Arc2 (p34) and Arc4 (p20) subunits (Gournier et al., 2001). The Arc2 and Arc4 subunits contact both Arp2 and Arp3 and therefore filament side-binding might favor association of Arp2 and Arp3. The fact that Arp2 ATP hydrolysis induced by VCA and an actin monomer requires filament side-binding strongly suggests that all Arp2/3-generated actin filaments are born on the side of pre-formed filaments.

Our results disagree with a recent paper which claims that ATP hydrolysis on Arp2 is slow and accompanies filament debranching (Le Clainche et al., 2003). Using similar experimental conditions, we observe similar slow ATP hydrolysis kinetics (Figure 4.2c) and we show that this ATP hydrolysis occurs on Arp2/3 complex recruited slowly from solution. The slow hydrolysis does not reflect delayed ATP hydrolysis on Arp2/3 complex rapidly incorporated into branches early in the experiment. ATP hydrolysis on Arp2, therefore, cannot be associated with

debranching. Le Clainche et al. (2003) claim that ATP hydrolysis does not oc-
cur during nucleation, and present data with a lag of several hundred seconds
between computer-simulated nucleation kinetics and measured ATP hydrolysis
kinetics (Le Clainche et al., 2003, Figure 1B of). In this experiment, Le Clainche
et al. (2003) initiate polymerization in the absence of free ATP. These conditions
would deactivate up to 97% of the Arp2/3 complex (that fraction which is not
crosslinked to ATP on both subunits). In our hands removal of free ATP in-
troduces an artificial lag in polymerization (unpublished observations). This lag
lasts until tightly-bound ATP is released from monomeric actin ($k^{-1}_{ATP\_release} = 330$ s
(Selden et al., 1999)) and is free to interact with the Arp2/3 complex. The claim
that the absence of free ATP does not affect ATP hydrolysis kinetics (Le Clainche
et al., 2003) is contradicted by the data, since the free ATP would activate un-
crosslinked Arp2/3 which would compete with crosslinked Arp2/3 and should
reduce the ^{32}P signal to approximately one fifth. The observation that the ^{32}P
signal is not reduced, rather than confirming that removal of free ATP has no
effect, instead confirms that contaminating ATP is present for the latter part of
the 'ATP free' condition, presumably released slowly from monomeric actin. The
use of a computer-simulation to derive the nucleation curve in this experiment
(Le Clainche et al., 2003) may explain why a lag in the polymerization created by
the initial absence of ATP was not apparent.

We find that ATP hydrolysis and phosphate release from Arp2 (~40 s) are
more than an order of magnitude faster than debranching of Arp2/3-generated

dendritic networks (~1000 s) (Blanchoin et al., 2000a). The kinetics of phosphate release from Arp2 are also about an order of magnitude faster than phosphate release from actin ($k^{-1}_{Pi\_release}$ = 384 s for skeletal muscle actin (Melki et al., 1996)), suggesting that, if phosphate release controls debranching, it is the phosphate release from the daughter actin filament that is important, not phosphate release from Arp2. This is supported by the observation that phalloidin, which slows phosphate release from actin, slows filament debranching, and cofilin, which accelerates phosphate release from actin, accelerates filament debranching (Blanchoin et al., 2000a). Le Clainche et al. (2003) claim (but do not demonstrate) that Cr^{2+}-ATP Arp2/3 releases phosphate more slowly than Mg^{2+}-ATP Arp2/3, and show that Cr^{2+}-ATP Arp2/3 debranches more slowly than Mg^{2+}-ATP Arp2/3. If chromium does slow the phosphate release from Arp2/3, in the light of our data, this would suggest that phosphate release from Arp2 may simply be a prerequisite for filament debranching—but cannot be a direct cause, since it occurs much too rapidly.

We previously showed that the Arp2/3 complex requires hydrolysable ATP for nucleation activity (Dayel et al., 2001), and the current study adds weight to the hypothesis that ATP hydrolysis has a direct role in nucleation, by showing that ATP is hydrolysed by Arp2 upon nucleation. The separation of the Arps in the crystal structure and the very low nucleation rate of the unactivated complex probably reflect the tendency of Arp2 and Arp3 to remain separated in the absence of all the required nucleation promoting factors. This suggests that there is a

large free energy barrier to the formation of an Arp2-Arp3 heterodimer. Our data indicate that there are two ways to overcome this energy barrier, both using the binding energy of actin: one using the combined binding energy of the two actin monomers at the pointed-end of an actin filament during pointed-end capping, and the other the combined binding energy of the side of the mother filament, the VCA domain and a single actin monomer. The surface area of the filament pointed end that would be buried by interaction with an Arp2-Arp3 dimer would be large ($\sim$6800 Å^2). This is consistent with the fact that *in vitro* the binding energy of this interface is sufficient to drive the interaction and promote the active conformation of the complex directly, even in the absence of VCA or a mother filament (Mullins et al., 1998). The binding of monomeric actin alone is insufficient to overcome the free-energy barrier, which ensures that the inactive conformation of the Arp2/3 complex is robust despite high cellular concentrations of actin. Because of the free energy of all the binding partners involved in nucleation, however, the energy of ATP hydrolysis may not be needed to stabilize the nucleus. Regardless, it is very likely that ATP hydrolysis on Arp2, like actin, provides a timing signal to the system. ATP hydrolysis on Arp2/3 would promote release of VCA from the complex and allow a new actin branch to move away from the site of its creation (Dayel et al., 2001). ATP hydrolysis may also regulate the timing of the interaction of the Arp2/3 complex with other binding partners such as cortactin and cofilin. Temporal regulation of these interactions is likely to be essential to construction of functional motile structures.

The Arp2/3 ATP hydrolysis assay presented here provides a novel assay for activation of the Arp2/3 complex that does not rely, as all previous assays have done, solely on actin polymerization. Pyrene actin polymerization is only useful over a limited range of actin concentrations because at high concentrations spontaneous assembly obscures Arp2/3-mediated nucleation. The pyrene actin assay also has temporal limits since it rapidly uses up one of the factors necessary for Arp2/3 activation—monomeric actin. Our observation that ATP is hydrolyzed by Arp2 rapidly during, or soon after, the nucleation reaction means that we can use ATP hydrolysis on Arp2 as an assay to study the factors required to promote activation of the Arp2/3 complex. The fact that non-polymerizable actin monomers are competent to stimulate hydrolysis enables us to investigate the conditions for Arp2/3 complex activation under a wider range of conditions. This system will be useful for further studies of the biophysics of Arp2/3-mediated actin assembly.

Chapter 5

The Structural Basis for Arp2/3 Activation

5.1   The Structural Basis for Arp2/3 Activation

This chapter is an expansion of the model for activation of the Arp2/3 com-
plex shown in Figure 4.5, including struture-based rendering of the molecular
components and a structure-based argument for Arp2/3 activation working as
an AND gate integrating signals from the Mother filament and VCA.

5.2   The Arp2-Arp3 heterodimer model of filament nucle-
ation

Figure 5.1 shows a representation of the Arp2/3 complex in the crystal-
structure conformation Figure 5.1a and in a hypothesized active conformation
Figure 5.1b by flexing around the p35 hinge. Rodal et al. (2005) recently found
a distribution of Arp2/3 conformations by electron microscopy single-particle re-
constructions supporting the possibility of a flexing of the complex. This con-
formation aligns Arp2 and Arp3 to be in the positions of two adjacent subunits
of an actin helix, and aligning the daughter filament so that the Arp2 and Arp3
subunits form a contiguous helix gives the arrangement shown in Figure 5.1c.

5.3   Pointed-end Capping

Figure 5.2 shows this docking as a model for pointed end capping by the
Arp2/3 complex. In this model, the binding energy of the association of the com-
plex with the pointed end of the actin filament drives Arp2 and Arp3 together by
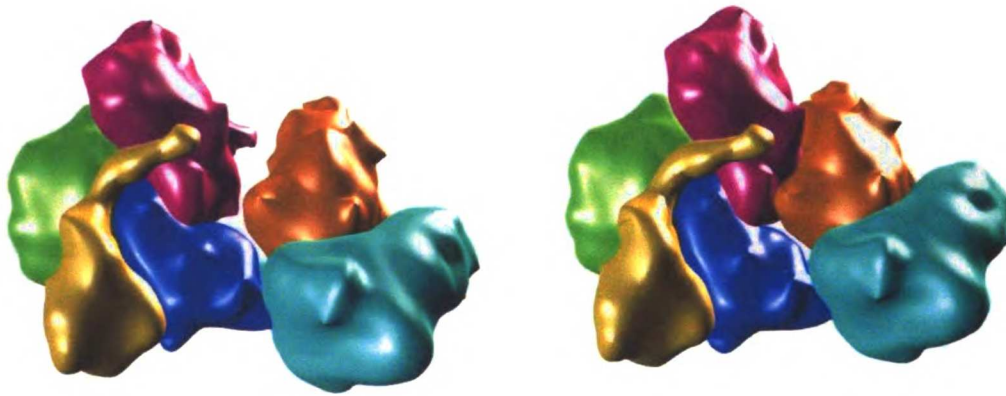
(a) Arp2/3 in open conformation (from crystal structure (Robinson et al., 2001))

(b) Postulated closed conformation, with Arp2 and Arp3 in an actin-like dimer conformation
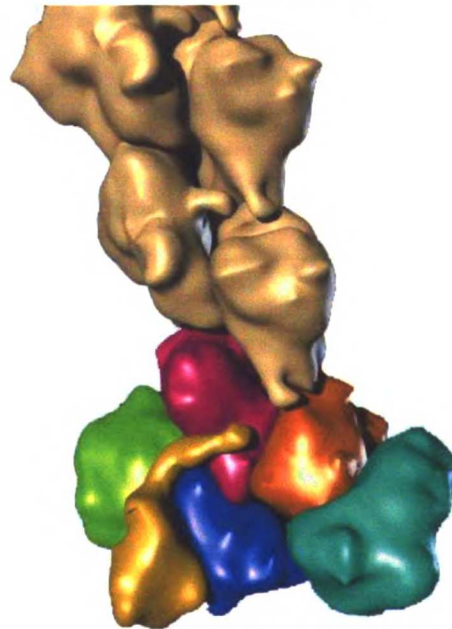
(c) Arp2/3 complex with closed structure docked onto daughter filament

Figure 5.1: The Arp2-Arp3 heterodimer model of filament nucleation

hinging around p35. This creates a pocket for Arp2, surrounded by Arp3 and the two monomers at the end of the filament. Since hydrolysis occurs with even one actin monomer (see We hypothezise that it is this particular conformation—with the end-most actin subunit and Arp3 in contact with Arp2 (and in the opposite helix) that triggers ATP hydrolysis. By extension we would predict this to be the trigger for ATP hydrolysis on a subunit within an actin filament, i.e. that an actin trimer is the minimal assembly required to trigger ATP hydrolysis on actin, and that ATP hydrolysis would occur on the middle subunit.

5.4 p21 as the Integrator of Activation Signals

Figure 5.2a shows a docking of the Arp2/3–pointed end assembly onto a mother actin filament. I docked this by hand, matching the shape of the complex to that of the side of the actin filament as closely as possible whilst avoiding steric overlap. Interestingly, this conformation not only produces a branch at the correct 70° angle to the mother filament, and the subunit arrangement matches the antibody map of the branch recently published by Egile et al. (2005) (the docking was performed before the publication of this map).

Not visible in the previous views was p21, hanging from the far side of Arp3. Even with the closure of Arp2 and Arp3, p21 does not dock well with the rest of the complex, nor with the mother filament (see Figure 5.3b.) It seems likely that activation of the complex involves not only a hinging of the complex to bring Arp2 and Arp3 together as has been previously proposed, but also a rotation of p21 on

(a) Arp2/3 and actin filament pointed end. Arp2/3 in open conformation free in solution

(b) Arp2/3 interacts with pointed end

(c) Pointed end (actin) binding energy drives conformational change and closes Arp2/3 conformation. Contact with actin triggers ATP hydrolysis on Arp2 (glow)

(d) Stable pointed end cap

Figure 5.2: Model for Arp2/3 pointed-end capping
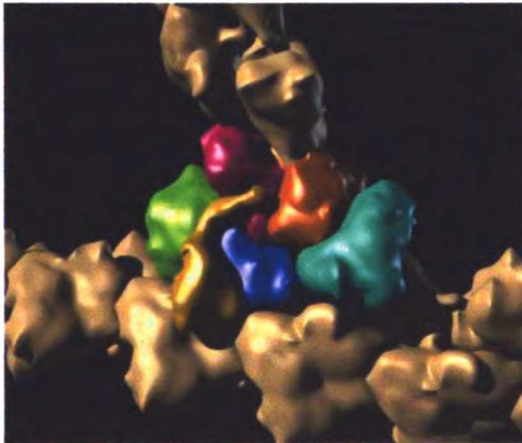
(a) Model for Arp2/3 branch
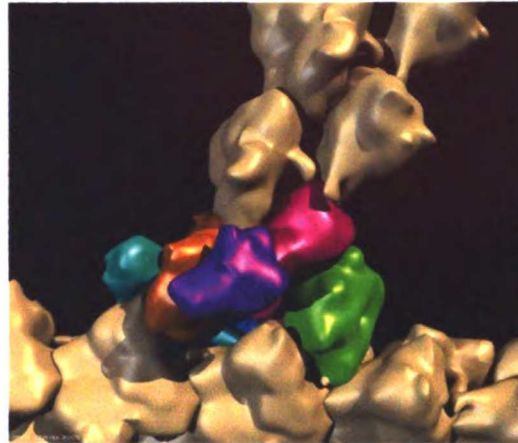
(b) Model for Arp2/3 branch showing that, without further rearrangement, p21 (purple) and Arp3 (orange) do not dock well onto the mother filament

Figure 5.3: Arp2/3 complex with closed structure docked onto mother and daughter filaments

Arp3 to associate with the mother filament. This is especially interesting because 1) p21 has been shown to bind the acidic domain of the VCA proteins 2) this conformational change would place p21 in a position to stimulate ATP hydrolysis on Arp3 (assuming that Arp2 behaves similarly to Arp2 and is stimulated by a protein-protein interaction close to the subdomain 3/4 loop) and 3) p21 would be in a position to contact the mother filament.

I propose that p21 is the key sensor for the Arp2/3 complex AND gate—it is poised at the position of the two inputs (VCA and the mother filament), and is ideally suited to trigger a closing of the complex conformation around the p35 hinge. In this scenario, the unactivated Arp2/3 complex would be in the open, crystal structure conformation (Figure 5.1a) and p21 would be swung away from the complex. To activate the complex requires both Mother Filament binding and

VCA binding (and that VCA carries an actin monomer). Without Mother Filament binding, when VCA binds it attaches to the p21 subunit via its acidic domain and p40 by the CA domain (Zalevsky et al., 2001b, Alex Kelly and Dyche Mullins, unpublished observations and), closing the Arp2/3 hinge slightly. p21 is still swung out, and this positions VCA so that the complex conformational closure is incomplete, and the actin monomer bound to the WH2 domain is unable to dock correctly onto the complex to form an Arp2-Arp3-actin nucleus. When the Mother filament binds, it interacts with Arp3 to bring p21 down and into a cleft formed between Arp2 and Arp3 and the mother filament. This further closes the complex via interaction with VCA and allows VCA to dock the actin monomer onto the Arp2-Arp3 dimer. If Arp2/3 complex binds the mother filament in the absence of VCA, the conformational change of Arp3 and p21 still occurs and Arp2 and Arp3 are brought closer into contact but do not close completely together because the allosteric interaction via VCA is absent. When VCA binds the closure is complete and VCA can dock the actin monomer onto the complex to form a nucleus. It should be noted that complete closure requires the binding energy of not only the mother filament, but also VCA and the actin monomer. This hypothesis also explains the Marchand et al. (2001) result that VCA and mother filament-binding are co-operative, and since the acidic domain is thought to bind p21, may explain why the number of acidic residues in the VCA domain has such a dramatic effect on nucleation (Zalevsky et al., 2001b).

(a) Mother filament, with Arp2/3 and VCA free in solution
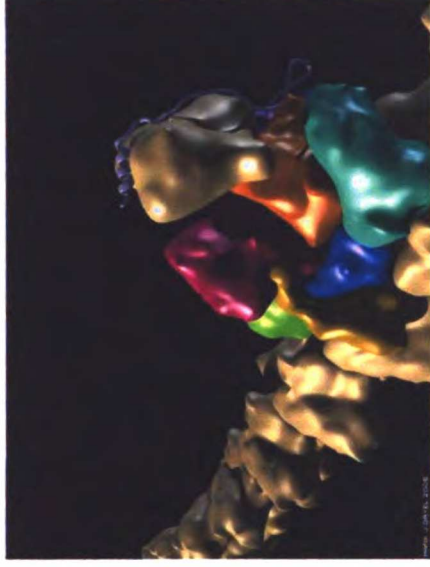
(b) Arp2/3 associates with VCA and Mother filament to form a pre-nucleus. VCA WH2 domain (helix) binds an actin monomer bringing it into contact with the complex
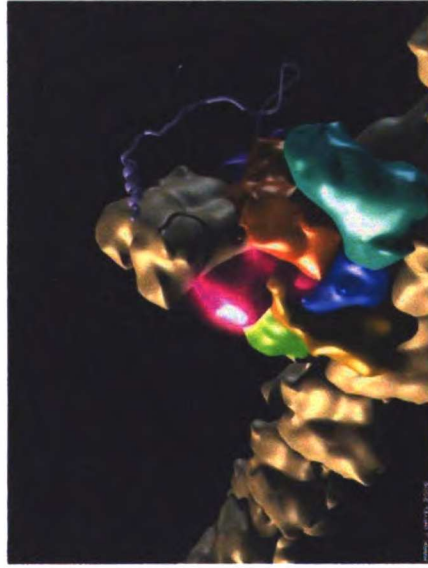
(c) VCA drives association of actin with Arp2/3 complex and drives the conformational change to the closed Arp2/3 conformation. Contact with actin triggers ATP hydrolysis on Arp2 (glow)

(d) Stable Arp2/3 branch. Actin polymerizes from nucleus and VCA is released after ATP hydrolysis on Arp2

Figure 5.4: Model for mechanism of actin filament nucleation by Arp2/3

5.5 Filament Nucleation

Figure 5.4 shows our complete model for nucleation of filaments by the Arp2/3 complex. Interaction with both the mother filament and VCA closes the complex conformation and allows VCA to dock an actin monomer onto the Arp2-Arp3 heterdimer. We don't currently know the order of assembly of the components, but from the capping result, we know that ATP hydrolysis is triggered by actin interacting with and bringing Arp2 and Arp3 together as the final step of nucleation.

Chapter 6

Inhibition of ATP hydrolysis on Arp2 does not affect nucleation

Because ATP hydrolysis occurs synchronously with nucleation and because hydrolysable ATP appeared to be required for filament nucleation, we thought that ATP hydrolysis might be the cause of the conformational change that leads to nucleation. If this were true, a delay or inhibition of ATP hydrolysis should delay or inhibit filament nucleation. We tested this in two ways, using Ca^{2+}-ATP bound Arp2/3 complex and using a hydrolysis deficient mutant Arp2.

6.1 Ca^{2+}-ATP bound Arp2/3 complex rapidly nucleates filaments

Members of the actin superfamily bind ATP in association with a divalent cation (i.e. Mg^{2+}-ATP, Ca^{2+}-ATP, Li^{2+}-ATP etc.). Due to the intracellular predominance of magnesium, Mg^{2+}-ATP Arp2/3 is likely to be the physologically relevant form, and is usually used in all our assays. Blanchoin and Pollard (2002) have shown that for actin, changing the divalent cation from Mg^{2+} to Ca^{2+} significantly slows the ATP hydrolysis rate, so we used Ca^{2+}-ATP bound Arp2/3 and determined the effect on the nucleation reaction (this was carried out with a similar techique to the control of nucleotide outlined in section 3.4.3). Since Arp2 is similar in sequence and structure to actin, we anticipated that it might slow the hydrolysis rate of Arp2 and thereby slow nucleation. No such slowing was observed (Figure 6.1). In the Ca^{2+}-ATP Arp2/3 condition of this assay, the effect of free Ca^{2+} in solution affects the actin, causing depolymerisation after the actin has exchanged its bound Mg^{2+} for Ca^{2+} (~100 s). The important result is that there

Figure 6.1: Ca^{2+}-ATP bound Arp2/3 complex rapidly nucleates actin filaments

is no lag between the initiation of the nucleation (~10 s in both cases) between the Mg^{2+} and Ca^{2+} conditions. If Ca^{2+} does slow ATP hydrolysis on Arp2, this result suggests that ATP hydrolysis is not required for filament nucleation.

6.2 Arp2 Q139A is hydrolysis dead, but nucleation kinetics are unaffected

To confirm that ATP hydrolysis is not required for filament nucleation, Rong Li's lab at Harvard kindly provided us with a set of yeast strains with mutations in the ATP-binding pocket of Arp2. We purified these mutated forms of Arp2/3 complex and tested them in the γ^{32}P-AzidoATP hydrolysis assay. We found that Arp2-Q139A mutation inhibits ATP hydrolysis (Figure 6.2(a)). The pyrene-actin based polymerisation assay showed that this mutant Arp2/3 complex is just as active as the wild-type complex, confirming that ATP hydrolysis on Arp2 is unnecessary for filament nucleation(Figure 6.2(b)).
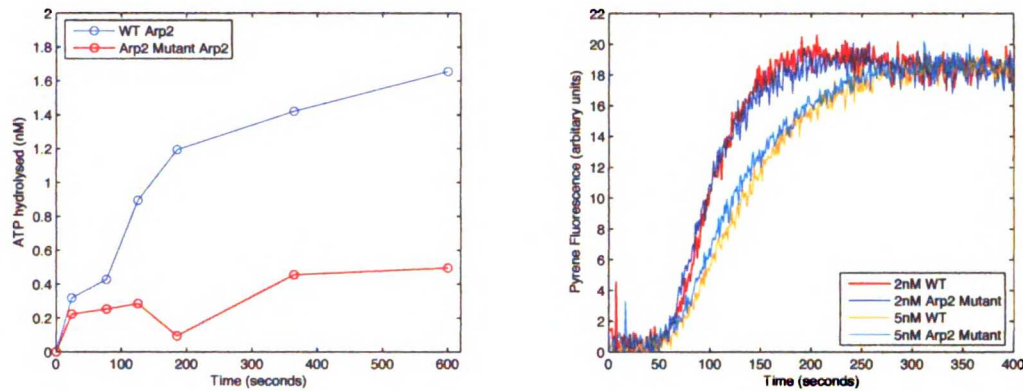
(a) Q139A Arp2 mutant binds but does not hydrolyse ATP

(b) Kinetics of filament nucleation are unaffected by Arp2 Q139A mutation

Figure 6.2: Q139A Arp2 mutant is hydrolysis dead, but kinetics of nucleation are unaffected

6.3 Reconciling the AMP-PNP and the Q139A results

The results in chapter 6 show that ATP hydrolysis is not required for filament nucleation, seeming to contradict the results in section 3.4.3, that 'hydrolysable ATP' is required for nucleation. There are, however, two important caveats with the results from section 3.4.3:

- Whilst our claim that ATP (rather than ADP) is required is strong, our claim that hydrolysable ATP is required is based on the inability of AMP-PNP to sustain nucleation activity, but this rests on the assumption that AMP-PNP is a good structural mimic for ATP in this context, for which we have no evidence for or against.

- Our method for controlling nucleotide was not precisely targeted. By changing nucleotide in solution, we changed the nucleotide on both Arp2 and Arp3 together, and were therefore unable to tell which subunit needed bound ATP.

In the light of the Q139A Arp2 mutant result, we believe that the failure of AMP-PNP bound Arp2/3 to nucleate is likely due to the failure of AMP-PNP to mimic the structure of ATP, rather than our initial interpretation (which was that AMP-PNP mimics ATP, and the inability of the complex to hydrolyse it prevented nucleation.)

This still leaves the question of why ADP-bound Arp2/3 is inactive. There are 2 possibilites:

1. That although Arp2 does not require ATP hydrolysis to nucleate, it does require *bound ATP*.

2. That although we have not detected significant ATP hydrolysis on Arp3, the complex still responds to the Arp3 nucleotide state and ADP bound to Arp3 inhibits nucleation.

Chapter 7

ATP hydrolysis and the Arp2/3 cycle

7.1 ATP hydrolysis on Arp2 as the initiation of an ATPase cycle

ATP hydrolysis on Arp2 occurs as a result—not the cause—of filament nucleation. Presumably, the energy of ATP hydrolysis is being used for some other process and the *timing* is determined by nucleation. This could be similar to actin, for which ATP hydrolysis occurs rapidly upon polymerisation (Blanchoin and Pollard, 2002) and set in motion the ATP → ADP-Pi → ADP → ATP cycle. Although the cycle is synchronized to the ATP → ADP-Pi transition upon polymerisation, to our knowledge it not this transition, but the ADP-Pi → ADP transition which has a discernible effect, reducing subunit-subunit affinity and allowing filament disassembly by cofilin (Blanchoin and Pollard, 1999; Pollard et al., 2000).

This underlines a key concept: Although the cycle may require energy, the energy can be coupled to *any* step in that cycle. Another example is the power stroke of myosin, which although driven by the energy of ATP hydrolysis, occurs on the ADP-Pi → ADP transition, and not the ATP hydrolysis step itself. The energy of ATP hydrolysis can be used at any stage: ATP hydrolysis (ATP → ADP-Pi), Phosphate release (ADP-Pi → ADP), or ATP re-loading (ADP → ATP)[1]. This raises the question: What are the other stages of the Arp2/3 cycle for which energy could be required?

---

[1]Formally, work could also be coupled to the ADP release step, but here this is collapsed into the ATP-reloading step for reasons of simplicity

7.2 Energetics of the Arp2/3 cycle

Both actin and Arp2/3 complex are components of a larger cellular module that produces motile force by treadmilling (Pollard and Borisy, 2003). Within this module actin is layed down at the leading edge producing protrucive force, and disassembled at the rear of the lamellipod, and just as actin cycles between monomeric and filamentous forms, the Arp2/3 complex cycles its association with partner proteins (Figure 7.1(a)). The basic set of Arp2/3 states within this system are shown in Figure 7.1(b): free, bound to VCA, filament nucleation, VCA Release, and debranching.

We are relatively confident of the stages illustrated in Figure 7.1(b), but there is reason to think that the Arp2/3 cycle may have more steps that this. In addition to binding VCA (Machesky and Insall, 1998) and actin (Mullins et al., 1998), the Arp2/3 complex has been shown to bind cortactin (Weaver et al., 2001), CARMIL (Jung et al., 2001) and cofilin (Zalevsky et al., 2001a). A more complete Arp2/3 cycle is shown in Figure 7.2, including the possibility of interaction with other binding partners such as Cortactin and CARMIL, and making explicit the difference between mother and daughter filament debranching.

For each of the steps, there is the potential for the use of energy from ATP hydrolysis on the Arp2/3 complex, but for many of these steps other sources of energy are available in the form of associations with other proteins in the system (binding energies, or ATP hydrolysis on other proteins such as actin), summarized in table Table 7.1.
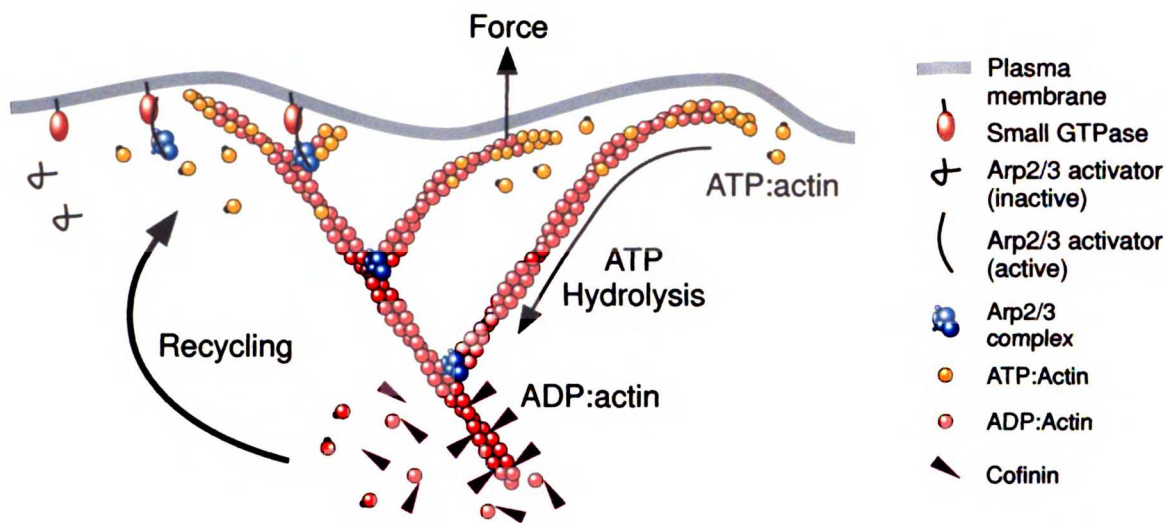
(a) The Arp2/3-actin lamellipodial treadmill
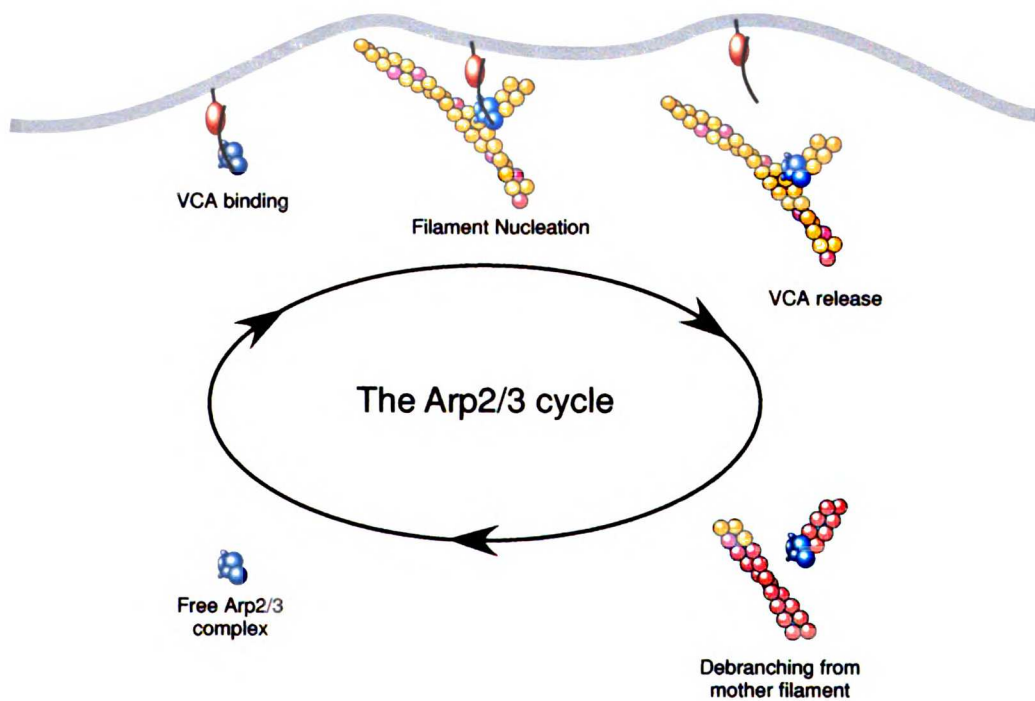
(b) The simplified Arp2/3 cycle

Figure 7.1: Both actin and the Arp2/3 complex cycle within the actin treadmill
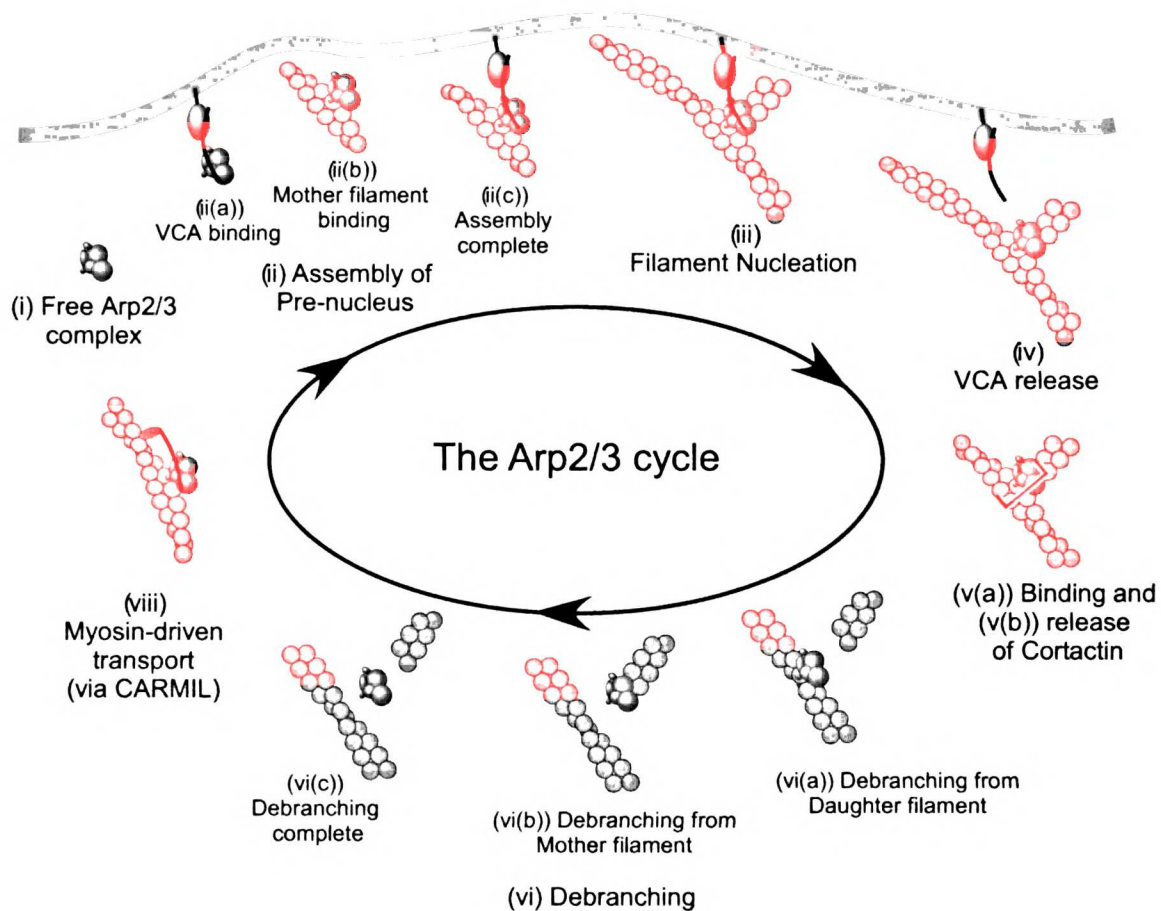
Figure 7.2: The Arp2/3 cycle

Stage	Process	Binding energy Input	Other energy sources
(ii)	Assembly of Prenucleus	VCA and Mother filament	–
(iii)	Filament Nucleation	Actin subunit(s)	ATP hydrolysis on Arp2
(iv)	VCA release	–	Polymerization Force
(v(a))	Cortactin binding	Cortactin	–
(v(b))	Cortactin release	–	ATP hydrolysis on Actin
(vi(a))	Daughter debranching	–	ATP hydrolysis on Actin
(vi(b))	Mother debranching	–	ATP hydrolysis on Actin
(vii)	CARMIL-transport	CARMIL	–
(i)	CARMIL release	–	–

Table 7.1: Sources of energy available in the Arp2/3 cycle

7.2.1 Assembly of Pre-nucleus

Assembly of the pre-nucleus (the step between stage (i) and (ii)) can be driven simply by the binding energy of the components, VCA and the Mother filament. Affinity measurements (Marchand et al., 2001) suggest this is a cooperative process, with both VCA and Mother filament binding stabilizing the same conformation of the Arp2/3 complex. We currently do not know the order of assembly, but from a logistical view it is likely that VCA binds first and promotes an increased association with the mother filament (filamentous actin concentration is very high at the leading edge of the cell and if Arp2/3 were first to attach to filaments, it would likely undergo unproductive attachments to filaments far from sites of activation).

7.2.2 Filament Nucleation

Energy must be put into the system at the point of nucleation to overcome an activation barrier (discussed in section 2.2.1). ATP hydrolysis occurs on Arp2 at this time, but since we know that hydrolysis is not required for nucleation this cannot be the energy source and it therefore must be from the binding energy of other components. Assembly of the pre-nucleus (binding energy of VCA and Mother filament) may provide part of the binding energy, but our results that ATP hydrolysis on Arp2 is stimulated by pointed-end capping suggest that the active conformation of Arp2/3 complex is primarily driven by interaction with actin subunit(s) from the daughter filament. This follows from 1) the deduction that

the pointed-end capping interface of Arp2/3 complex must be the same interface that interacts with the pointed-end of the daughter filament 2) that during this interaction it must also be in the active conformation (else it would not interface with the filament), and 3) that this conformation is driven by interaction with filament pointed ends in the absence of either VCA or Mother filament binding (see section 4.4.8). We believe the binding energy of the first subunit of the daughter filament drives nucleation, with VCA and the mother filament acting together as as a catalyst, reducing the energy barrier for association of this subunit. Once associated, another actin monomer can quickly add onto this nucleus, providing additional binding energy (from the free energy of polymerization pool) to stabilize the interaction of the first subunit.

7.2.3 VCA release

We previously measured the affinity of Arp2/3 complex for VCA and found that ADP-bound Arp2/3 complex binds less tightly than ATP-bound Arp2/3 (Dayel et al., 2001). This led us to put forward the model of ATP hydrolysis on the Arp2/3 complex inducing VCA release, since release of VCA is vital for efficient force production and ATP hydrolysis on Arp2 occurs upon nucleation—the correct time for VCA release (see section 3.4.2 on page 34 for more details).

We do not yet know whether native VCA-containing proteins are released and remain at the membrane after activating Arp2/3 complex, or remain attached and traffic back with Arp2/3 in lamellipod. The *Listeria* ActA protein, however, the VCA domain must be released for motility, since ActA is attached to the Listerium,

so there is reason to believe that the native Wasp-family proteins are also released. If the VCA domain works to drive the Arp2/3 complex into an active form, it would be anticipated to bind tighter to the activated than the inactive form (corroborated by the co-operativity observed in pre-nucleus formation (Marchand et al., 2001)). Release of VCA (stage (iv)) would seem to be an important requirement, and there are two possible sources of energy for this process, the hydrolysis of ATP from Arp2, and the energy of polymerization itself—forcibly releasing the activator.

7.2.4   Cortactin binding and release

The exact function of Arp2/3's interaction with cortactin is uncertain, but it is speculated to stabilize the Arp2/3–actin branch (Weaver et al., 2001). There is evidence that the interaction of Arp2/3 with VCA and cortactin is sequential, with cortactin associating with the Arp2/3 branch after the release of VCA (Uruno et al., 2003). Such a sequential association is a good candidate for control by ATP hydrolysis, especially as the association would be expected to occur following filament nucleation and VCA release. This hypothesis would predict a higher affinity of cortactin for ADP– (or ADP-Pi–) bound Arp2/3 than ATP-bound.

Whilst VCA release would occur relatively quickly after nucleation, we don't have a good idea of the timing or function of Cortactin association and release (stage (v)). It is believed to stabilize the branch (Weaver et al., 2001), suggesting a high affinity for the post-nucleated branch state. Association could occur simply by the binding energy of Cortactin for the branch, but dissociation would have to be driven by some other energy-release step. The next step in the cycle is

dissassembly of the branch (functionally opposite to stabilzation by cortactin), and cortactin release may be linked to whatever promotes this step (below).

7.2.5 Debranching

The Arp2/3 complex must be released from its branch (Figure 7.2(vii)) before it can be recycled. Since the complex interacts with both the mother filament and the pointed end of the daughter, debranching must occur in two steps, release from both the daughter (Figure 7.2(vi(a))) the mother (Figure 7.2(vi(b))) filament. We don't know the cause or order of these processes, though ATP hydrolysis on the complex (Le Clainche et al., 2003), the nucleotide state of the filament and association with cofilin (Blanchoin et al., 2000b) have all been implicated.

The phosphate release following ATP hydrolysis on actin subunits increases their affinity for cofilin, which disassembles the filament (Blanchoin and Pollard, 1999; Pollard et al., 2000). Cofilin is also known to bind Arp2/3 complex (Zalevsky et al., 2001a). The debranching of Arp2/3 complex could therefore be driven by 1) ATP hydrolysis on the mother filament 2) ATP hydrolysis on the daughter filament 3) some other process e.g. Phosphate release from Arp2, ATP hydrolysis on Arp3 etc. The possibility of ATP hydrolysis on Arp3 is interesting, since Arp3 contacts the mother filament. Le Clainche et al. (2003) found that Cr^{2+}-ATP –bound Arp2/3 complex has slower debranching kinetics than the more physological Mg^{2+}-ATP –bound ATP. Since Cr^{2+}-ATP slows the release of phosphate from actin, this suggests that phosphate release from Arp2 may be involved in debranching. Since there are two steps to debranching, release from the daughter (Figure 7.2(vi(a)))

and from the mother (Figure 7.2(vi(b))) filaments, a combination of these might be expected.

7.2.6 Interaction with CARMIL: Myosin-driven transport

Jung et al. (2001) identified CARMIL (Capping protein, Arp2/3, and Myosin I Linker, also known as Acan-125) as a protein that binds Arp2/3 complex, capping protein and myosin. This is a particularly interesting protein, since capping protein and Arp2/3 complex are known to be the primary regulators of free barbed ends in the cell (which in turn detemines actin polymerisation), and function mainly at the leading edge—there is a good possibility of active myosin-driven transport of these components to the leading edge via CARMIL. Yang et al. (2005) recently found that CARMIL induces capping protein to release from the barbed ends of actin filaments, indicating that CARMIL preferentially binds the free form of capping protein, and it may possibly act to uncap filaments at the leading edge. Yeast lack a leading edge but also have a potential for localizing Arp2/3 complex via Myosin, since yeast Myosin I contains an acidic Arp2/3 binding domain (Evangelista et al., 2000). Perhaps yeast do not require the active localization of capping-protein, because of the different actin structures constructed.

If CARMIL is involved in Arp2/3 transport, regulation of this protein is a particularly interesting question, since CARMIL binding may be involved in blocking the interaction of Arp2/3 with filaments to allow Arp2/3 transport through the network. Again, the possibility of ATP hydrolysis on Arp3 being involved with

this process is intreging, since Arp3 contacts the mother filament, so regulated interaction between Arp3 and CARMIL might block filament-binding directly.

7.3   The Function of ATP hydrolysis on Arp2

Phosphate release from actin has been shown destablize the filament by breaking the contact between subdomain 2 and the subunit below it (Belmont et al., 1999; Muhlrad et al., 1994), and allow filament dissassembly. The crystal structure of Arp2/3 complex (Figure 5.1 on page 77) shows subdomain 2 of Arp2 to be in place to contact Arp3 (if Arp2 and Arp3 come together in an actin-dimer like arrangement), and subdomain 2 of Arp3 presumably contacts the mother filament (based on crosslinking data (Mullins et al., 1997))

If Arp2 works in a similar way to actin, we therefore would expect the nucleotide state of Arp2 to regulate its interaction with Arp3 (i.e. regulate the stability of an Arp2-Arp3 heterodimer nucleus). This would suggest that it would be involved either in nucleation (which we know is not the case from the data in section 6) or in *daughter* filament debranching which is supported by the Cr^{2+}-ATP of (Le Clainche et al., 2003). Our favored interpretation of the results is that ATP hydrolysis on Arp2 promotes VCA release, and phosphate release favors debranching from the daughter filament.

7.4 The Function of ATP hydrolysis on Arp3

By the same logic, the nucleotide state of Arp3 would be expected to regulate the interaction with the Mother Filament. Since we do not see significant ATP hydrolysis by Arp3, presumably the stimulus is absent in our experiments. We tested several hypotheses for the stimulus for ATP hydrolysis on Arp3: Force (by shearing the filaments after the branches had formed), Cofilin (adding during or after the polymerization), debranching (by waiting several hours, or adding cofilin).

It should be noted that true mother filament debranching may not be occuring in our assays. We and others assay for debranching by observing fluorescent actin filaments under the microscope. Over time we observe the disappearence of the characteristic Y-branches, but if Arp2/3 releases the daughter filament (Figure 7.2(vi(a))) and remains attached to the mother filament, it is indistinguishable in this assay from complete debranching (Figure 7.2(vi(c))). It may also be possible that pseudo-debranching by cofilin (by simply disassembling the mother and daughter filaments), leaving the Arp2/3 complex behind) is not equivalent to an as yet unknown active mother filament debranching mechanism that may be governed by Arp3 ATP hydrolysis.

If we accept the hypothesis that the Arp3 nucleotide state governs the affinity for the mother filament, there is one (known) interactant that might be expected to be involved: Cortactin. This would be directly analogous to what we believe occurs on Arp2 in the formation of the branch. With Arp2, actin (brougt in

by VCA) stimulates ATP hydrolysis on Arp2, and later phosphate release causes release of this subunit of the daughter filament and debranching. Essentially, the binding energy of the actin subunit triggers the release of ATP energy which will later be used to combat this binding energy. With Arp3, Cortactin could be the stimulus for ATP hydrolysis on Arp3, and the energy of ATP hydrolysis could later be used to disassemble the cortactin-stabilised branch.
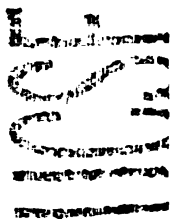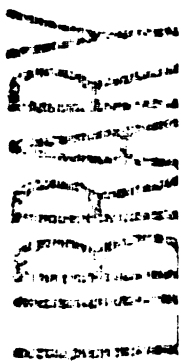
Chapter 8

Future Directions

8.1 Tools to investigate the function of Arp2/3 ATP hydrolysis

8.1.1 ATP hydrolysis mutants

To understand the role of ATP hydrolysis on Arp2/3, we need to observe the effects of inhibition of ATP hydrolysis. We can use mutants such as Arp2 Q139A to inhibit Arp2 ATP hydrolysis, and the corresponding Arp3 Q183A mutation to inhibit ATP hydrolysis (Figure 8.1). Note, since we have no known way of stimulating ATP hydrolysis on Arp3, the Arp3 Q182A mutation is untested. Since the Arp2/3 complex goes through a cycle of activities (Figure 7.2), disruption of this cycling may shed light on the role of ATP hydrolysis.

8.1.2 Steady-state polarized systems

8.1.2.1 The S2 lamellipod

The S2 lamellipod provides an excellent *in vivo* model for the lamellipod (Rogers et al., 2003), well suited for examining the role of Arp2/3 ATP hydrolysis. This system uses a ConA-coated coverslip as a substrate that prevents cell movement and allows localization of proteins within a dynamic but stationary lamellipod. The use of S2 cells allows for specific knockdown of proteins using RNAi.

This experiment involves the construction of two fluorescently tagged versions of the Arp2/3 complex (by CFP/YFP etc.). One color tag would mark a

```
           .   .:*:*:*:*: * * **:: *   .**                      * ** *    .:
Actin -MHSEVAALVIDNGSGMCKAGFAGDDAPRAVFP--------------SIVGRP---RHQG          42
Arp2  -MDPHI-PIVLDQGTGFVKIGRAGENFPDYTFP--------------SIVGRPILRAEMR          44
Arp3  MSYLNPAVVMDNGTGLIKLGFAGNSPSWVFPAIAIAAPLTKKSGVGAPLAVSNEA                60
ruler 1.......10........20........30........40........50........60

           .:                                    * .:*:** :  **:.:*
Actin IIVG-----------------------MGQKDSYVGDQAQSKRG--ILTLRYPIEHGI          75
Arp2  ASVA---------------------DPLKDIMIGDEASEVRS---YLQISYPMENGI           77
Arp3  SIFGNNTHATNFIGANTGGLLSNNILGKRGTEDLDFYIGNALVASQGPSYELSYPIRHGQ      120
ruler .......70........80........90.......100.......110.......120

        : ** .** :*. :::: ::       . .:  .****.*:** .** : :::**.::   ..*:
Actin VTNWDDMEKIWHHTFYNELRVAPEEHP-VLLTAPMNPKSRXXXEIMFETFNVPAFYV         134
Arp2  IKNWTDMELLWDYAFFEDMKLPSTSNGKILLTEPPMNPLKNREKMCEVMFEKYDFGGVYV      137
Arp3  VEDWDHMERFWENIFKYLRLEPEDHEF-FLLTEPPLNPPENREQVAEIFFESFNCAGLYI      179
ruler .......130.......140.......150.......160.......170.......180

        :;****;* :.  :            :* *:*********:;*;  .   :       .: :****;*
Actin SIQAVLSLYSSGR--------GIVLDSGDGVTHVVPITAGFSLPHAILRLDLAGRDL         186
Arp2  AIQAVLALYAQGL--------SGVVVDSGDGVTHIVPVYSVVLSHLTRRLDVAGRDVT        189
Arp3  AVQAVLALAAWTSRKVTDRLLTGTVIDSGDGVTHVIPVAEGYVIGSAIKNIPIAGRDIT      239
ruler .......190.......200.......210.......220.......230.......240

        .: .:* .** .**      :      .    **:: ***. *:  : :    : .:       : :. *
Actin DYLMKILSERGYSFSTSAEREIVRDIKEKLCYVALDFEQEMQTAASSSL-----IEKSYE      241
Arp2  RHLIDLLSRRGYAFNRTADFETVRQIKEKLCYVSYDLQLDKKLARETTA-----LVESYE      244
Arp3  LFIQSLLRKRG---EADLSLRTAEKIKQEYCYVCPDIVKEFNKFDKDPSKFASFVVENQ       296
ruler .......250.......260.......270.......280.......290.......300

        .   :.: :* *** *** :*:* : .  :        :     ::: . :*:*. ** **:*
Actin LPDGQVITIGNERFRAPEALFHPSVLGLESAG-IDQTTYNSIMKCDVDVRKELYGNIVM       300
Arp2  LPDGRTIKVGQFRFEAPECLFQPGLVDVEQPG-VGELLFNTVSADVDIRSSLYKAIVLS      303
Arp3  KTRRKVVDIGYERFLAPEIFFNPEIASSDFLTPLPTVVDQIIQACPIDVRKGLYKNIVLS     356
ruler .......310.......320.......330.......340.......350.......360

        **::*: .:  *:::::*. : .                     ..* :   .:: *::**::*
Actin GGTTMFPSIAERMQKEITALAP-----------------SMKVKIIAPPERKYSVWIGGSIL      346
Arp2  GGSSMYPGLPSRLEKELKQLWFGRVLHNDPQR---LDKFKVRIEDPPRRKHMVFIGGAVL     360
Arp3  GGSTMFKDFGRRLQRDLKSIVNNRIAFNLGGTIPGLTEGVDVSVSHRKFRNAVWFGGSLL     416
ruler .......370.......380.......390.......400.......410.......420

        *   :    .   .:*::::* ** : :
Actin AELE-FQQMWISKQEYDESGPXIVHHKCF----                                375
Arp2  ASIMADKDHMWLSKQEWQESGPSAMTKTFGPR---                              391
Arp3  A-QEAEFKGYCHTKKDYEEYGPEIVRNFSLFQMV                               449
ruler .......430.......440.......450....
```

Figure 8.1: Sequence alignment of actin, Arp2 and Arp3 from *Saccharomyces cerevisiae*. Arp2 Q139A mutation inhibits ATP hydrolysis (at ruler position 183, corresponding to actin Q137A and Arp3 Q182A)

wild-type Arp2/3 complex, whilst the other color marks the ATPase mutant. Expression is kept low, so that 1) the structure and kinetics of the lamellipod are unaffected and 2) we can visualize Arp2/3 complex by fluorescence speckle microscopy (FSM) (Waterman-Storer et al., 1998). Because individual Arp2/3 molecules diffuse quickly unless they are attached to some substrate such as the lamellipodial network, this allows us to distinguish free and bound Arp2/3 complex. The spatial distribution of both speckles (network bound) and intensity (network and free), and movement of individual speckles will enable us to determine the dynamics of Arp2/3 complex within the cycle. By then comparing the behaviour of the two colored versions of Arp2/3 complex we will determine the effects of ATPase mutants. e.g. if the Arp2 ATPase mutant is defective in debranching, it would be preferentially localized toward the rear of the lamellipod compared to wild-type.

8.1.2.2 Bead motility experiments

The actin tail that forms on ActA coated beads (Bernheim-Groswasser et al., 2002) provides a similar polarized actin network to the S2 lamellipod (stationary in the reference frame of the bead). The reconstitution of the system using purified components (Loisel et al., 1999) provides opportunity to investigate the activity of the Arp2/3 complex in a very well controlled environment. Comparing the behavior of wild-type and ATPase mutant Arp2/3 complexes in this system will help determine the exact mechanism for differential localization, and the in-

volvement of individual proteins (e.g. the addition of Cortactin, CARMIL/myosin, etc.)

8.1.3 Conformational probes

Since actin undergoes a conformational change in response to a change in nucleotide state (Belmont et al., 1999) we expect Arp2/3 to undergo an analogous conformational change. Several methods could be used to measure such a change:

8.1.3.1 Crosslinking

Our lab has previously used chemical crosslinking to successfully locate protein-protein interactions and conformational changes with Arp2/3 complex (Mullins et al., 1997; Zalevsky et al., 2001a). I attempted to examine an Arp2-Arp3 association using EDC-NHS crosslinking of Arp2/3 mixed with actin filaments. Our prediction was that Arp2 and Arp3 would come closer together upon shearing of the filaments, since this would capping is predicted to induce the Arp2-Arp3 heterodimer conformation. I saw no difference between the crosslinking profiles, but saw an Arp2-Arp3 crosslink in both conditions, suggesting that mother filament binding may be sufficient to bring Arp2 and Arp3 together, and that nucleation involves a more subtle conformational change after these subunits are already in contact.

A more thorough crosslinking experiment may help map the conformational changes that occur upon activation. Filament side-binding of Arp2/3 could

be blocked with a p35 antibody, or by filament side-binding proteins such as tropomyosin.

8.1.3.2 FRET

Attaching a FRET-pair of fluorophores to the complex at approximately the Förster distance allows read-out of conformational changes by changes in fluorescence lifetime and intensity. Previous studies using CFP attached to p21 and YFP attached to p40 Goley et al. (2004) demonstrated a conformational change upon VCA and nucleotide binding, but surprisingly, no further change upon nucleation. This may be due to the large relative size of the CFP and YFP conjugates—the activation of the Arp2/3 complex involves interaction with two actin filaments and these filaments may have physically separated the CFP and YFP, obscuring any further conformational change upon nucleation, or the fluorophores may have already been too far within the Förster distance.

Specific localized labeling of Arp2/3 complex with multiple FRET pairs using small molecule fluorophores would allow mapping of conformational changes without concern of disruption by the mother and daughter filaments or Förster distance constraints (and multiple FRET pairs are needed to map a conformational change by triangulation.) The logistics of achieving this are challenging, but a relatively simple way may be to remove endogenous cysteines, engineer specifically localized cysteines for the FRET pairs, and label with the two fluorophores at once. There will be a probabilistic distribution between singly labeled, doubly homogeneously labeled, and doubly heterogeneously labeled, from which the

conformational changes can be deconvolved. Single molecule experiments would also make it easy to distinguish the labellings.

8.1.3.3 Electron Microscopy

Egile et al. (2005) recently used antibody mapping of negative-stain EM to reconstruct the Arp2/3 branch structure which produced results in line with crosslinking data, and confirms that Arp2 and Arp3 interface with the daughter filament. The results of negative stain EM of Arp2/3 branches (Egile et al., 2005; Volkmann et al., 2001) remain disappointing, however, possibly due to interactions with the EM grid. The Arp2/3 branch is a planar structure, and the plane of the branch is forced into the plane of the grid, it would be expected to cause severe distortion of the branch. Cryo-EM of the branch may therefore be necessary to determine the true Arp2/3 branch structure.

8.1.3.4 Crystallography

The crystal structure of the Arp2/3 complex showed Arp2 and Arp3 separated, and speculated that they come together in the activated state to form a nucleus Robinson et al. (2001). The ultimate goal in understanding the conformational changes upon nucleation is to obtain a crystallographic resolution. This would also help uncover the trigger for ATP hydrolysis. One possible way of achieving this may be to crystallize the Arp2/3 complex bound to the pointed end of the daughter filament.

As yet, crystallizing filamentous actin has been impossible. The tendency to form filaments is incompatible with crystallization. A recent attempt (Dawson et al., 2003) was made to crystallize an actin trimer by crosslinking polymerized actin and disassembling with gelsolin. Unfortunately the gelsolin also disrupted the structure of the trimer.

A better way to crystallize an actin trimer (and later an actin trimer in association with Arp2/3 complex to determine the activated Arp2/3 complex crystal structure) may be to use solid-phase directional crosslinking. Actin monomers would be attached a solid-phase support via Cys 374, e.g. by crosslinking to biotin and using a streptavidin column where the streptavidin is reversibly linked to the matrix e.g. via a protease cleavage site. The EDC-NHS reaction can be performed in a directional manner, priming one side of the reaction components, then introducing the second so that self-crosslinking between the second component is eliminated. This would enable priming of the actin-streptavidin complex, then flowing in of actin monomers under polymerizing conditions to allow polymerization of actin from the actin-streptavidin complex. Washing the column would remove free actin and allow dissociation of uncrosslinked actin monomers. The process (priming, adding actin, washing) could then be repeated to crosslink the third (or more) actin monomer(s). The final species would be eluted by cleaving the streptavidin from the column, with the streptavidin remaining attached to the barbed end of the filament to prevent self association (annealing). This would then be gel filtered and crystallized.

The association (and directional crosslinking) of Arp2/3 with the free pointed end of this actin trimer may allow crystallization of the activated state the complex. A reverse approach, nucleating from crosslink-primed Arp2/3 complex may allow crystallization of activated Arp2/3 with its contact actin subunits.

8.2 Investigating Specific hypotheses

8.2.1 Does ATP hydrolysis on Arp2 causes VCA release?

We previously measured the affinity of Arp2/3 complex for VCA, finding this to drop for ADP-bound Arp2/3 compared to ATP-bound Arp2/3 complex (see section section 3.4.2). If VCA release is a physiological of ATP hydrolysis on Arp2, we would expect this difference in affinity to also be observed in the branch, and the difference be much greater than the 3-fold difference we measured for free complex. The challenge is to measure the affinity of VCA for branches, when the concentration of branches in our assays is usually ~1–2 nM.

8.2.1.1 Anisotropy

I initially attempted to measure the affinity of VCA for the branch by nucleating branches with labeled VCA and competing off with an excess of unlabeled VCA whilst monitoring the anisotropy. Our fluorescence anisotropy measurements are unfortunately not sensitive to such low labeled protein of (~1–2 nM). This experiment may work if the volume of the sample is increased or the equipment is changed in some other way to yield greater signal.

8.2.1.2 Bead force measurements

We postulate that the function of ATP hydrolysis induced VCA release is to allow Arp2/3 to travel away from a membrane-bound activator, or for ActA, a listeria-bound activator. Reconstituted motility experiments based on Loisel et al. (1999) have provided a means to investigate the attachment force by pulling the tail from a motile bead using an atomic force microscope (AFM) (Marcy et al., 2004). This yielded an estimate of $0.25\,\mathrm{nN\cdot\mu m^{-2}}$ for the detachement force under their conditions. Comparing wild-type and ATPase deficient mutants using this experiment, and normalizing for actin, Arp2/3 and VCA density is one way to determine whether ATP hydrolysis helps release VCA from Arp2/3 complex.

8.2.1.3 Single molecule release from VCA-coated slides

Fujiwara et al. (2002) measured the force of VCA–Arp2/3 attachment directly by growing branched actin filaments from VCA-coated slides and using an optical trap to pull individual branched from the slide, determining the detachment force to be 6–7 pN. This is a better way of measuring the attachment force than AFM measurements, since it is not dependent on actin meshwork density.

An simpler version of this experiment may be possible, by observing detachment of branches from the ActA coated coverslip without the optical trap. In this situation, some degree of flow would be required to prevent re-association with ActA on the coverslip, but the experiment should be tractible.

8.2.2 Does ATP hydrolysis regulate interaction with actin filaments?

Blanchoin et al. (2000b) made measurements of Arp2/3 debranching ki-
netics by observing the decrease in concentration of branches over time by mi-
croscopy of fluorescently labeled filaments. A simple extension of this experiment
would enable the measurement of Mother and Daughter filament debranching.
By fluorescently labeling Arp2/3 complex itself with a second color, we should
be able to determine whether the complex remains associated with the mother or
daughter filament following debranching. By comparing the effects of Arp2 and
Arp3 ATPase mutations, we can determine whether either of these subunits are
involved in regulating the separate debranching steps.

8.2.3 Is p21 the integrator of Arp2/3 activation signals?

In section 5.4, I outlined an argument for p21 being the key to the oper-
ation of Arp2/3 complex as an AND gate, integrating the signals from VCA and
the mother filament. Previous crosslinking studies show that the p35 and Arp3
subunits bind mother actin filaments, but not p21 (Mullins and Pollard, 1999b),
however these were conducted with unactivated Arp2/3 complex. To investigate
the possibility of an activation-dependent association of p21 with the mother fil-
ament, similar EDC-NHS crosslinking could be carried out and the appearance
of an actin-p21 crosslink upon nucleation be assayed. This is a somewhat chal-
lenging experiment, since the concentrations of Arp2/3 are low in a nucleation
reaction, but the trick of using latrunculin–bound actin to prevent polymerization

may allow this to be carried out. If there turns out to be an activation-dependent crosslink between p21 and actin, a next step would be to perform a more systematic docking of p21 to complex and the mother filament to determine the predicted structure of the activated complex, and perform mutagenesis of p21 to dissect the activation mechanism by specifically reducing binding to VCA and the mother filament. An attractive and simple hypothesis is that that there is a charge-charge interaction between the basic patch of p21 (Figure 8.2a) and the acidic patch of the actin filament adjacent (Figure 8.2b), but that these charges are unbalanced. This imbalance could be neutralized by the acidic residues the VCA acidic domain allowing filament docking. This hypothesis would predict that mutation of certain basic surface-exposed residues on p21 to neutral would not only make nucleation by activators with fewer acidic residues (e.g. SCAR1 VCA) more efficient, and nucleation by activators with more acidic residues (e.g. N-WASP VCA) less efficient, but would also increase the baseline activity of Arp2/3 complex.
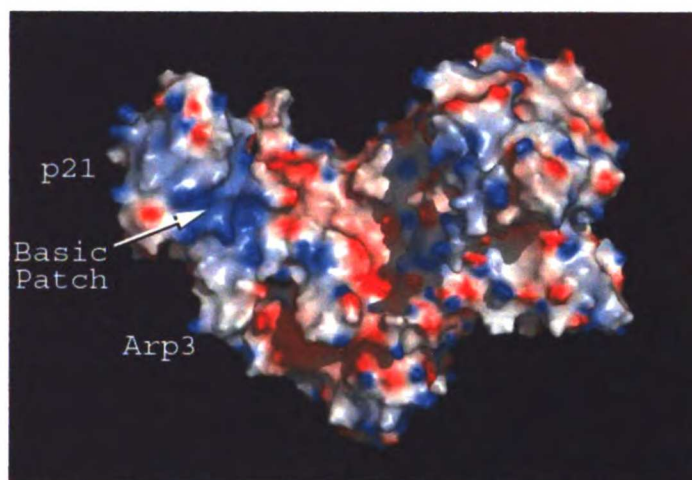
(a) Electrostatic map of Arp2/3 complex
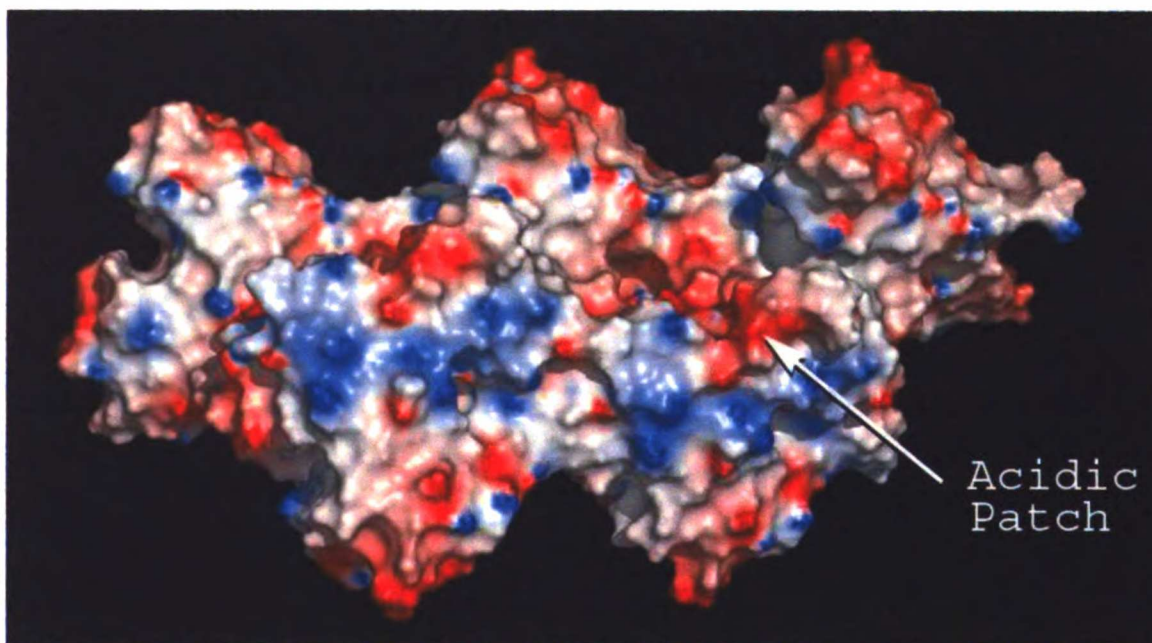
(b) Electrostatic map of actin filament

Figure 8.2: Electrostatic maps of Arp2/3 complex and actin filament (acidic=red, basic=blue). c.f. Figure 5.3 on page 80

Part II

Computational Model of the Mechanism of Force Generation by Actin Networks

Abstract

The goal of this study is to explain how eukaryotic cells move by determining the mechanism by which actin polymerization produces force on a *micron* scale—the scale of the structures created *in vivo*. A biochemical model system for force producing actin networks is *Listeria* motility. To reconstitute this minimal actin-based force generation system requires four components: Arp2/3 complex, actin, capping protein and an Arp2/3 activator on the surface to be pushed. The biochemical properties of these components are well known and the question of how these proteins could come together to produce force has yielded multiple models e.g. elasticity on sub-microscopic scale; elasticity on the mesoscopic scale; filament tethering and pushing; and squeezing.

The experimental system is underdetermined—we do not yet have enough data to eliminate any model nor distinguish the relative contributions of these different mechanisms to motility. Nor do we know the exact experimental questions to ask, because the models have hitherto been largely conceptual. Analytic treatments have been made, but the system is sufficiently complex that it us unclear whether the argued contributions are correct.

In this study, by systematically introducing the known properties of the actin system into a computer model, I will determine the specific requirements and contributions of these properties to force production.

Specific Aims

1. To generate a computational model that simulates the elastic and compressive properties of an actin network and determine whether mesoscopic elastic properties alone are sufficient to produce symmetry breaking, sustained force and directional motility.

2. Systematically introduce known properties of the system to evoke the spectrum of observed behavior, and determine their importance and redundancy, and design and conduct experiments to verify the model.

3. Explicitly add filament Brownian Motion and the Elastic Browinan Ratchet model to the elastic gel model and determine its effects and predict filament architecture under different load and concentration regimes

4. Apply the model to make specific predictions of how actin networks will behave *in vivo*. Predict the effect of e.g. membrane forces at the lamellipod, cellular crosslinking proteins, spatially regulated actin nucleation, and forces exerted by motor proteins on the biological function of actin networks.

Chapter 9

Introduction

9.1 Actin polymerization generates motile force

Listeria Monocytogenes is a commonly used model system for investigating the way actin polymerization produces force. This intracellular bacterium usurps the actin machinery of its host cell to propel itself on an actin 'comet' tail and invade neighboring cells. Loisel et al. (1999) have shown that production of motile force does not involve motor proteins such as myosin but originates directly from the polymerization of actin.

Electron microscopy of the *Listeria* tail reveals a dense network of actin filaments. Actin networks that result in motility are assembled by the Arp2/3 complex (Pollard and Borisy, 2003) which forms dendritic arrays by nucleating new filaments from the sides of existing filaments to form branches at angles of ~70°. As explained in detail in Part I, before it will nucleate a branch, Arp2/3 complex requires an existing actin filament to branch from and an activator protein. Na-

tive Arp2/3 activators are tightly regulated, but *Listeria* expresses a constitutively active activator of Arp2/3 complex, ActA, on its surface (Welch and Mullins, 2002) allowing investigation of the force generation system independent of complications from upstream signaling events.

Three components, in addition to ActA on the Listerium itself, are required for *in vitro* reconstitution of motility: Arp2/3 complex, actin monomers and capping protein (Loisel et al., 1999). Activated by ActA at the surface, Arp2/3 complex nucleates filaments into a branched array. Capping protein caps growing actin filaments, preventing them from polymerizing, effectively restricting actin polymerization to the sites of new nucleation, and reducing the average lengths of individual filaments.

9.2 Experimental Observations

9.2.1 Filament and Network Elasticity

Actin filaments are semi-flexible polymers with a persistence length of ~9 μM (Liu and Pollack, 2002). Individual actin filaments stabilized with the mushroom toxin phalloidin have biphasic length-tension relation, nonlinear within a low-tension range of 0–50 pN (~0.5% resultant strain), becoming linear in the range 50–230 pN and in the linear range, a 1 μM filament has a stretching stiffness of ~35 pN/nM (Liu and Pollack, 2002). Isambert et al. (1995) used thermal fluctiuations to measure the relative persistance lengths of phalloidin, ADP-BeF₃, and ADP –bound actin filaments and found 18, 13.5 and 9 μM respectively, suggest-

ing that phalloidin filaments are flexurally more rigid than unstabilized filaments, and that upon phosphate release, the filament becomes even more flexible. Extensive measurements of the tensile strength of phallodin stabilized actin filaments have been carried out, yieling breakage strengths of ~430 pN (Tsuda et al., 1996). Unfortunately, the subunit dissociation constant is dramatically reduced by phalloidin, and this is likely to be the primary determinant of yield strength and flexural rigidity, phallodin-free actin filaments yielding tensile strengths of ~3.5 pN (Adami et al., 2003). *In vivo* tensile strength is likely to be some intermediate value (Grazi et al., 2004). The tensile strength of the Arp2/3–actin bond has been shown to be >6 pN (Fujiwara et al., 2002) and probably much higher.

The actin network nucleated by *Listeria* is elastic. Measurements of the mechanical properties of the *Listeria* tail using optical tweezers (Gerbal et al., 2000b) and micromanipulation (Marcy et al., 2004) show the tail to behave as an elastic gel with a Young's modulus of 10^3–10^4 Pa. The elastic properties and tensile strength of the actin network likely play an important role in the mechanism of force generation and the mechanism of actin-based motility.

9.2.2 Bead motility and symmetry breaking

Asymmetric distribution of the ActA protein on the *Listeria* surface biases actin polymerization to one end of the rod-shaped bacterium and defines the direction of motility (Kocks et al., 1993). A simplified system replaces the *Listeria* with spherical beads coated with a symmetric distribution of ActA (Cameron et al., 1999). These beads polymerize a symmetric actin shell and under cer-

tain conditions, this shell eventually fractures resulting in an asymmetric actin distribution—a process known as 'symmetry breaking'. The bead then moves on an actin comet in a way similar to *Listeria* motility (Bernheim-Groswasser et al., 2002). The time required for symmetry breaking to occur is observed to increase linearly with bead diameter, and for larger beads (> 3 μM diameter), the bead motion after symmetry breaking becomes irregular, with repeated apparent shell formation and shell breakage. Although *Listeria* has a cylindrical diameter of ~ 0.5 μM a similar behavior is seen with a mutant ActA which produces a 'hopping' Listeria phenotype. Bernheim-Groswasser et al. (2002) proposed that the actin shell around the bead behaves as an elastic gel, with Young's modulus C and breaking stress $\sigma_{\theta\theta}^c$. Assuming constant polymerization velocity at the bead v_p, this reduces to a linear relation, as observed, between time to symmetry breaking t_c and bead radius R:

$$t_c = \frac{\sigma_{\theta\theta}^c R}{v_p C}$$

For motility to continue in the same direction, the same asymmetry must be maintained after symmetry breaking. One possibility is that asymmetry is maintained by an asymmetry in polymerization due to positive feedback: i.e. more actin is polymerized on the side of the bead with more actin. In solution experiments, Arp2/3–mediated nucleation is a process dominated by positive feedback (Zalevsky et al., 2001b) because Arp2/3 complex requires existing filaments to branch from. In the bead motility experiments, ActA is distributed evenly across the bead but the tail, once formed, is asymmetric. The asymmetric distribution of

actin could drive an asymmetric activation of Arp2/3, re-inforcing the asymmetry. It is unclear whether this is the case, or whether it is required for motility.

9.2.3 Tail attachment and stepping motions

Motile *Listeria* and beads are firmly attached to their actin tails with a strength > 10 pN (Gerbal et al., 2000b). Using *in vivo* laser tracking microrheology Kuo and McGrath (2000) have shown that *Listeria* undergo discrete stepping motions of ~5 nM. Firm attachment to the tail is thought to occur by ActA directly interacting with actin filaments or interacting with Arp2/3 complex in the tail.

9.2.4 Vesicle motility and squeezing forces

Vesicles have also been shown to display actin-based motility *in vivo* similar to *Listeria* and beads (Taunton et al., 2000). *In vitro* experiments with ActA coated vesicles by Giardini et al. (2003) show that the vesicles are deformed in a way consistent with squeezing forces driving the vesicles forward. Forces calculated from bead deformation. This suggests the vesicle experiences significant retrograde as well as anterograde forces and that the small imbalance results in motility. This hypothesis is in line with the symmetry breaking model proposed by Bernheim-Groswasser et al. (2002) and supports the elastic gel model (Gerbal et al., 2000a).

9.3 Target behavior for models

9.3.1 Essential behavior

There are several essential observed behaviors that a model for *Listeria* and bead motility must produce:

- Build-up of a symmetric actin shell
- Symmetry breaking
- Higher actin density in shell than tail
- Linear dependence of time to symmetry breaking on bead diameter
- Pulsatile motion at large bead diameters
- Sustained directional motility
- Discrete stepping motions
- Tail attachment
- Squeezing Forces at edge of tail
- Rearward forces at center of tail

9.3.2 Predictive power of model

The models should also produce qualitative and testable explanations for the following behavior:

- The mechanism of tail attachment
- The cause of nM stepping motions
- The cause of squeezing and rearward force
- The robustness and sensitivity of motility to parameters e.g.

  - Diameter of bead

- Network elastic properties (e.g. modified by crosslinking proteins)

- The positive feedback of the actin nucleation reaction (e.g. modified by asymmetric vs symmetric distribution of ActA)

9.4 Existing models for actin-based motility

Two complementary theoretical models to explain force generation have been proposed and refined over the last few years. Both models link the free energy of polymerization and elastic properties of actin to the generation of motile force, but operate on different spacial scales. A third, computational model has recently been introduced.

9.4.1 The Elastic Tethered Brownian Ratchet Model

Mogilner and Oster (1996) propose a mechanism by which force could be produced by actin polymerization purely considering processes occurring on a microscopic ($x < 100$ nM) scale. In this model, actin filaments are nucleated by Arp2/3 complex at the Listerium surface. Filaments are theorized to encounter the surface at ~35° (half the 70° branching angle created by Arp2/3 complex) and thermal bending motion of the individual filaments causes the tips to transiently move away from the surface. The gaps thus created would allow actin monomers to polymerize onto the ends before elastic recoil would drive the tips of the filaments back into contact with the Listerium surface. Due to the elongation of the filament, the filament would no longer fit, and the elastic restoring force push on

the surface of the Listerium, driving it forwards. In a minor update to this model, Mogilner and Oster (2003) add explicit ActA-tail binding interactions are added to cause tail attachment and keep the model in line with the observed data.

9.4.2 The Elastic Gel Model

Gerbal et al. (2000a) propose a mechanism by which the relaxation of elastic energy on a mesoscopic scale $(100\,nM < x < 5\,\mu M)$ may generate motile force. In this model, actin polymerization at the surface of the Listerium would create a crosslinked network that behaves as an elastic gel. Material polymerized at the surface would push older material out, stretching it and building up elastic energy. To release this energy, the Listerium is driven forwards, allowing the elastic gel to collapse. This model is known colloquially as the 'soap-squeezing' model.

9.4.3 Alberts model

A recent computational model (Alberts and Odell, 2004) has been used to simulate *Listeria* motility. This model simulates nucleation of actin filaments at one end of the Listerium, and models actin filaments as rigid rods that become locked immovably in space. In this model the bacteria experiences random Brownian forces in all directions, but lateral movement is prevented by a rigid sleeve of actin filaments that form a cylinder around the bacterium. Retrograde diffusion of the bacterium is prevented by the immovable actin filaments at one end, but anterograde diffusion is uninhibited—resulting in linear motion of the Listerium. The introduction of an elastic ActA-filament attachment also produced

stepping motions as attachments are built up and catastrophically broken. The weaknesses of this model are that it violates the known elastic properties of both actin filaments and the network, the known diffusive behavior of the bacterium, the known requirement of existing filaments for Arp2/3 nucleation, and by its assumption of immovable, inflexible filaments, rules out the contribution of elastic energy to motility.

Chapter 10

Plan for the computational Model

10.1 My starting hypothesis: Motility by steady-state symmetry breaking

10.1.1 Sustained motility by steady-state symmetry breaking

My hypothesis for the mechanism of bead (and *Listeria*) motility is essentially an extension and modification of the elastic gel model proposed by Gerbal et al. (2000a) and the symmetry breaking model proposed by Giardini et al. (2003).

I propose that sustained bead motility is nothing more than steady-state symmetry breaking. The first step in this model is identical to that described by Giardini et al. (2003) i.e. material is symmetrically deposited on the bead surface, tension builds up and the network eventually ruptures. Once symmetry is broken, however, actin continues to be deposited symmetrically on the bead surface. Asymmetry is maintained by the asymmetric distribution of the existing network: one side the network is in contact with and stabilized by the old shell, and will therefore be more difficult to deform. As elastic energy builds up once more, the thin shell (relative to the initial symmetry breaking shell) immediately rips along its weakest point: opposite the original shell. This ripping continues in a steady state manner as motility is sustained.

10.1.2 Predictions of this hypothesis

1. That explicit attachment between the bead and the tail in the form of actin–ActA or Arp2/3–ActA binding is not necessary. The network will form a 'ball-

and-socket' attachment to the tail: removal of the bead from the tail would require energy to rip open this 'socket'. This would predict the attachment of the tail to a hemispherically coated bead to be weaker than a spherically coated bead.

2. That the stepping motions may be caused by filaments at the front of the bead tearing: This would predict that stepping motions would be observed with spherically coated beads, but not at all with hemispherically coated beads. All other models include explicit tail attachments via ActA and predict stepping in both cases.

3. That the erratic motion of beads and the 'hopping' of *Listeria* is caused by temporary build up and breakage of partial shells at the front of the bead.

4. That the forces that act on vesicles to cause the tear-drop shape are caused not by 'squeezing' per se (i.e. the relaxation of lateral gel stress), but an asymmetric steady-state symmetry-breaking (i.e. compression in all directions relative to the network but relieved directly at the rear since the relative bead velocity is maximal and negative at this point.

10.2 Testing the hypothesis *in silico*

To test my hypothesis, I will develop a computational model to determine whether motility can be reconstituted from only these basic properties of the network. By using a computer simulation, I can explicitly simplify the model as

much as possible and will be left with the essential components that are absolutely required for motility. I can also introduce more aspects to evoke more esoteric behaviors such as stepping etc. I will implement the models in stages of increasing physical accuracy and complexity. Each stage will have a specific goal.

10.2.1 1st Generation Model: Implementation of the elastic network

Objective: To determine if the mesoscopic elastic network properties alone are sufficient to cause symmetry breaking and motility

The first stage model will be the simplest, implementing a bare minimum of physical behaviors. The goal of this model will be to determine the minimal set of undeniable physical properties that will reconstitute the behavior of symmetry breaking and sustained motility. I will therefore assume that the network behaves as an elastic material with finite compressibility and the has a finite tensile strength.

I will also explicitly reduce the likelihood of being able to re-create bead motility if the hypothesis is false by assuming:

- there is no explicit attachment between the bead and the tail: the bead is essentially frictionless

- there is no positive feedback to cause greater actin polymerization at the side of the bead with a higher concentration of existing actin

- the crosslinking of the actin network is spatially isotropic

(a) First Generation Model showing node connectivity for two nodes represented by coloured links

(b) Third Generation Model showing Arp2/3 branches (green nodes), capped filaments (red nodes) and entanglement (blue node)
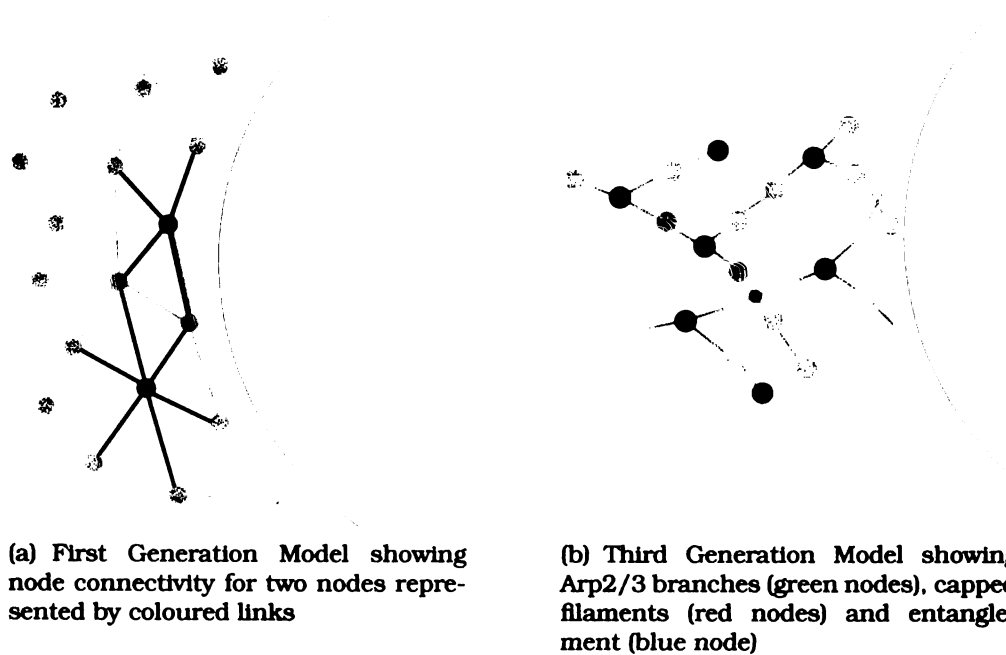
Figure 10.1: Conceptual illustration of first and third generation models

The elastic material will be deposited at the surface of a bead or Listerium, becoming crosslinked to adjacent material to form a network (Figure 10.1(a)). This crosslinking represents both individual actin filaments linking one area to another directly and also the entanglement linking filaments that are not directly attached. This material will have finite compressibility and finite strength, thereby allowing buildup of elastic energy, network fracture and release of that energy.

10.2.2 2nd Generation Model: Introduction of network anisotropy

Objective: To refine the elastic model including the effects of network anisotropy and long-distance filament crosslinks

The second generation model extends the first by introducing additional physical properties of the network, but again in a simplified way. Polymerization rate at the bead surface will be reduced as pressure increases. Attachments between the bead and the tail will be modeled as adhesive properties, and the anisotropy of the network will be introduced:

The actin network is composed of filaments which inherently have polarity. Filaments are nucleated with their fast-growing 'barbed' ends towards the nucleator surface and by electron microscopy it appears that there is a tendency for filaments to have some alignment in the direction of motility. During the formation of the initial shell, it is assumed that filaments will align more parallel to the surface, under compressive pressure from the outer layers.

The second generation model will incorporate anisotropic crosslinking and tensile strength, in order to incorporate the anisotropic nature of filaments. This model will also be extended to allow for longer, flexible crosslinks that behave more like filamentous material. Bead motility nucleated by the ParM–ParR–ParC system (Garner, Campbell and Mullins, unpublished observations) appears similar to actin-nucleated bead motility except that the tails appear to contain long unbranched filaments that tightly bundle, and that motility ceases with a large concentration of filaments at the front of the bead, as though the bead is entan-

gled and halted in its motion. We will begin modeling this behavior using isotropic filament-like crosslinking.

10.2.3 3rd Generation Model: Filaments and crosslinks

Objective: To explicitly add filament Brownian Motion and the Elastic Brownian Ratchet model to the elastic gel model and determine its effects and predict filament architecture under different load and concentration regimes

The isotropic nature of the material as simulated crudely in the second generation model will be simulated explicitly here by introducing directionality and polymerizability to each node.. The nodes will represent junction points on filaments. The direction vector of a node will represent the direction of polymerization. New nodes will form linked to existing nodes, with their direction vectors aligned with the link and with the position of nodes restricted by physical curvature of actin filaments (Figure 10.1(b)). Linked nodes will experience a restoring moment proportional to the angular difference in the direction vectors, except in the following case: If within range of an ActA molecule, there will be a certain probability of branch formation. This will be represented by two new nodes linked to the existing node, on in line with the original direction vector and the second at a 70° angle. This node will have a restoring moment towards this 70° angle. Filament capping will be simulated by preventing polymerization and branching. Explict tail attachment will be modeled directly. Entanglement of will be modeled by calculating the trajectory of filaments as they are nucleated and determining

their proximity to other nearby links. If links are crossing, half will be modeled as entangled by introducing a special node at the crossover point, shared by both 'filaments'.

Once implemented, this model will also allow us to incorporate more complex behaviors, such as the effect of anti-capping factors such as vasp which appear to be able to invoke another regime of motility in which Arp2/3 based branching does not occur, motility is 10 times faster and the comet tails are hollow Plastino et al. (2004).

The advantage of this method is that it will be possible to simulate very advanced morphologies of actin filaments, incorporate elongation rates measured by kinetic experiments, physical properties of individual filaments, but to do so with very little computational resources, since filaments are still simulated as nodes and not individual molecules.

10.2.4   4th Generation Model: Extension to other cellular geometries

Objective: To extend the model to cellular geometries, predict mechanisms of force generation *in vivo*, **and incorporate additional network proteins**

Lastly, we will extend the model by incorporating the effects of different cellular geometries: e.g. Flat lamellipodia involved in cell motility and macropinosomes involved in phagocytosis. The effects of membranes will be modelled in their effect of compressing and resisting deformation forces exerted by the network.

The effect of crosslinking proteins will also be modelled as reversible changes in crosslinking properties dependent on local geometries.

Chapter 11

Implementation of the Model

11.1   General Principle

The `comet` program is a Monte-Carlo/Lagrangian model that calculates the 3 dimensional positions of a large number (1000's) of 'nodes' representing material in an actin network. For each timestep `DELTA_T`, nodes move a displacement proportional to the force acting upon them. There is no inertia, since this is a low Reynolds number regime. The forces actin on each node are as follows:

- Repulsive forces between nodes

- Link forces between nodes

There is also an imposed incompressibility of the nucleator object. This is implemented as a *displacement* rather than a force: e.g. if a node enters the nucleator due to other forces, then in the next iteration, it is simply moved out of the nucleator along a normal to the nucleator surface.

Nodes are nucleated at a constant rate, proportional to `P_NUC`, at the nucleator surface. A new node has its `harbinger` flag set and while a harbinger it experiences only repulsive forces to allow it to find an equilibrium position (for `CROSSLINKDELAY` iterations) before being crosslinked into the network. Crosslinks are formed as follows: All nodes with within `XLINK_NODE_RANGE` are counted, and links are formed at random until the number of crosslinks reaches `MAX_LINKS_PER_NODE`. Once a link is formed, its original distance is stored and used to calculate link forces. If the link is stretched or compressed away from its original length it behaves as a Hooke's Law spring and excerts a force proportional to, and opposing,

the displacment. The scale factor for this force is LINK_FORCE. This is to simulate an actin filament acting as an entropic spring by flexing motions. If the link is stretched beyond a certain factor of its original distance (LINK_TAUGHT_RATIO) it becomes 'taught' and exerts a much greater force, proportional to the product of the distance beyond the taught distance and LINK_TAUGHT_FORCE. If for any reason the link force exceeds LINK_BREAKAGE_FORCE then the link breaks.

The nucleator is allowed to move, subject to a vector equal and opposite to the summed node repulsion from the nucleator, and scaled by the nucleator 'movability'. Movement of the nucleator is really implemented as movement of the nodes in an equal and opposite displacement. The position is kept track of in a vector that is used to displace the reference frame when generating bitmaps etc.

Output files are saved as jpgs for the x,y and z projections (convolved with a gaussian to make it look like a microscope image) and wrz (gzipped vrml wrl file) for 3D viewing of the nodes in a web browser.

Note: the program calls the Imagemagick convert program to add text to the images and save as jpgs and calls gzip to compress the vrml and text files.

11.2 Implementation in C++

The current implementation is very hodge-podge, and is not really object oriented at all. There are nominal attempts to use an object-based approach. A good many of the member variables are declared globally static to allow their access across threads.

Here is a breakdown of the main functions in the program. There are numerous other functions that do housekeeping tasks, or are not finished yet and are not included, but this is the core of the program:

- Main()

  - Spawns threads. Always spawns the `compressfilesthread`, can spawn other threads: `collisiondetectionthread`, `linkforcesthread` and `applyforcesthread`

  - Parses the `comet_params.ini` file to read parameters. All of the parameters are implemented as globals

  - Creates the main `theactin` and `nuc_object` objects.

  - Runs through the main iteration loop, calling `theactin.iterate()` and saving snapshots every so often.

- Actin class

  - There is only one actin object, `theactin`, which contains the nodes and the functions that deal with them

  - The `iterate()` function does one iteration pass, calling:

    * `ejectfromnucleator()` displaces any nodes out of the nucleator object along a normal to the nucleator surface

    * `nucleate()` adds new harbinger nodes to the surface of the nucleator

    * `crosslinknewnodes()` crosslinks harbingers once they are ready

* `sortnodesbygridpoint()` orders nodes by gridpoint. The *only* reason for this is for the division of labor when using threads: We do repulsion by gridpoint to save re-calculating nearby nodes if there are multiple nodes on one gridpoint, and we do not want to divide nodes on one gridpoint across multiple threads. [This is probably not helping at all at the moment. The grid resolution may be completely wrong.]

* `collisiondetection()` detects whether nodes are within `NODE_REPULSIVE_RANGE` of one another and adds the repulsive force to `rep_force_vec[]`. If nodes are also within `NODE_INCOMPRESSIBLE_RADIUS`, adds ejection to `repulsion_displacement_vec[]`. Currently adds equal and opposite to each pair of nodes. This shouldn't be necessary, but on safe side in case any asymmetry at the moment.

* `linkforces()` Calculates the forces between nodes due to links and puts into `link_force_vec[]`. If a link goes above a certain threshold force, marks it as broken and removes next time (again to prevent thread problems—since a link is removed both ways and we can't guarentee that both nodes are being processed by same thread)

       * `applyforces()` updates the positions of all the nodes. Sums over the threads for `rep_force_vec[]`, `link_force_vec[]` and `repulsion_displacement_vec[]`.

- Numerous other functions for little things like saving bmps, vrml etc.

- Nucleator class

  - There is only one nucleator object, `nuc_object`, which is closely linked to the actin object

  - The nucleator is either a sphere or a capsule (i.e. a sphere with a cylindrical segment stuck in the middle).

  - `addnodes()` adds harbingers to the surface of the nucleator. The probability of addition of nodes is normalized by surface area and is symmetric if `ASYMMETRIC_NUCLEATION` is zero, or asymmetric if 1 or 2 (stepped or linear bias)

  - `definenucleatorgrid()` sets a list of gridpoints to check in case of nodes entering the nucleator. Called once at the beginning.

  - `iswithinnucleator()` returns true if the node is within the nucleator

  - `collision()` moves a node out of the nucleator along a normal vector

- Nodes class

  - Nodes exist only as members of the actin object

- `nodegrid` (now global) is a 3 dimensional C++ vector of node pointers. Each nodegrid entry starts a circularly linked list of nodes representing the nodes within that gridpoint voxel.

- The actin class contains a vector of nodes. Each node has an associated `nodenum`, `x` `y` and `z` position, `nextnode` and `prevnode` node pointers for the nodegrid linked list, `rep_force_vec[]`, `link_force_vec[]` and `repulsion_displacement_vec[]` as described above, the grid position of the node, `harbinger` and `polymer` flags and a `listoflinks` i.e. a vector of link object which attach this node to other nodes.

- `polymerize()` Creates a node as a harbinger. Adds its pointer to the gridpoint linked list.

- `depolymerize()` Removes a node, deletes all links and removes from grid.

- `setgridcoords()` Calculates new grid co-ordinates based on x,y,z position

- `addtogrid()` adds the node to the current gridpoint

- `removefromgrid()` removes node from the grid

- `updategrid()` checks to see if node has moved gridpoints, and updates grid is needs to

- `removelink()` removes the specified node from the list of links

- Links class

- Links exist only as members of the node objects

- Each link has an associated `linkednodeptr` which points to the target node that the link is to and a `broken` flag which is read by `actin::linkforces()` and tells it to delete the link if it broke.

- `orig_dist` and `orig_distsqr` store the original distance of the link (and the square of that in a misguided attempt to avoid taking square roots.)

- `breakcount` stores the number of consecutive iterations the link force has been above `LINK_BREAKAGE_FORCE` and is used to increase the probability of breakage

- `getlinkforces()` returns the force acting on the link. Also sets the `broken` flag and increments `breakcount` if appropriate

Chapter 12

Results

12.1 Preliminary Results

I have implemented the first generation model in Ansi C++. Material is represented as a network of nodes as shown in figure 10.1(a): spatial node density correlates directly with network density. Nodes are deposited randomly on the surface of the nucleator at constant rate (the nucleator is a rigid sphere or capsule, to simulate a bead or Listerium). Nodes exert a repulsive force against one another and cannot enter the nucleator. New nodes crosslink to existing nodes if any are close by. Crosslinks behave as Hookes Law springs with equilibrium length equal to the length of the original crosslink. If the tensile force of a crosslink exceeds a certain limit, the link breaks. Data is output at at regular intervals both as 3D coordinate files (VRML) and X, Y and Z projections calculated by convolving the node distribution with a gaussian representing a microscope point spread function.

12.1.1 Shell buildup, symmetry breaking and directional motility

Initial simulations produced by the model have yielded excellent results. A symmetric shell of material is of course produced under all conditions tested. Many sets of parameters conditions I have tested result in plastic deformation of the shell, and maintenance of symmetry with shell growth balanced by continual approximately symmetric link breakage. By varying crosslinking strength and range I have determined a set of gel properties that produce shell fracture and persistent motility (Figure 12.1).

The behavior of the model, specifically the movement of the network material during symmetry breaking and motility mimics the observation of the experimental *in vitro* motility system remarkably well. There is shell recoil and the subsequent motility is smooth and in a constant direction. This result shows steady-state symmetry breaking model as a reasonable explanation of motility. Occam's razor supports this hypothesis: Behavior which replicates the experimental results is produced by simple deposition of an elastic network with finite strength at the surface of the bead.

12.1.2 Pulsatile motion

Currently the visco part of the 'viscoelastic' network is implemented relative to the lab reference frame. I.e. the viscous drag on each part of the network is not relative to the neighboring parts of the network. This is a first approximation for reasons of simplicity of implementation, and will be refined later.

Lowering this viscous drag coefficient makes it easier for the nodes to move. Running simulations with a lower viscous drag leads to pulsatile motion which is particularly interesting because under certain conditions pulsatile motion on these spatial scales has been observed by experiment (Bernheim-Groswasser et al., 2005, 2002). Figure 12.2 shows how the bead velocity vaires over time for three different viscosities. At high viscosity (Figure 12.2a), the bead velocity gradually builds up as symmetry breaks and reaches a constant steady-state velocity. As viscosity is lowered the bead velocity becomes more chaotic, with some continued motion, but some sporadic bursts (Figure 12.2b). This corresponds to some

(a) Frame 86

(b) Frame 138

(c) Frame 223

(d) Frame 314

Figure 12.1: Symmetry breaking and directional motility of a spherical bead

(a) High viscosity   (b) Medium viscosity   (c) Low viscosity
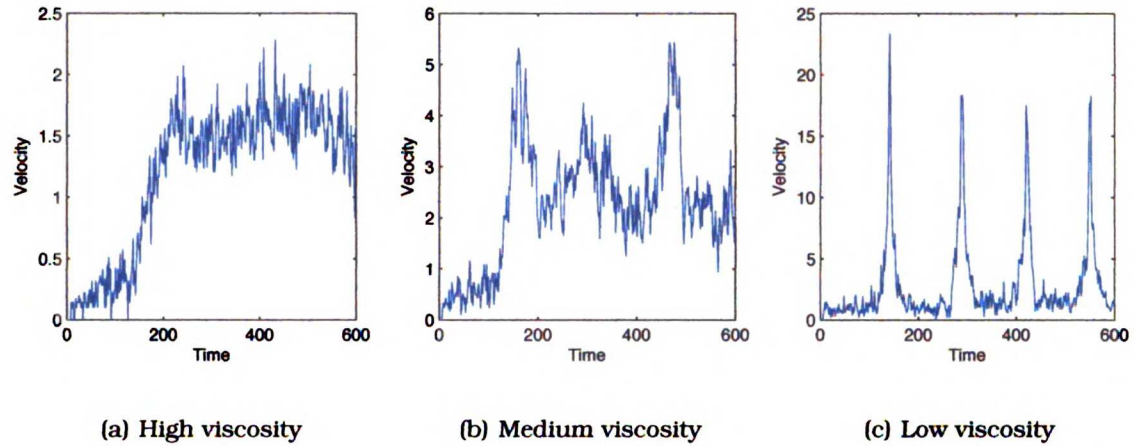
Figure 12.2: Whether motion is smooth or pulsatile depends on viscosity

steady-state symmertry breaking, but in the times where velocity is low, a new shell can be observed building up, and the peaks in the velocity correspond to the breaking of these partial shells. Lowering viscosity still further (Figure 12.2c) produces a very regular pulsatile motion, as each shell builds up, breaks, and is completely ejected.

This same switching behavior between smooth and pulsatile motion can also be produced by changing the nucleation rate (rate of material production at the bead surface). For a high viscosity that produces smooth motion, decreasing the rate of nucleation will cause it to become pulsatile, and for a low viscosity that produces pulsatile motion, increasing the nucleation rate will cause it to switch to a smooth motion. This relationship between viscosity and nucleation rate reveals the cause of the switching: the relative balance between the kinetics of energy build up (by deposition of material) and energy release (by node move-

(a) High viscosity   (b) Low viscosity
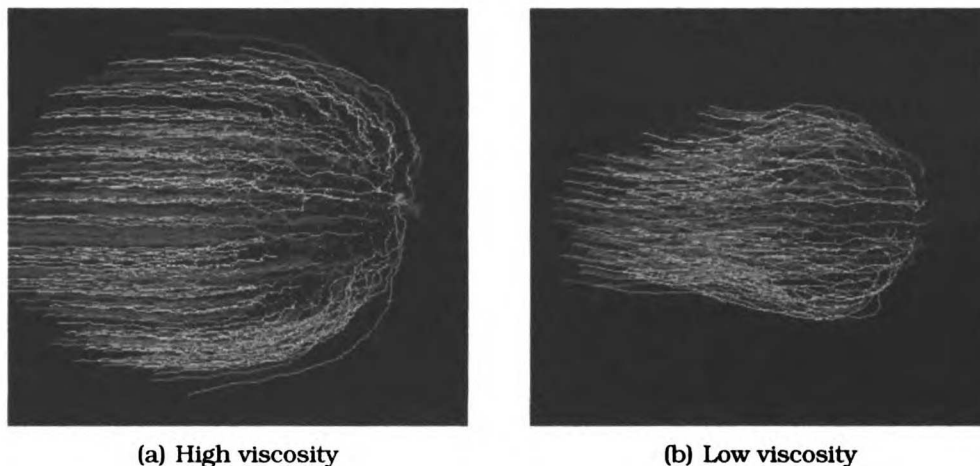
Figure 12.3: Node trajectories upon bead movement. Note for (a) this movement is constant but for (b) the movement is transient and pulsatile—most of the time the bead is stationary.

ment). When the kinetics of energy release are fast (i.e. low viscosity) the network can move quickly and the network can quickly reach its equilibrium state. When a symmetric shell is building up, equilibrium cannot be attained, since the route to equilibrium (collapse of the shell) is blocked by the bead. As soon as symmetry is broken there is elastic collapse of the shell and ejection of the bead—under low viscosity conditions this happens quickly, under higher viscosity conditions, more slowly. If this equilibration happens sufficiently quickly compared to the nucleation rate, then the system is essentially nearly completely at equilibrium by the time new elastic energy (new material) is introduced, and the process repeats (Figure 12.2c). For a high viscosity situation where the material moves slowly this does not occur. New material and new elastic energy is introduced before the bead has fully escaped the old shell, and an steady-state disequilibrium is reached in

which the shell recoils at a constant rate that balances the input of new material (Figure 12.2c).

The behavior of the network itself as the bead moves is not only fast, but is qualitatively different under low viscosity conditions. Figure 12.3 shows the trajectories of nodes from as the bead moves under high and low viscosity regimes. Whereas in the high viscosity regime, the material expands away from the bead, under the low viscosity regime the rapid symmetry breaking allows the stretched elastic shell to collapse after the bead moves out of the way, producing a squeezing motion.

Bernheim-Groswasser et al. (2005) recently characterized the regimes in which beads move under smooth or pulsatile motion. Although changing network viscosity experimentally is not possible, one of their experimental results is that beads will switch from pulsatile to smooth motion upon increasing the surface density of the nucleator ActA. This supports the result of the model that increasing nucleation rate can compensate for low viscosity and lead to smooth motion, and supports the steady-state symmetry breaking hypothesis.

12.2 Listeria

motility

Listeria are observed to move along thier long axis, driven by actin polymerisation in a similar way as described for beads. The capsule geometry of listeria

(a) Frame 50

(b) Frame 128

(c) Frame 141

(d) Frame 155
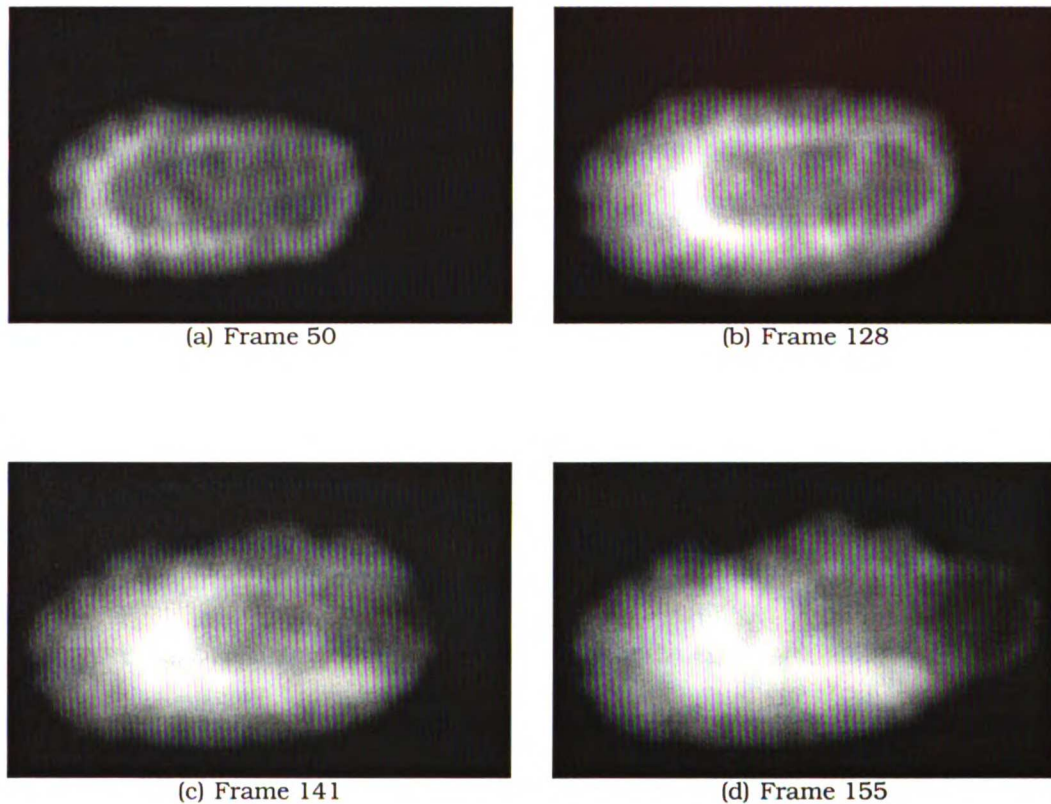
Figure 12.4: Model of motility of asymetrically coated listeria

introduces an asymmetry into the system and allows us another way to investi-gate the forces leading to symmetry breaking and motility.

ActA is asymmetrically distributed on the Listerium surface (Rafelski and Theriot, 2005; Smith et al., 1995). A linear density distribution of nucleator on a capsule geometry produces linear listeria motion in the direction of the long-axis (Figure 12.4). The shell naturally breaks at its weakest point, on the end with lowest nucleator density, and motility continues from there.

Using a symmetrically coated listeria geometry produces a different behavior. Instead of symmetry-breaking and moving lengthways, the symmetrically coated capsule breaks symmetry along its side and moves sideways (Figure 12.5a–d). Based on the model of the rate of stress buildup being higher for higher curvatures (Bernheim-Groswasser et al., 2002), this might initially seem a surprising result since the ends of the listerium clearly have a higher curvature (the ends are hemispheres, so have 2-dimesional curvature as opposed to the cylindrical long axis which is only has one dimensional curvature).

Careful observation of the motion of the actin network immediately prior to symmetry breaking reveals the cause of the sideways symmetry breaking and motion. (Figure 12.5e) shows the trajectories of the initial shell as it is pushed away from the listerium surface by deposition of material on the surface. The nodes that are part way toward the ends of the listerium are being drawn toward the ends as they are pushed out. This is due to the higher strain build up caused by the higher curvature of the ends being relieved by stretching the linear section of the network. The circumferential strain on the cylinder, however, although it builds up slower does not have a linear section and so does not get relieved. Without this strain relief, the highest strain is circumferentially around the cylinder, and this is where symmetry breaks. Motion continues in a sideways direction by a similar mechanism of steady-state symmetry breaking.

(a) Frame 50

(b) Frame 128

(c) Frame 141

(d) Frame 155

(e) Node trajectories for symmetrically coated listeria just before symmetry breaking
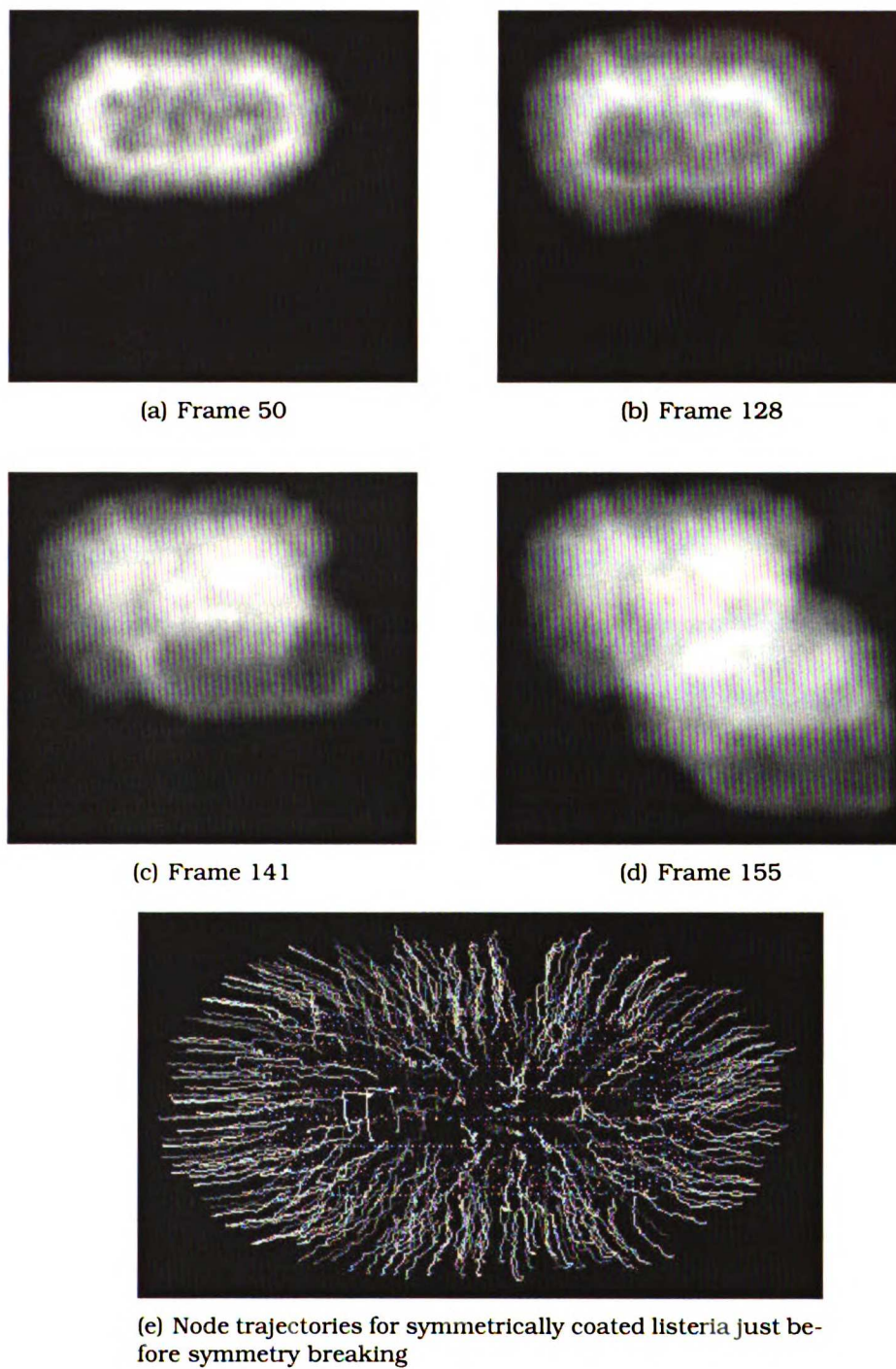
Figure 12.5: Model of motility of symetrically coated listeria

This result suggests that the skidding listeria phenotype seen by the skidding ActA mutant (residues 231-238 to alanine mutation) Lauer et al. (2001) may have caused a defect in ActA localization leading to sideways motion seen *in vivo*.

12.3 Future Directions

The above results are produced with a first pass at the first generation model. The future plans are to implement the other 3 generations, but short term goals for are the incorporation of explicit bead attachments and true network viscoelasticity.

These simulations have led to a number of experimentally testable ideas. For example, we are currently investigating the behavior of actin polymerized from elliptical and capsule-shaped geometries. Does the movement of the real actin matches our predictions in Figure 12.5e? And does the switch from smooth to pulsatile motion correspond to a switch from an extrusion to a squeezing motion of the network as in Figure 12.3? Data from these experiments will allow us validate the model, and use it as a way to understand these complex emergent behaviors.

Conclusions

The Arp2/3 complex represents a molecular device that bridges the gap between the worlds of biochemistry (a protein), information (functioning as a molecular AND gate) and the physical (co-ordinating the building of higher-order structures). Much remains to be understood about the Arp2/3 complex, but we currently have a good understanding of its basic functioning.

The use of computational models to help us understand the emergent behavior of biochemical and cell biological systems is in its infancy. The actin cytoskeleton represents an ideal starting point for such models—the physical properties of viscoelastic networks are well understood from the field of materials science, the interactions of the components are understood from our biochemical experiments and the biophysical properties are currently being revealed. Such systems are sufficiently complex that rigorous simulations are required to show the validity and robustness of any explanations put forth. These simulations represent the beginnings of our understanding of cell biology as an integrated system.

Bibliography

Abdul-Manan, N., Aghazadeh, B., Liu, G., Majumdar, A., Ouerfelli, O., Siminovitch, K., and Rosen, M. (1999). Structure of Cdc42 in complex with the GTPase-binding domain of the 'Wiskott-Aldrich syndrome' protein. *Nature*, 399(6734):379–383. Cited on p. 7

Adami, R., Cintio, O., Trombetta, G., Choquet, D., and Grazi, E. (2003). On the stiffness of the natural actin filament decorated with alexa fluor tropomyosin. *Biophys Chem*, 104(2):469–476. Cited on p. 121

Alberts, J. and Odell, G. (2004). In silico reconstitution of Listeria propulsion exhibits nano-saltation. *PLoS Biol*, 2(12). Cited on p. 126

Amann, K. and Pollard, T. (2001a). Direct real-time observation of actin filament branching mediated by Arp2/3 complex using total internal reflection fluorescence microscopy. *Proc Natl Acad Sci U S A*, 98(26):15009–15013. Cited on p. 66

Amann, K. and Pollard, T. (2001b). The Arp2/3 complex nucleates actin filament branches from the sides of pre-existing filaments. *Nat Cell Biol*, 3(3):306–310. Cited on p. 66, 67

Andrianantoandro, E., Blanchoin, L., Sept, D., McCammon, J., and Pollard, T. (2001). Kinetic mechanism of end-to-end annealing of actin filaments. *J Mol Biol*, 312(4):721–730. Cited on p. 63

Bai, R., Choe, K., Ewell, J., Nguyen, N., and Hamel, E. (1998). Direct photoaffinity labeling of cysteine-295 of alpha-tubulin by guanosine 5'-triphosphate bound in the nonexchangeable site. *J Biol Chem*, 273(16):9894–9897. Cited on p. 32

Ball, L., Kühne, R., Hoffmann, B., Häfner, A., Schmieder, P., Volkmer-Engert, R., Hof, M., Wahl, M., Schneider-Mergener, J., Walter, U., Oschkinat, H., and Jarchau, T. (2000). Dual epitope recognition by the VASP EVH1 domain modulates polyproline ligand specificity and binding affinity. *EMBO J*, 19(18):4903–4914. Cited on p. 35

Belmont, L., Orlova, A., Drubin, D., and Egelman, E. (1999). A change in actin conformation associated with filament instability after Pi release. *Proc Natl Acad Sci U S A*, 96(1):29–34. Cited on p. 22, 99, 106

Bernheim-Groswasser, A., Prost, J., and Sykes, C. (2005). Mechanism of actin-based motility: a dynamic state diagram. *Biophys J*, 89(2):1411–1419. Cited on p. 147, 151

Bernheim-Groswasser, A., Wiesner, S., Golsteyn, R., Carlier, M., and Sykes, C. (2002). The dynamics of actin-based motility depend on surface parameters. *Nature*, 417(6886):308–311. Cited on p. 105, 122, 123, 147, 153

Biswas, S. and Kornberg, A. (1984). Nucleoside triphosphate binding to DNA polymerase III holoenzyme of Escherichia coli. A direct photoaffinity labeling study. *J Biol Chem*, 259(12):7990–7993. Cited on p. 25

Blanchoin, L., Amann, K., Higgs, H., Marchand, J., Kaiser, D., and Pollard, T. (2000a). Direct observation of dendritic actin filament networks nucleated by Arp2/3 complex and WASP/Scar proteins. *Nature*, 404(6781):1007–1011. Cited on p. 22, 45, 61, 66, 72

Blanchoin, L. and Pollard, T. (1999). Mechanism of interaction of Acanthamoeba actophorin (ADF/Cofilin) with actin filaments. *J Biol Chem*, 274(22):15538–15546. Cited on p. 47, 90, 97

Blanchoin, L. and Pollard, T. (2002). Hydrolysis of ATP by polymerized actin depends on the bound divalent cation but not profilin. *Biochemistry*, 41(2):597–602. Cited on p. 46, 66, 85, 90

Blanchoin, L., Pollard, T., and Hitchcock-DeGregori, S. (2001). Inhibition of the Arp2/3 complex-nucleated actin polymerization and branch formation by tropomyosin. *Curr Biol*, 11(16):1300–1304. Cited on p. 45, 46, 61, 66

Blanchoin, L., Pollard, T., and Mullins, R. (2000b). Interactions of ADF/cofilin, Arp2/3 complex, capping protein and profilin in remodeling of branched actin filament networks. *Curr Biol*, 10(20):1273–1282. Cited on p. 97, 112

Bork, P., Sander, C., and Valencia, A. (1992). An ATPase domain common to prokaryotic cell cycle proteins, sugar kinases, actin, and hsp70 heat shock proteins. *Proc Natl Acad Sci U S A*, 89(16):7290–7294. Cited on p. 22

Cameron, L., Footer, M., van Oudenaarden, A., and Theriot, J. (1999). Motility of ActA protein-coated microspheres driven by actin polymerization. *Proc Natl Acad Sci U S A*, 96(9):4908–4913. Cited on p. 121

Childs, K., Ning, X., and Bolling, S. (1996). Simultaneous detection of nucleotides, nucleosides and oxidative metabolites in myocardial biopsies. *J Chromatogr B Biomed Appl*, 678(2):181–186. Cited on p. 26

Combeau, C. and Carlier, M. (1988). Probing the mechanism of ATP hydrolysis on F-actin using vanadate and the structural analogs of phosphate BeF-3 and AlF-4. *J Biol Chem*, 263(33):17429–17436. Cited on p. 37

Cooper, J. and Pollard, T. (1982). Methods to measure actin polymerization. *Methods Enzymol*, 85 Pt B:182–210. Cited on p. 28

Dawson, J., Sablin, E., Spudich, J., and Fletterick, R. (2003). Structure of an F-actin trimer disrupted by gelsolin and implications for the mechanism of severing. *J Biol Chem*, 278(2):1229–1238. Cited on p. 109

Dayel, M., Holleran, E., and Mullins, R. (2001). Arp2/3 complex requires hydrolyzable ATP for nucleation of new actin filaments. *Proc Natl Acad Sci U S A*, 98(26):14871–14876. Cited on p. 19, 46, 49, 52, 72, 73, 95

Dayel, M. and Mullins, R. (2004). Activation of Arp2/3 complex: addition of the first subunit of the new filament by a WASP protein triggers rapid ATP hydrolysis on Arp2. *PLoS Biol*, 2(4). Cited on p. 43

De La Cruz, E. and Pollard, T. (1995). Nucleotide-free actin: stabilization by sucrose and nucleotide binding kinetics. *Biochemistry*, 34(16):5452–5461. Cited on p. 32, 33

Egile, C., Rouiller, I., Xu, X., Volkmann, N., Li, R., and Hanein, D. (2005). Mechanism of filament nucleation and branch stability revealed by the structure of the Arp2/3 complex at actin branch junctions. *PLoS Biol*, 3(11). Cited on p. 78, 108

Evangelista, M., Klebl, B., Tong, A., Webb, B., Leeuw, T., Leberer, E., Whiteway, M., Thomas, D., and Boone, C. (2000). A role for myosin-I in actin assembly through interactions with Vrp1p, Bee1p, and the Arp2/3 complex. *J Cell Biol*, 148(2):353–362. Cited on p. 98

Fujiwara, I., Suetsugu, S., Uemura, S., Takenawa, T., and Ishiwata, S. (2002). Visualization and force measurement of branching by Arp2/3 complex and N-WASP in actin filament. *Biochem Biophys Res Commun*, 293(5):1550–1555. Cited on p. 111, 121

Gardel, M., Shin, J., MacKintosh, F., Mahadevan, L., Matsudaira, P., and Weitz, D. (2004). Elastic behavior of cross-linked and bundled actin networks. *Science*, 304(5675):1301–1305. Cited on p. 9

Gautreau, A., Ho, H., Li, J., Steen, H., Gygi, S., and Kirschner, M. (2004). Purification and architecture of the ubiquitous Wave complex. *Proc Natl Acad Sci U S A*, 101(13):4379–4383. Cited on p. 9

Gerbal, F., Chaikin, P., Rabin, Y., and Prost, J. (2000a). An elastic analysis of Listeria monocytogenes propulsion. *Biophys J*, 79(5):2259–2275. Cited on p. 10, 123, 126, 129

Gerbal, F., Laurent, V., Ott, A., Carlier, M., Chaikin, P., and Prost, J. (2000b). Measurement of the elasticity of the actin tail of Listeria monocytogenes. *Eur Biophys J*, 29(2):134–140. Cited on p. 10, 121, 123

Giardini, P., Fletcher, D., and Theriot, J. (2003). Compression forces generated by actin comet tails on lipid vesicles. *Proc Natl Acad Sci U S A*, 100(11):6493–6498. Cited on p. 123, 129

Goley, E., Rodenbusch, S., Martin, A., and Welch, M. (2004). Critical conformational changes in the Arp2/3 complex are induced by nucleotide and nucleation promoting factor. *Mol Cell*, 16(2):269–279. Cited on p. 107

Gournier, H., Goley, E., Niederstrasser, H., Trinh, T., and Welch, M. (2001). Reconstitution of human Arp2/3 complex reveals critical roles of individual subunits in complex structure and activity. *Mol Cell*, 8(5):1041–1052. Cited on p. 70

Grazi, E., Cintio, O., and Trombetta, G. (2004). On the mechanics of the actin filament: the linear relationship between stiffness and yield strength allows

estimation of the yield strength of thin filament in vivo. *J Muscle Res Cell Motil*, 25(1):103–105. Cited on p. 121

Isambert, H., Venier, P., Maggs, A., Fattoum, A., Kassab, R., Pantaloni, D., and Carlier, M. (1995). Flexibility of actin filaments derived from thermal fluctuations. Effect of bound nucleotide, phalloidin, and muscle regulatory proteins. *J Biol Chem*, 270(19):11437–11444. Cited on p. 120

Jung, G., Remmert, K., Wu, X., Volosky, J., and Hammer, J. (2001). The Dictyostelium CARMIL protein links capping protein and the Arp2/3 complex to type I myosins through their SH3 domains. *J Cell Biol*, 153(7):1479–1497. Cited on p. 91, 98

Kelleher, J., Atkinson, S., and Pollard, T. (1995). Sequences, structural models, and cellular localization of the actin-related proteins Arp2 and Arp3 from Acanthamoeba. *J Cell Biol*, 131(2):385–397. Cited on p. 13, 22, 30, 68

Kocks, C., Hellio, R., Gounon, P., Ohayon, H., and Cossart, P. (1993). Polarized distribution of Listeria monocytogenes surface protein ActA at the site of directional actin assembly. *J Cell Sci*, 105 (Pt 3):699–710. Cited on p. 121

Korn, E., Carlier, M., and Pantaloni, D. (1987). Actin polymerization and ATP hydrolysis. *Science*, 238(4827):638–644. Cited on p. 22

Kuang, B. and Rubenstein, P. (1997). The effects of severely decreased hydrophobicity in a subdomain 3/4 loop on the dynamics and stability of yeast G-actin. *J Biol Chem*, 272(7):4412–4418. Cited on p. 67, 68

Kuo, S. and McGrath, J. (2000). Steps and fluctuations of Listeria monocytogenes during actin-based motility. *Nature*, 407(6807):1026–1029. Cited on p. 35, 123

Lauer, P., Theriot, J., Skoble, J., Welch, M., and Portnoy, D. (2001). Systematic mutational analysis of the amino-terminal domain of the Listeria monocytogenes ActA protein reveals novel functions in actin-based motility. *Mol Microbiol*, 42(5):1163–1177. Cited on p. 155

Laurent, V., Loisel, T., Harbeck, B., Wehman, A., Gröbe, L., Jockusch, B., Wehland, J., Gertler, F., and Carlier, M. (1999). Role of proteins of the Ena/VASP family in actin-based motility of Listeria monocytogenes. *J Cell Biol*, 144(6):1245–1258. Cited on p. 35

Le Clainche, C., Pantaloni, D., and Carlier, M. (2003). ATP hydrolysis on actin-related protein 2/3 complex causes debranching of dendritic actin arrays. *Proc Natl Acad Sci U S A*, 100(11):6337–6342. Cited on p. 58, 70, 71, 72, 97, 99

Liberek, K., Skowyra, D., Zylicz, M., Johnson, C., and Georgopoulos, C. (1991). The Escherichia coli DnaK chaperone, the 70-kDa heat shock protein eukaryotic equivalent, changes conformation upon ATP hydrolysis, thus triggering its dissociation from a bound target protein. *J Biol Chem*, 266(22):14491–14496. Cited on p. 22

Liu, X. and Pollack, G. (2002). Mechanics of F-actin characterized with microfabricated cantilevers. *Biophys J*, 83(5):2705–2715. Cited on p. 120

Loisel, T., Boujemaa, R., Pantaloni, D., and , M. (1999). Reconstitution of actin-based motility of Listeria and Shigella using pure proteins. *Nature*, 401(6753):613–616. Cited on p. 105, 111, 119, 120

Lorenz, M., Popp, D., and Holmes, K. (1993). Refinement of the F-actin model against X-ray fiber diffraction data by the use of a directed mutation algorithm. *J Mol Biol*, 234(3):826–836. Cited on p. 68

Machesky, L., Atkinson, S., Ampe, C., Vandekerckhove, J., and Pollard, T. (1994). Purification of a cortical complex containing two unconventional actins from Acanthamoeba by affinity chromatography on profilin-agarose. *J Cell Biol*, 127(1):107–115. Cited on p. 13

Machesky, L. and Insall, R. (1998). Scar1 and the related Wiskott-Aldrich syndrome protein, WASP, regulate the actin cytoskeleton through the Arp2/3 complex. *Curr Biol*, 8(25):1347–1356. Cited on p. 21, 91

Machesky, L., Mullins, R., Higgs, H., Kaiser, D., Blanchoin, L., May, R., Hall, M., and Pollard, T. (1999). Scar, a WASp-related protein, activates nucleation of actin filaments by the Arp2/3 complex. *Proc Natl Acad Sci U S A*, 96(7):3739–3744. Cited on p. 13, 45

Maciver, S., Zot, H., and Pollard, T. (1991). Characterization of actin filament severing by actophorin from Acanthamoeba castellanii. *J Cell Biol*, 115(6):1611–1620. Cited on p. 22

MacLean-Fletcher, S. and Pollard, T. (1980). Mechanism of action of cytochalasin B on actin. *Cell*, 20(2):329–341. Cited on p. 24

Marchand, J., Kaiser, D., Pollard, T., and Higgs, H. (2001). Interaction of WASP/Scar proteins with actin and vertebrate Arp2/3 complex. *Nat Cell Biol*, 3(1):76–82. Cited on p. 9, 39, 46, 67, 81, 94, 96

Marcy, Y., Prost, J., Carlier, M., and Sykes, C. (2004). Forces generated during actin-based propulsion: a direct measurement by micromanipulation. *Proc Natl Acad Sci U S A*, 101(16):5992–5997. Cited on p. 111, 121

Melki, R., Fievez, S., and Carlier, M. (1996). Continuous monitoring of Pi release following nucleotide hydrolysis in actin or tubulin assembly using 2-amino-6-mercapto-7-methylpurine ribonucleoside and purine-nucleoside phosphorylase as an enzyme-linked assay. *Biochemistry*, 35(37):12038–12045. Cited on p. 46, 72

Miki, H., Sasaki, T., Takai, Y., and Takenawa, T. (1998a). Induction of filopodium formation by a WASP-related actin-depolymerizing protein N-WASP. *Nature*, 391(6662):93–96. Cited on p. 21

Miki, H., Suetsugu, S., and Takenawa, T. (1998b). WAVE, a novel WASP-family protein involved in actin reorganization induced by Rac. *EMBO J*, 17(23):6932–6941. Cited on p. 21

Mogilner, A. and Oster, G. (1996). Cell motility driven by actin polymerization. *Biophys J*, 71(6):3030–3045. Cited on p. 125

Mogilner, A. and Oster, G. (2003). Force generation by actin polymerization II: the elastic ratchet and tethered filaments. *Biophys J*, 84(3):1591–1605. Cited on p. 126

Muhlrad, A., Cheung, P., Phan, B., Miller, C., and Reisler, E. (1994). Dynamic properties of actin. Structural changes induced by beryllium fluoride. *J Biol Chem*, 269(16):11852–11858. Cited on p. 99

Mullins, R. (2000). How WASP-family proteins and the Arp2/3 complex convert intracellular signals into cytoskeletal structures. *Curr Opin Cell Biol*, 12(1):91–96. Cited on p. 21

Mullins, R., Heuser, J., and Pollard, T. (1998). The interaction of Arp2/3 complex with actin: nucleation, high affinity pointed end capping, and formation of branching networks of filaments. *Proc Natl Acad Sci U S A*, 95(11):6181–6186. Cited on p. 4, 13, 22, 35, 39, 45, 63, 66, 73, 91

Mullins, R. and Machesky, L. (2000). Actin assembly mediated by Arp2/3 complex and WASP family proteins. *Methods Enzymol*, 325:214–237. Cited on p. 29, 51

Mullins, R. and Pollard, T. (1999a). Rho-family GTPases require the Arp2/3 complex to stimulate actin polymerization in Acanthamoeba extracts. *Curr Biol*, 9(8):405–415. Cited on p. 37

Mullins, R. and Pollard, T. (1999b). Structure and function of the Arp2/3 complex. *Curr Opin Struct Biol*, 9(2):244–249. Cited on p. 22, 112

Mullins, R., Stafford, W., and Pollard, T. (1997). Structure, subunit topology, and actin-binding activity of the Arp2/3 complex from Acanthamoeba. *J Cell Biol*, 136(2):331–343. Cited on p. 99, 106

Murphy, D., Gray, R., Grasser, W., and Pollard, T. (1988). Direct demonstration of actin filament annealing in vitro. *J Cell Biol*, 106(6):1947–1954. Cited on p. 63

Orlova, A. and Egelman, E. (1992). Structural basis for the destabilization of F-actin by phosphate release following ATP hydrolysis. *J Mol Biol*, 227(4):1043–1053. Cited on p. 22, 37

Otterbein, L., Graceffa, P., and Dominguez, R. (2001). The crystal structure of uncomplexed actin in the ADP state. *Science*, 293(5530):708–711. Cited on p. 22

Panchal, S., Kaiser, D., Torres, E., Pollard, T., and Rosen, M. (2003). A conserved amphipathic helix in WASP/Scar proteins is essential for activation of Arp2/3 complex. *Nat Struct Biol*, 10(8):591–598. Cited on p. 46, 67

Plastino, J., Olivier, S., and Sykes, C. (2004). Actin filaments align into hollow comets for rapid VASP-mediated propulsion. *Curr Biol*, 14(19):1766–1771. Cited on p. 135

Pollard, T., Blanchoin, L., and Mullins, R. (2000). Molecular mechanisms controlling actin filament dynamics in nonmuscle cells. *Annu Rev Biophys Biomol Struct*, 29:545–576. Cited on p. 21, 45, 90, 97

Pollard, T. and Borisy, G. (2003). Cellular motility driven by assembly and disassembly of actin filaments. *Cell*, 112(4):453–465. Cited on p. 4, 91, 119

Rafelski, S. and Theriot, J. (2005). Bacterial shape and ActA distribution affect initiation of Listeria monocytogenes actin-based motility. *Biophys J*, 89(3):2146–2158. Cited on p. 152

Ridley, A. and Hall, A. (1992). The small GTP-binding protein rho regulates the assembly of focal adhesions and actin stress fibers in response to growth factors. *Cell*, 70(3):389–399. Cited on p. 21

Ridley, A., Paterson, H., Johnston, C., Diekmann, D., and Hall, A. (1992). The small GTP-binding protein rac regulates growth factor-induced membrane ruffling. *Cell*, 70(3):401–410. Cited on p. 21

Robinson, R., Turbedsky, K., Kaiser, D., Marchand, J., Higgs, H., Choe, S., and Pollard, T. (2001). Crystal structure of Arp2/3 complex. *Science*, 294(5547):1679–1684. Cited on p. 45, 46, 68, 77, 108

Rodal, A., Sokolova, O., Robins, D., Daugherty, K., Hippenmeyer, S., Riezman, H., Grigorieff, N., and Goode, B. (2005). Conformational changes in the Arp2/3 complex leading to actin nucleation. *Nat Struct Mol Biol*, 12(1):26–31. Cited on p. 76

Rogers, S., Wiedemann, U., Stuurman, N., and Vale, R. (2003). Molecular requirements for actin-based lamella formation in Drosophila S2 cells. *J Cell Biol*, 162(6):1079–1088. Cited on p. 103

Rohatgi, R., Ma, L., Miki, H., Lopez, M., Kirchhausen, T., Takenawa, T., and Kirschner, M. (1999). The interaction between N-WASP and the Arp2/3 complex links Cdc42-dependent signals to actin assembly. *Cell,* 97(2):221–231. Cited on p. 21, 45

Rosenfeld, S. and Taylor, E. (1984). Reactions of 1-N6-ethenoadenosine nucleotides with myosin subfragment 1 and acto-subfragment 1 of skeletal and smooth muscle. *J Biol Chem,* 259(19):11920–11929. Cited on p. 26

Selden, L., Kinosian, H., Estes, J., and Gershman, L. (1999). Impact of profilin on actin-bound nucleotide exchange and actin polymerization dynamics. *Biochemistry,* 38(9):2769–2778. Cited on p. 37, 71

Shacter, E. (1984). Organic extraction of Pi with isobutanol/toluene. *Anal Biochem,* 138(2):416–420. Cited on p. 50

Smith, G., Portnoy, D., and Theriot, J. (1995). Asymmetric distribution of the Listeria monocytogenes ActA protein is required and sufficient to direct actin-based motility. *Mol Microbiol,* 17(5):945–951. Cited on p. 152

Svitkina, T. and Borisy, G. (1999). Arp2/3 complex and actin depolymerizing factor/cofilin in dendritic organization and treadmilling of actin filament array in lamellipodia. *J Cell Biol,* 145(5):1009–1026. Cited on p. 22

Takeda, S. and McKay, D. (1996). Kinetics of peptide binding to the bovine 70 kDa heat shock cognate protein, a molecular chaperone. *Biochemistry,* 35(14):4636–4644. Cited on p. 22

Taunton, J. (2001). Actin filament nucleation by endosomes, lysosomes and secretory vesicles. *Curr Opin Cell Biol*, 13(1):85–91. Cited on p. 21

Taunton, J., Rowning, B., Coughlin, M., Wu, M., Moon, R., Mitchison, T., and Larabell, C. (2000). Actin-dependent propulsion of endosomes and lysosomes by recruitment of N-WASP. *J Cell Biol*, 148(3):519–530. Cited on p. 123

Tsuda, Y., Yasutake, H., Ishijima, A., and Yanagida, T. (1996). Torsional rigidity of single actin filaments and actin-actin bond breaking force under torsion measured directly by in vitro micromanipulation. *Proc Natl Acad Sci U S A*, 93(23):12937–12942. Cited on p. 121

Uruno, T., Liu, J., Li, Y., Smith, N., and Zhan, X. (2003). Sequential interaction of actin-related proteins 2 and 3 (Arp2/3) complex with neural Wiscott-Aldrich syndrome protein (N-WASP) and cortactin during branched actin filament network formation. *J Biol Chem*, 278(28):26086–26093. Cited on p. 96

Volkmann, N., Amann, K., Stoilova-McPhie, S., Egile, C., Winter, D., Hazelwood, L., Heuser, J., Li, R., Pollard, T., and Hanein, D. (2001). Structure of Arp2/3 complex in its activated state and in actin filament branch junctions. *Science*, 293(5539):2456–2459. Cited on p. 108

Waterman-Storer, C., Desai, A., Bulinski, J., and Salmon, E. (1998). Fluorescent speckle microscopy, a method to visualize the dynamics of protein assemblies in living cells. *Curr Biol*, 8(22):1227–1230. Cited on p. 4, 105

Weaver, A., Karginov, A., Kinley, A., Weed, S., Li, Y., Parsons, J., and Cooper, J. (2001). Cortactin promotes and stabilizes Arp2/3-induced actin filament network formation. *Curr Biol*, 11(5):370–374. Cited on p. 91, 96

Welch, M. and Mullins, R. (2002). Cellular control of actin nucleation. *Annu Rev Cell Dev Biol*, 18:247–288. Cited on p. 120

Welch, M., Rosenblatt, J., Skoble, J., Portnoy, D., and Mitchison, T. (1998). Interaction of human Arp2/3 complex and the Listeria monocytogenes ActA protein in actin filament nucleation. *Science*, 281(5373):105–108. Cited on p. 45

Xu, J., Schwarz, W., Käs, J., Stossel, T., Janmey, P., and Pollard, T. (1998). Mechanical properties of actin filament networks depend on preparation, polymerization conditions, and storage of actin monomers. *Biophys J*, 74(5):2731–2740. Cited on p. 16

Yang, C., Pring, M., Wear, M., Huang, M., Cooper, J., Svitkina, T., and Zigmond, S. (2005). Mammalian CARMIL inhibits actin filament capping by capping protein. *Dev Cell*, 9(2):209–221. Cited on p. 98

Yarar, D., To, W., Abo, A., and Welch, M. (1999). The Wiskott-Aldrich syndrome protein directs actin-based motility by stimulating actin nucleation with the Arp2/3 complex. *Curr Biol*, 9(10):555–558. Cited on p. 21

Zalevsky, J., Grigorova, I., and Mullins, R. (2001a). Activation of the Arp2/3 complex by the Listeria acta protein. Acta binds two actin monomers and three

subunits of the Arp2/3 complex. *J Biol Chem*, 276(5):3468–3475. Cited on p. 28, 35, 39, 91, 97, 106

Zalevsky, J., Lempert, L., Kranitz, H., and Mullins, R. (2001b). Different WASP family proteins stimulate different Arp2/3 complex-dependent actin-nucleating activities. *Curr Biol*, 11(24):1903–1913. Cited on p. 33, 45, 51, 61, 67, 81, 122